Holographic Memory Photopolymer Materials

Katherine B. Pacheco

UNIVERSITE D'ANGERS

Année 2007
N° d'ordre 847

Photopolymères pour mémoire holographiques.

Thèse de Doctorat
Spécialité : Physique

Ecole Doctorale d'Angers

Présentée et soutenue publiquement

Le 14 Décembre 2007 à Angers

Par **Katherine B. PACHECO**

Devant le jury ci-dessous :

Rapporteurs : M. Alain Fort, *DR1, Institut de Physique et Chimique des Matériaux de Strasbourg, France*
Mme. Chantal Andraud, *Professeur Ecole Normale Supérieure de Lyon, France*
Examinateurs : M. Mamadou Sylla, *MC-HDR, Université d'Angers, France*
M. Jean-Michel NUNZI, *Professeur, Université d'Angers, France*

Directeur de thèse : **Pr. Jean-Michel NUNZI**

Laboratoire POMA, UMR CNRS 6136
Université d'Angers, bâtiment Db
2, boulevard Lavoisier, 49045 Angers.

ED 363

Abstract

Data flow and its storage is one of the immediate requirements in present information age. There is a huge demand for a suitable storage media for immediate use and for data archive. Photopolymers are one of the most interesting materials with great storage potentials at extremely low cost. Photopolymers are attractive optical recording materials for holography, optical image multiplexing, holographic optical devices, and so forth because they have the capabilities of recording holograms of high spatial frequency and exhibit high diffraction efficiency.

In this thesis we study and optimize various water soluble photopolymer compositions for their data storage capability as well as a good recording media using optical interferometry. Such optimized compositions are selectively sensitized using red to blue sensitizing dyes for optimum information storage. We also present two newly synthesized dyes absorbing in blue region as a promising media for holographic data storage with high resolution embedded grating structures. The experimental results are explained using several supporting characterizations and measurements such as UV-VIS, FT-IR Spectroscopy, CV, DSC, TGA and NMR. For enhancing the refractive index modulation the addition of dispersed SiO_2 nanoparticles is used which also leads to remarkable reduction of film shrinkage.

Résumé

Le flux de données et son stockage est un besoin immédiat de l'ère de l'information. Il existe une demande énorme de supports de stockage appropriés pour l'usage immédiat et pour l'archivage de données. Les Photopolymères sont des matériaux le plus intéressants avec des grands potentiels de stockage à un coût extrêmement bas. Les photopolymères sont des matériaux attrayants pour l'enregistrement holographique, le multiplexage d'images, les circuit optiques, et ainsi de suite parce qu'ils ont la possibilité d'enregistrer des hologrammes avec une bonne fréquence spatiale et l'efficacité de diffraction.

Dans cette thèse nous étudions et optimisons les diverses compositions de photopolymères solubles dans l'eau pour leur capacité de stockage et comme medias d'enregistrement en utilisant l'interférométrie optique. De telles compositions optimisées sont sélectivement sensibilisées en utilisant des colorants dans le bleu pour le stockage optimum d'information. Nous présentons également deux colorants nouvellement synthétises absorbant dans la région bleue en tant que medias promoteurs pour le stockage de données à haute densité. Les résultats expérimentaux sont expliqués en utilisant plusieurs caractérisations et mesures de support telles qu'UV-Vis, la spectroscopie de FT-IR, CV, DSC, TGA, RMN. Pour augmenter la modulation d'indice de réfraction la dispersion des nanoparticles de SiO_2 conduit, également à une réduction remarquable de rétreint du film.

Acknowledgements

Firstly, I would like to thank my thesis supervisor Prof. Jean-Michel Nunzi for his continuing guidance and encouragement during the whole period of my thesis.

On a different note, I would like to thank Christophe Cassagne for his initial but crucial help with experimental set up and timely discussions. Also thanks to Alain Mahot for his assistance with all types of technical problems at all times.

I would like to thank all my colleagues that I had worked with: Sophie Dixneuf, Gabriela, Hassina, Ajay and Marcos.

Thanks to: Prof. Pietrick Hudhomme for his donation of Perylene molecule to be tested as photosensitizer in photopolymers, Eric Levillain and Lionel Sanguinet for their help on electro-chemical measurements, Prof. Jack Couseau and Nicolas Mercier for letting me to use their laboratory facilities to carry out my experiments, Jacques Delaneau for NMR measurements; Magali Allain and Nicolas Louvain for their help with DSC and TGA measurements.

I would like to say thank to all the collaborators of the MICROHOLAS European project. My thank goes to Prof. Francesco Simoni from the University of Marche, Ancona, Italy and Prof. Susana Orlic from TUB, Berlin, Germany for the collaborations and research visits on holographic related measurements.

I would like to thank to Prof. Humberto Soscun and his wife, Olga for introducing me to the world of science and their friendship.

I have to say thank-you to: all my family members and friends in different parts of the world, particularly my Mother and Father; and most importantly of all to Karina, Auxi and Andreina, for their strong support, help and friendship throughout

different phases of my research work. Before I conclude the list I can't leave out my beloved Ponky for his beautiful company through out my life even you are not with me but you still remain close to my heart and special …

Finally, I am forever grateful to you my *best friend* for your understanding, endless patience and encouragement when it was most required.

Contents

List of figures.

List of Tables.

Introduction

We live in an era where flow and storage of data has become one of the integral parts of our daily life. With recent digital revolution every thing from general documentation to entertainment and photography requires huge amount of data to be archived. This raises the requirement for a suitable storage media to keep the huge quantity of such valuable data available for immediate use and storage [1]. With further demand for high definition data storage and visualisation, the existing data storage and handling media are hence pushed to their limit in terms of their general allowed capacity. Historically there are various recording and storage media available to us in form of magnetic tapes, photographic plates to compact discs. Optical data storage is one versatile optical tool which permits volume data storage in form of thin recording films often made up of photosensitive materials and this has been driving the storage technology for recent developments in high capacity optical data storage in form of blue ray discs, which takes the advantage of data recording using short optical wavelengths in order to enhance the capacity of the storage media [2]. Optical data storage in form of holograms has been historically studied as one of the promising medium where data storage can have virtually no limits taking advantage of optical interferometric techniques.

This thesis presents the study on development of water soluble photopolymer systems and their suitability as volume information storage media. There are many

types of photopolymers that may be differentiated by the type of binder, since this component determines to a great extent the choice of monomer, dye and initiator used in the photopolymer. Photopolymers with a poly(vinyl alcohol) or gelatin binder and monomers related to acrylamide (AA) are also hydrophilic. All these photopolymers have a desirable feature, the low toxicity of most of their components and high environmental compatibility. The environmental compatibility and life cycle are important features that must always be considered when developing new materials. In hydrophobic photopolymers, the organic solvents during their production are used. These solvents are not environmental friendly thus creating a considerable pollution in further years.

Here the emphasis is increase the capacity of the information storage in terms of raising the spatial frequency. Thus different sensitizing dyes with sensitivity from red to blue spectral region are studied and presented with experimentally demonstrated spatial frequency as high as 4760 lines/mm. We studied different photopolymer systems in transmission as well as in reflection geometry.

In the chapter 1 we discuss the principle of holography and different photosensitive media commonly used for recording purposes and the need of novel recording media such as photopolymers as a solution to high capacity data storage.

In the chapter 2 we describe the development and optimization of different components of photopolymer system suitable for red wavelength recording in transmission geometry. The results are analysed with help of optical techniques and through diffraction grating formation in the bulk of the recording medium.

In chapter 3 we present the studies on photopolymer system in transmission as well as reflection geometry recording using green sensitizing dyes, which takes advantage of high capacity grating storage over red sensitized dye studied in chapter 2. Different compositions are studied and optimized using different material characterization techniques.

In chapter 4 we develop novel photopolymer system suitable for blue wavelength recording. Two new water soluble blue sensitizing dyes are synthesized and their information storage capacity is demonstrated.

Finally; in chapter 5 we study, in detail, the refractive index modulation while incorporating low index in-organic nanoparticles in the photopolymer composition. Large modulation of index is thus created in recording system. This also helps us to understand the monomer diffusion process involved in the photopolymerization process.

1

Chapter 1

1.1 Hologram and History of Holography

A hologram is a record of the interaction of two mutually coherent light beams, in the form of a microscopic pattern of interference fringes. The principles of holography came in the late 1940's by Denis Gabor [3]. In 1948 Dennis Gabor fabricated the first hologram using one mercury line and a pinhole of 3 microns diameter. He created a hologram of an object of about 1 cm diameter. With the most sensitive emulsions then available in that period. The small coherence length forced him to arrange everything in one axis. Well known as "in line" holography and it was the only one possibility at that time. It was far from perfect. There were random disturbances and defects in the holograms. The disturbance arises from the fact that there is not one image but two. Each point of the object emits a spherical secondary wave, which interferes with the background and produces a system of circular Fresnel zones [2].

After the discovery of laser in 1962, Leith and Upatnieks invented the method of eliminating the second image; this became possible by the great coherence length of the He-Ne laser, which exceeded that of the mercury lamp by a factor of about 3000

[4]. Which makes it possible to separate the reference beam from the illuminating beam; instead of going through the object, it could now go around it [5]. The result was that the two reconstructed images were now separated not only in depth, but also by twice the incidence angle of the reference beam.

After the development of colour and pulsed laser holography in subsequent years, in 1968, Dr. Stephen A. Benton invented white-light transmission holography which leads the path for development towards first moving 3-dimensional images by combining white-light transmission holography with conventional cinematography [2].

1.2 Holographic recording materials

1.2.1 The ideal holographic recording material

There are several criteria, which an ideal material would satisfy [4]:

- The material must have a high resolution and a flat spatial frequency response. This will ensure that the desired interference pattern is completely stored, i.e. that no fine fringe detail is lost.
- There must be a linear relationship between exposure and the amplitude of the reconstructed wave. This ensures the fidelity of the image at replay.
- The material's dynamic range must be large enough for a sufficient modulation to be formed during recording, which will lead to a good signal to noise ratio.

- The material should be of high optical quality and lossless. This will lead to high optical efficiencies (bright images).
- Changes in environmental conditions should not affect the material and the recorded hologram should be stable for long periods of time.
- The material should be sensitive enough to react to a low energy exposure.

1.2.2 Silver Halide sensitized gelatine

Silver halide photographic emulsion (SHPE) is one of the oldest and most commonly used recording materials. It was originally used as it was both inexpensive and sensitive to common laser wavelengths. SHPE can be used to record holograms in reflection and transmission geometry and is suitable for both amplitude and phase holograms [4]. It is popular because of its very high sensitivity (10^5 to 10^3 mJ/cm^2) compared to other materials and can also record with good resolution (greater than 6000 lines/mm). Its main drawbacks are: (a) the need for wet chemical post-processing, which can lead to shrinking or swelling of the material, which affects the grating replay wavelength, and (b) random scatter due to particles dispersed in the material, which can lead to reduced dynamical range and the production of noise gratings [5]. SHPE consists of a gelatin layer in which microscopic grains of silver halide (usually AgBr) are dispersed. This layer is coated onto a glass or film substrate, with an emulsion thickness of between 5 and 15 mm being typical. The material works by recording a latent image, which is then developed by chemical post-

processing. The latent image is formed when the material absorbs an incident photon.

1.2.3 Dichromated gelatine

Dichromated gelatine is an almost ideal recording material; it has large refractive index modulation capability, high resolution and low absorption and scattering [5]. Hologram recording in Dichromated gelatine makes use of that fact a gelatine layer containing a small amount of a dichromate such as $(NH_4)_2Cr_2O_7$ becomes progressively harder on exposure light [4]. This hardening is due to photochemically produced Cr^{3+} ion forming localized cross-links between the carboxylate groups of neighbouring gelatine chains. For recording, a glass plate coated with gelatine sensitized with dichromate is given a holographic exposure, and the fringe pattern is then developed in a plain water bath [4]. This causes differential swelling of the exposed and unexposed areas [5]. The plate is then dehydrated in an alcohol bath and dried rapidly. The fringe pattern is thus 'frozen' into the gelatine structure, which serves as a phase hologram, with high diffraction efficiency and almost no scattering.

1.2.4 Photopolymers

Photopolymers are systems of organic molecules that rely on photo-initiated polymerization to record volume phase holograms [6]. Characteristics such as good

light sensitivity, large dynamic range, good optical properties and relatively low cost make photopolymers one of the most promising materials for write-one, read-many (WORM) holographic data storage applications [3,6]. Photopolymers, unlike dichromate gelatine based recording material do not require complicated holographic development processes. Photopolymers typically consist of one or more acrylic monomers and a photo-initiator complex, all dispersed within an inactive component, a polymer matrix, also referred to as a binder. Other components are sometime added to control a variety of properties such as pre-exposure shelf life, and viscosity of the recording medium [3]. The resulting formulation is typically a viscous fluid, or a solid with a low glass transition temperature, that is prepared for exposure either by coating on a solid or flexible substrate, or by containing it between two transparent solid substrates [5]. These materials have several advantages; because thick layers can be fabricated they act as a true volume material giving high diffraction efficiency and good angular selectivity. Most of the materials are self-developing or require only some simple post-processing such as an exposure to light or heat treatment. This eliminates the need for wet chemical development, which makes photopolymers suitable for applications such as holographic interferometry [3].

As described in this section, photopolymers are inexpensive and self processing media for information storage. In coming sections we will describe, in detail, the composition of a photopolymer system and various physical and chemical processes attached with photopolymer based holographic recording.

1.3 Terminology used in photopolymer holography

1.3.1 Refractive index modulation (RIM)

The refractive index modulation is related to the difference between the index of polymer formed and the un-reacted monomer in non-illuminated areas [6]. The photo-induced polymerization of the acrylic monomer in the bright regions of the interference pattern produces a refractive index increase in the illuminated regions compared to the dark regions. This occurs due to the actual conversion of chemical bonds during the polymerization process and the density modulation produced as the monomer migrates into the polymer regions during recording to form the higher density polymer [7]. The index modulation increases when the concentration of the monomer is raised but the scattering is practically constant.

A large refractive index (Δn) between these two regions is desired to minimize the dynamic range, or the data storage capacity of the material [6]. A combination of one or more large refractive index (e.g. aromatic monomers) with low refractive index binder is known to be advantageous for maximizing the Δn [6].

Achieving Δn larger than ca. 5×10^{-3} has proven to be difficult in photopolymer compositions [8], in part because of the limited diffusion of monomer molecules in binders and also because of relatively limited RI differences between the available monomers and binders.

In the hologram recording using photopolymers comprise the alternation in molecular electronic structure, density changes and spatial segregation of system

components. Examination of the Lorentz-Lorentz relationship of eq (1) for an isotropic, ideal mixture can give estimations of these effects [9]:

$$\frac{n^2-1}{n^2+2}=\sum_i \frac{\rho_i R_i}{M_i} \quad (1)$$

Here n is the average refractive index, ρ_I is the density, M_i is the molecular weight and R_i is the molar refraction of the ith component of the mixture. Differentiation of eq (2) for a single component reveals the effects that small changes in ρ and R have on the refractive index.

$$\Delta n=\left\{\frac{(n^2+2)(n^2-1)}{6n}\right\}\left\{\frac{\Delta R}{R}+\frac{\Delta\rho}{\rho}\right\} \quad (2)$$

Change of electronic structure upon polymerization is accounted for by changes in molar refraction when a monomer is incorporated into the polymer chain [9]. During vinyl polymerization the double bond of the monomer is converted to a single bond in the backbone structure of the polymer. This change in bond order can be responsible for a significant change in molar refraction; previously the polymerization of the monomers cannot approach closer to one another than the sum of their individual van der Waals radii. After the polymerization process occurs the monomers are linked by covalent bonds and thus the distance between connected monomers is shortened. When polymerization takes place almost always produces a decrease in volume and a concomitant increase in density.

1.3.2 Diffraction Efficiency

Diffraction efficiency is defined as a value that expresses the amount to which energy can be obtained from the diffracted light with respect to the energy of the incident light. We expressed the DE in our experiments as the ratio between diffracted light and the sum of the diffracted and the transmittance light respectively as shown as:

$$\eta = \frac{I_D}{I_D + I_T} \qquad (3)$$

where I_D and I_T are diffracted and transmitted intensities.

1.3.3 Sensitivity

Sensitivity gives the response of the material under incident light [11]. In other words, sensitivity is the measure of the energy necessary to obtain the maximum DE. The Sensitivity of the material is defined as:

$$Sensitivity\,(S) = \frac{\sqrt{\eta}}{I\,t\,d} \ \text{(cm/J)} \qquad (4)$$

where η is the diffraction efficiency, I is the total intensity in mW/cm^2, t is the exposure time and d is the thickness of the material. Sensitivity is related to the absorption of the material: this can be optimized for a given material.

1.3.4 Bragg angle and Bragg condition.

The Bragg condition for a plane, parallel grating with fringes those are normal to the grating surface (the case shown in Figure 1.1 is given by

$$m\,\lambda = \Lambda\,2\,n_2 \sin(\alpha_{2B}) \qquad (5)$$

where Λ is the fringe spacing of the grating equal to 1/ν for fringe planes orthogonal to the grating surface, and α_{2B} is the Bragg angle in the grating medium. The Bragg condition is met when *m* is an integer and the wavelength and fringe spacing are such that the angles of incidence and diffraction are equal and opposite (with respect to the surface normal). The formulation of the Bragg condition for slanted fringes is slightly more complex, but in that case the angles of incidence and diffraction are symmetric within the grating medium about the fringe planes. Light illuminating the grating at angles significantly outside of the Bragg condition may pass through the grating without being diffracted [12].

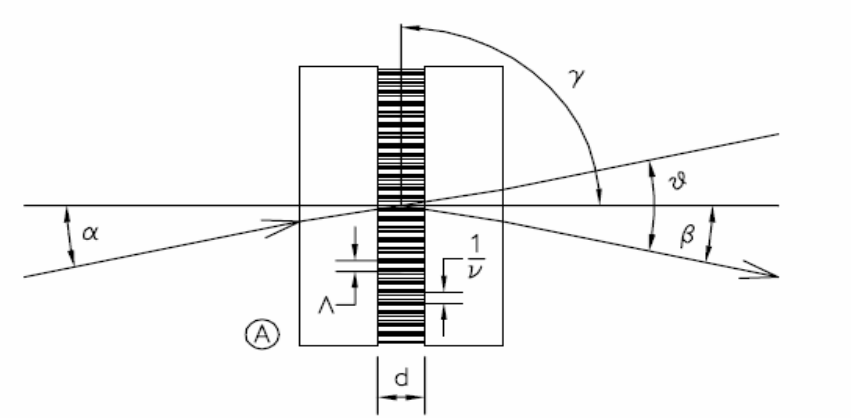

Fig. 1.1 Transmission grating with fringes perpendicular to the grating (unslanted fringes).

1.3.5 Fringe Spacing

The pitch of the grating or the grating period is measure of the spatial distance between two interference fringes and is determined by the Bragg's Law:

$$\Lambda = \frac{\lambda}{2 \sin \theta} \qquad (7)$$

where λ is recording wavelength and θ is the half-angle between the recording beams inside the material [3].

1.3.6 Shrinkage

One of the greatest potential disadvantages of photopolymer is that they are prone to undergo shrinkage during processing [3,14]. In general, shrinkage is essentially, after hologram recording, observed in all photopolymer systems [14]. Each time a monomer adds to a growing polymer chain the volume of the system decreases as a covalent bond replaces a near van der Waals contact [4]. For photopolymer systems, including multifunctional monomers, the degree of volume shrinkage is usually not directly proportional to the degree of conversion to polymer. Rapid polymerization produces a kinetic lag between polymer conversion and volume shrinkage [15]. This effect is particularly pronounced during the latter stages of polymerization after the system has solidified [16]. Apparently, for high cross-linked, very viscous systems, relatively rapid polymerization produces excess free volume at a greater rate than is dissipated by diffusion and thermal relaxation. This excess free volume allows continued monomer diffusion, and promotes a greater degree of polymer conversion for rapid reaction compared with slow reactions. These considerations suggest that the free volume excess present in freshly recorded holograms will relax to a stable volume over a time period that varies from minutes to days. In substantially solidified systems such relaxation can effect degradation of image fidelity over time.

The existence of shrinking of the photopolymer layers results in a change in the fringe spacing [7]. Due to this it is required to alter the readout beam angle to achieve the maximum diffraction efficiency.

The value of the shrinkage changes dramatically in Reflection hologram but is not severely affected in transmission hologram because it is difficult for the material to shrink along the direction of the substrate, which is usually glass [3].

Shrinkage has been observed to cause: wavelength shift (and/or) and the angular rotation for maximum DE reconstruction [14]. Figure 1.2 shows the origin of shrinkage in a photopolymer recording film.

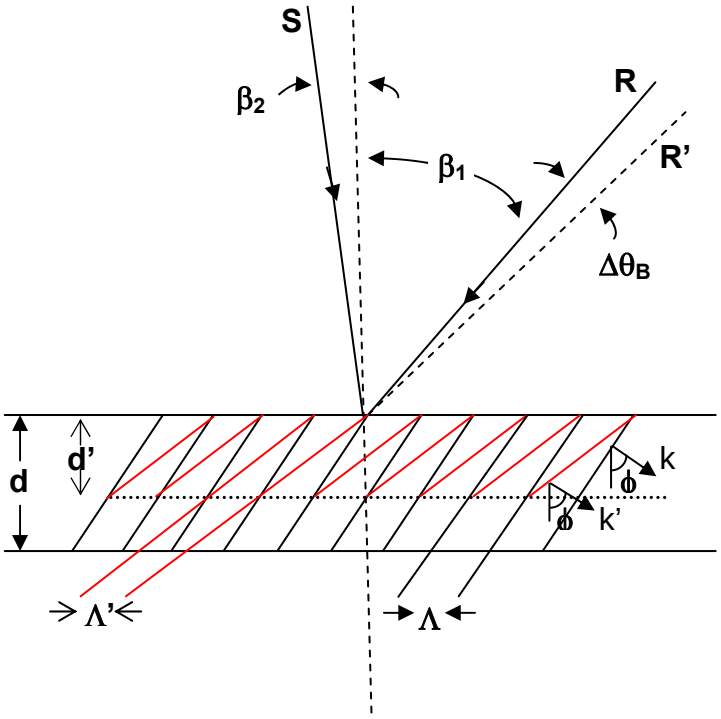

Fig. 1.2 Fringe-plane model for a plane-wave grating.

In figure 1.2, R and S are reference and signal beams which intersect the material at angles of β_1 and β_2 with respect to the surface normal. The sign of β_1 is positive and β_2

is negative. Before Shrinkage, the material has thickness d and the planar parallel fringes are defined by the grating vector K, the fringe spacing Λ, and the slant angle ϕ. The primed values indicate the new parameter values after shrinkage. The grating vector is defined by [14]

$$K = \frac{2\pi}{\Lambda}$$

where Λ is the fringe spacing. It should be mentioned that the maximum DE changes because Λ also changes with shrinkage. The change is the slant angle of the fringes is equivalent to the rotation in Bragg angle required for maximum DE reconstruction. The amount by which the DE is reduced increases with the amount of shrinkage and with spatial frequency of the object.

The fractional change in material thickness, Δd, can be obtained by knowing the initial slant change of the grating ϕ_o and the final slant angle, ϕ_f [7].

$$\Delta d = d_o\left[\frac{\tan\phi_f}{\tan\phi_o} - 1\right] \qquad (9)$$

1.3.7 Angular selectivity

The angular selectivity of volume holograms is responsible for their diverse applications in the spatial domain. Various spatial-domain properties and applications of holograms are attributed to their angular selectivity; for instance, angle multiplexing, shift multiplexing, holographic storage, image processing and pattern recognition, among others [7].

1.4 Composition of Photopolymer

As described earlier, photopolymer is a multi component system where some components serve multifunctional roles. The main constituents of a photopolymer recording medium are; monomer, cross-linker, dye or sensitizer, initiator and binder [6]. The first work was reported by Close et al.[17] which system comprised of a mixture of acrylamide and metal acrylate as monomers, methylene blue and p-toluene sodium salt as photosensitizers. The liquid system was sandwich between two glasses for the recording. Diffraction efficiencies of 45% were achieved with exposure energy of 300 mJ/cm2. The spatial frequency of the photopolymer was found to be 3000 lines/mm. The shelf life of the photopolymer was very short. Jenney [18,19] ameliorated the sensitivity of Close's system by diminishing the exposure energy required to 0.6 mJ/cm2 and employing lead or barium acrylate along with acrylamide as monomers.

Sugawara et al. [20] formulated a second liquid system comprised of acrylamide as monomer, N,N methylene bisacrylamide as crosslinker, methylene blue as phtosensitiser and either triethanolamine or acetylacetone as initiator. Diffraction efficiencies of 65% were achieved with exposure energies of 50 mJ/cm2 and 550 lines/mm of spatial frequency.

By adding poly-vinylalcohol as binder, Sadlej et al. [21] amended the system developed by Close and Jenney. The inclusion of binder allowed the formation of dry layers, which are easier to handle than liquid systems thus improving the shelf life of

the original material demonstrating that the binder can improve the stability of recorded holograms. The sensitivity of 10 mJ/cm^2 and spatial frequencies of 4700 lines/mm could be registered. Low diffraction efficiencies up to 4% were found.

Jeudy et al. [22] described a variation in the liquid system proposed by Sugawara. A reversible photochrome (indolino-spiropyran) was used as sensitizer and poly-vinylalcohol as binder. The photochrome, transparent in visible light, could be activated by ultraviolet (UV) light shifting its absorption band to allow recording at 633 nm. Once the recording was accomplished the UV was switched off and the photochrome became inactive leading to a transparent and stable hologram of 90% of diffraction efficiency with exposure energy of 100 mJ/cm^2 and 3000 lines/mm of spatial frequency.

Calixto [23], kept working on these kind of systems. It was formulated a material containing acrylamide as monomer, triethanolamine as electron donor, methylene blue as photosensitizer and poly-vinylalcohol as binder. The exposure energy was found to be low approximately 94 mJ/cm2 and maximum diffraction efficiencies of 10% were achieved.

A method was prepared by Fimia et al. [24,25] to raise the sensitivity of acrylamide photopolymers by dropping the inhibition time caused by oxygen. The system comprised two photosensitizer, Methylene Blue (sensitive at 633 nm) and Rose Bengal (sensitive at 546 nm). The film was pre-exposed to a 546 nm beam. The Rose Bengal dye produces radicals, which then react with oxygen within the layer. When the recording at 633 nm occurs, amount of oxygen is reduced and enough Methylene

Blue polymerises the monomer. Employing this system, diffraction efficiencies of 40% at spatial frequency of 1000 lines/mm could be achieved with exposure energy of 3 mJ/cm2.

The photopolymer proposed by Calixto et al. [26] was an optimization of the previous system for 514 nm region recording by replacing the photosensitizer for a xanthene one. Diffraction efficiencies greater than 80% were obtained with exposure energy of 80 mJ/cm2. The spatial frequency of the material was reported as 2750 lines/mm.

An improvement of Close and Sugara's material at 514 nm as recording wavelength was reported by Weiss et al. [27] by including diphenyl iodonium chloride to act as a photosensitizer along with material triethanolamine. Glutaraldehyde was used as a second crosslinker causing an increase in the refractive index modulation. Diffraction efficiencies of 90% at 2000 lines/mm of spatial frequency were achieved with exposure energy of 12 mJ/cm^2.

The sensitivity of the acrylamide photopolymer for recording at 633 nm was enhanced by Blaya et al. [28] by replacing the crosslinker for N,N-dihydroethylenebisacrylamide, causing an augment in the rate of polymerisation thus reducing the exposure energy required. Diffraction efficiencies of 70% at a spatial frequency of 1000 lines/mm were obtained with exposure energy of 5 mJ/cm^2.

Zhao [29] proposed a new material. It consisted in a mixture of acrylamide and acrylic as monomers, methylene Blue as photosensitizer, triethanolamine and p-toluenesulfonic acid as sensitizers and gelatin as a binder. The maximum spatial

frequency achieved for recording was 4000 lines/mm. The maximum diffraction efficiency obtained was above 80% with exposure energy of 2 mJ/cm^2

Lawrence et al. [4] proposed a photopolymer based on acrylamide. The photopolymer consisted in acrylamide and N,N'-methylenebisacrylamide as monomer and cross-linking agent, erythrosine B as photosensitizer, triethanolamine as initiator dissolved all in poly-vinylalcohol as binder. The diffraction efficiencies found were approximately of 80% using a 120 μm thick film at 1000 lines/mm of spatial frequency using an intensity of 2 mW/cm^2. By increasing the spatial frequency to 2750 lines/mm the diffraction efficiency decayed to 30%

Neipp et al. [30] prepared a photopolymer using acrylamide (AA), N,N'-methylenebisacrylamide as monomers, triethanolamine as initiator, yellowish eosin as photosensitizer in a polyvinylalcohol matrix as a binder. The gratings were recorded using two different spatial frequencies: 545 lines/mm and 1125 lines/mm in order to observe the effect of the spatial frequency on the efficiency. At 545 lines/mm of spatial frequency the diffraction efficiency was found to be 80% and 0.015 of refractive index modulation were achieved using a 73 μm of thick film. At 1125 lines/mm of spatial frequency almost 60% of efficiency was obtained and 0.011 of RIM was estimated in a 33 μm thick film.

Kim et al. [31] reported a novel photopolymer satisfying both phase stability and high diffraction efficiency by replacing the poly-vinylalcohol for a modified poly(methyl methacrylate) as a polymer matrix. The rest of the components of the system were acrylamide and N,N'-methylenebisacrlamide as monomers,

triethanolamine as initiator and methylene blue as photosensitizer. A methacrylic acid unit was inserted into the poly(methyl methacrylate) in order to enhance the phase stability without decreasing the difference between the refractive index of polymer matrix and photopolymerized polymer. By the inclusion of hydrophilic acid unit, the transparency of the photopolymer was greatly improved and high diffraction efficiency close to 90% could be achieved after 200 sec of exposure time and a total intensity of 8 mW/cm2 using symmetric geometry. The refractive index modulation calculated was 1.385 $x10^{-3}$ for the maximum efficiency.

Jeong et al. [32] proposed a system based on epoxy resin with longer length. The photopolymer comprised Polypropylenediglycidylether and polyethyleneimine for the synthesis of epoxy resin, acrylamide as monomer, triethanolamine as initiator and yellowish eosin as a photosensitizer. Holographic diffraction gratings were recording with a spatial frequency of aprox 1940 lines/mm in this photopolymerisable epoxy resin material. Diffraction efficiencies of 92% with an energetic energy of $11.7x10^{-3}cm^2/J$ were achieved in 200~400μm thick films by optimizing the structure of the matrix and the reactants compositions. The refractive index modulation for the maximum diffraction efficiency was estimated to be $9.03x10^{-4}$.

R. Jallapuram et al. [33] studied an acrylamide based photopolymer in transmission and reflection geometries. The transmission gratings were recorded at 3000 lines/mm spatial frequency using a continuous wave intensity of 17 mW/cm^2. Diffraction efficiency of 50% was achieved in 4 sec exposure time. A refractive index modulation

of $0.5x10^{-3}$ was calculated for the maximum diffraction efficiency. The thickness of the layer used for the study was approximately 100 μm and the sensitivity 1450 cm/J. Diffraction efficiency up to 0.2% was achieved in reflection geometry with a spatial frequency of 5640 lines/mm using 1μJ as writing energy.

In this section we will elaborate the precise function of each and every component and their influence on the various parameters, before and after recording.

1.4.1 Monomer

The function of the monomer is to polymerize upon exposure to form a highly crosslinked web, entangling the binder, so that the exposed areas exhibits sufficient mechanical and chemical resistance after recording [3,34]. It also determines the difference in the RI of the exposed and non exposed areas [35]. Typically, monomers contain more than one vinyl groups, for example added to produce a molecular architecture comprising a cross-linking network of polymer chains to improve dimensional stability and image fidelity. Also, monomer should contain at least one double bond to react with a free radical [34]. Suitable monomers belong to the family of polyfunctional acrylate and methacrylate, often modified with alcoxyside chains [34]. Vinyl monomers such as acrylate and methacrylate esters are used in most photopolymer systems. These monomers polymerize through a free radical mechanism [36]. The photopolymerization is initiated when a monomer combines with a reactive radical species to produce the first unit in an actively growing chain.

Chain growth then proceeds through successive addition of monomers to the active chain end. Growth steeps when one of several possible termination reactions deactivates the radical at the growing chain end [36].

(I) Acrylamide

Acrylamide (AA) is commonly used monomer in photopolymer systems due to its high rate of reaction and high solubility in water [35]. The sensitivity of the recording material is improved with the increase of AA concentration [35]. However, it is impossible to increase the concentration of AA indefinitely because the compatibility and solubility of this monomer in the polymer matrix such as PVA, PMMA are limited [37]. At high concentration of AA, precipitation occurs on the surface of the film; this gives rise to the observation of noise gratings, which are produced by the interference of the scattered light of these solid monomer particles with the incident laser beam in the process of hologram formation [38]. Moreover, high concentration of AA makes the film shrink greatly [37].

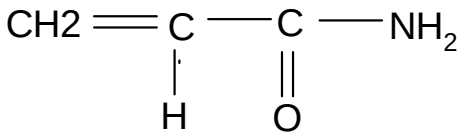

Fig.1.3 Chemical structure of Acrylamide

1.4.2 Cross-linker

The presence of a bifunctional cross-linking monomer in a photopolymer system enhances the capacity of uniting the polyacrylamide chains among them with the

aim to obtain polymer chains with higher length [7]. The creation of these macromolecules helps to maintain the recorded information in the material for longer periods by hindering the monomer diffusion in the polymer chain. One such well known cross-linker is N'N-methylenebisacrylamide (BSA)**.**

(II) N'N-methylenebisacrylamide

N'N-methylenebisacrylamide (BSA) is a cross-linking agent. It gives a cross-linked polymer with higher density and also lower mobility than the linear polyacrylamide obtained when only acrylamide is used [39]. This can be understood if one takes into account that the addition of a cross-linking monomer supports a quick rise of polymer molecular weight obtained in the bright zones by cross-linking of polyacrylamide chains, thus increasing the polymerization rate [34].

The existence of BSA creates an increase of the polarization and the refractive index within the material and/ or in the polymer [40]. In general, when the concentration of AA monomer is low, the diffraction efficiency is also low. BSA can speed-up the polymerization reaction of AA in the photopolymer [41], so the materials with high concentration of BSA have high diffraction efficiency and sensitivity at the same time, but too much BSA leads to high shrinkage of the material. These testify the fact that BSA can ameliorate the characters of the material.

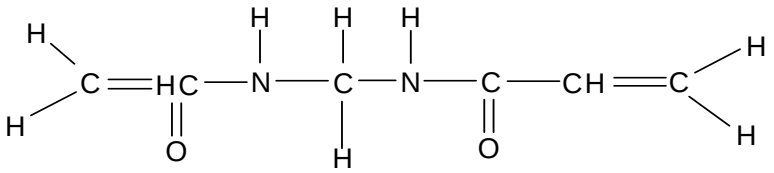

Fig.1.4 Chemical structure of N,N'-methylenebisacrylamide

1.4.3 Dye or photosensitizer

Dye or sensitizer determines the zone of absorption which determines the wavelength used to record and read the holographic gratings [35]. The recording of thick holograms therefore requires special care in the choice of sensitizer. A high concentration of a sensitizer with low extinction coefficient allows the necessary degree of polymerization to occur during holographic exposure without exceeding the desired maximum light absorption in thick samples.

A photosensitizer molecule absorbs the imaging light and in its excited state interacts with a radical generator or acid generator molecule, either through energy transfer or though a redox reaction, to produce the initiating species [42]. Many sensitizers are bleached during hologram recording and produce hologram that do not absorb light at the recording/reading wavelength. With an appropriate selection of sensitizer, holograms can be recorded throughout the spectral range from 400 nm to 650 m as indicated in the following figure 1.5.

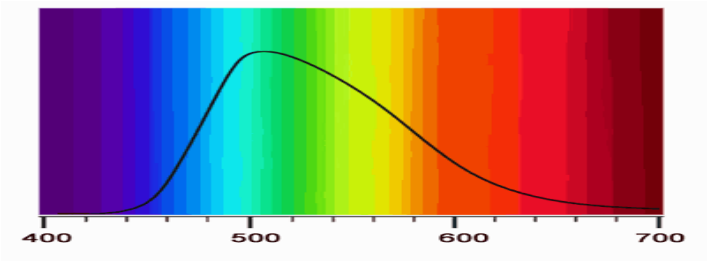

Fig. 1.5 UV/Vis Spectra of the sensitizer.

The bleaching of the dye is an important process that allows a hologram to be fixed after recording [4]. By bleaching any remaining dye cannot form any extra free radical meaning no unwanted polymerization occurs after holographic recording [4]. Concentration of dye is a crucial step in polymerization process. The high dye concentration leads to lower diffraction efficiency, a great deal of dispersion and large number of irregularities [42]. The low dye concentration, are often required to maintain acceptable optical densities for holograms recording at an optimum thickness. In many cases sensitizer molecules are converted to an active form during the photochemical process that leads to polymer chain initiation [4].

1.4.4 Initiator

They are compounds with the ability to produce electron transfer reactions with the dye thereby increasing the polymerization rate [35]. The dye radical is not usually reactive enough to initiate polymerization so the initiators like tertiary amine radical reacts with an AA molecule which initiates the polymerization process [4].

(III) Triethanolamine

Secondary and tertiary amines are compounds capable of reducing the excited dye molecule and of generating radicals that can initiate the radical polymerization [4]. Triethanolamine (TEA) has the ability to produce photoreduction reactions in dyes and has been used as coinitiator, producing an increase in the energetic sensitivity

[35]. It is easy to understand that the more the dye molecules, the more the photons being absorbed, and the more the excited states of the dye, the easier the triethanolamine is excited and the quicker is the monomer's polymerization rate [41]. This compound is a plasticizer also, and its high concentration in the photopolymer system improves the quality of the material, reducing the precipitation of monomer over the surface of the film and consequently reducing the noise gratings as well [41]. Triethanolamine does not give pronounced variations in the conversion of monomer in polymer or length of the chains [35].

Fig.1.6 Chemical structure of Triethanolamine

1.4.5 Binder

Binder is the final and crucial component of a photopolymer system where monomers and the photo initiating systems are usually combined with this component to form a final photopolymer system [4,43]. The binder acts as supporting matrix for monomer mixture which preferentially diffuses and reacts in volume of highest irradiance [8]. The binder is sometimes a polymer that is included to modify the viscosity of the formulation, to aid sample preparation, and to enhance holographic exposure [43]. Binders can also be small molecules or oligomers that are required for the development of the holographic image [43].

Also, binder allows the production of dry photopolymer layers which are easier to use than the earlier liquid systems [4]. In this way, the shelf life of the original

material greatly improves proving conclusively that binder can improve the stability of recorded holograms [4]. The molecular weight and refractive index and other properties of binder have a major effect on the characteristics of the materials [4]. For example changing the binder to one which has a different RI than that of the polymer can lead to higher RIM and therefore higher DE [4].

(IV) Poly vinyl alcohol (PVA)

The choice of PVA is a fundamental factor in obtaining a material of great thickness. PVA with high molecular weight usually have very long polymer chains and when it is dissolved in water gives highly viscous solution with a great capacity per unit of mass to retain water [42]. The presence of long chains also gives rise to a high light dispersion. It is necessary to find a type of PVA that allows sufficient water to be retained so as to obtain layers of the required thickness and has a molecular weight such that the material does not exhibit excessive dispersion of light [42].

If the molecular weight is small, higher concentration of PVA is necessary which hinders the photopolymerization process [41]. Moreover, a great deal of solution must be deposited in order to obtain the required thickness and given the small amount of water retained, the concentration of active substances in the dry film increases excessively giving rise to poor photopolymerization results, since this process depends directly on the concentration in the film of material and not on the concentrations in the initial solution. Preferably a binder with suitable molecular

weight should give dry thin samples [42]. As in thinner samples, a diminished amount of light would be absorbed before it reaches the back plane of the sample, and thus the amount of light absorbed throughout the sample thickness would be more uniform during recording [42].

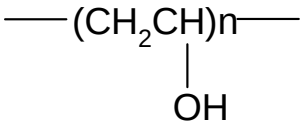

Fig.1.7 Chemical structure of Poly viny lalcohol

1.5 Photopolymerization process

(A) Photophysical process

As described in the previous section, a photopolymer contains several components in different roles giving rise to a suitable recording medium. Now, we present the step wise photo-physical and photo-chemical process taking place when such a multi-component system undergoes photo-excitation during recording process [2].

When the dye molecule D, is exposed to light of suitable wavelength, it absorbs a photon and is promoted into a singlet excited state $^1D^*$

$$D + h\nu \rightarrow {}^1D^* \qquad (10)$$

This singlet excited state dye $^1D^*$ can return to the ground state by radiationless transfer to another molecule such as the electron donor, ED. This process is known as Fluorescence quenching

$$^1D^* + ED \rightarrow D + ED^* \qquad (11)$$

It can also revert back to the ground state, D by emission of a photon, by a process called fluorescence

$$^{1}D^{*} \rightarrow D + h\nu \qquad (12)$$

The singlet state can also undergo inter-system crossing into more stable and longer lived triplet excited state

$$^{3}D^{*} \rightarrow {}^{3}D \qquad (13)$$

This triplet dye molecule can return to the ground state by radiationless transfer or by the delayed emission of a photon.

At high dye concentration it can be deactivated by collision with another dye molecule

$$3D^{*} + D \rightarrow 2D \qquad (14)$$

The dye molecule can also undergo a reaction whereby it abstracts two hydrogens from the ED to form the transparent (leuco) form of the dye. The actual production of free radicals takes place when the triplet state dye reacts with the electron donor [4].

The electron donor used in this thesis is triethanolamine (HOCH2CH2)3N. The triethanolamine (TEA) donates an electron to the excited triplet state of the dye leaving the dye with one unpaired electron and an overall negative charge [4]:

$$^{3}D^{*} + (HOCH_2CH_2)_3N: \rightarrow D^{\cdot -} + (HOCH_2CH_2)_3N^{\cdot +} \qquad (15)$$

The TEA radical cation then loses a proton and becomes a free radical:

$$(HOCH_2CH_2)_3N^{\cdot +} \rightarrow (HOCH_2CH_2)_2\,NCH{\cdot}CH_2OH + H^{+} \qquad (16)$$

When the acrylamide monomer is present the free radical can undergo two different reactions. The first possible reaction is the initiation of the acrylamide (AA) polymerisation [4].

$$TEA^{\cdot +} \rightarrow TEA + AA^{\cdot} \qquad (17)$$

The second reaction the radical can undergo is dye bleaching. This occurs when the dye radical formed in eq. (17) abstracts hydrogen from the TEA free radical. An unstable TEA intermediate and the transparent dihydro dye are formed by this reaction [4]

$$(HOCH_2CH_2)_3NCH{\cdot}CH_2OH + H^+ + D^{\cdot -} \rightarrow (HOCH_2CH_2)_2NCH{=}CHOH + H_2D \qquad (18)$$

The unstable intermediate then rearranges to form a more stable intermediate

$$(HOCH_2CH_2)_3NCH{=}CHOH + H^+ \rightarrow (HOCH_2CH_2)_2NCH_2CHO \qquad (19)$$

Dye bleaching is an important process because it allows a hologram to be fixed after recording. By bleaching any remaining dye no extra free radicals can be formed. This means that no unwanted polymerisation occurs after holographic recording. It also makes the final hologram transparent. Figure 1.8 summarises the various mechanisms which can occur under photo-excitation.

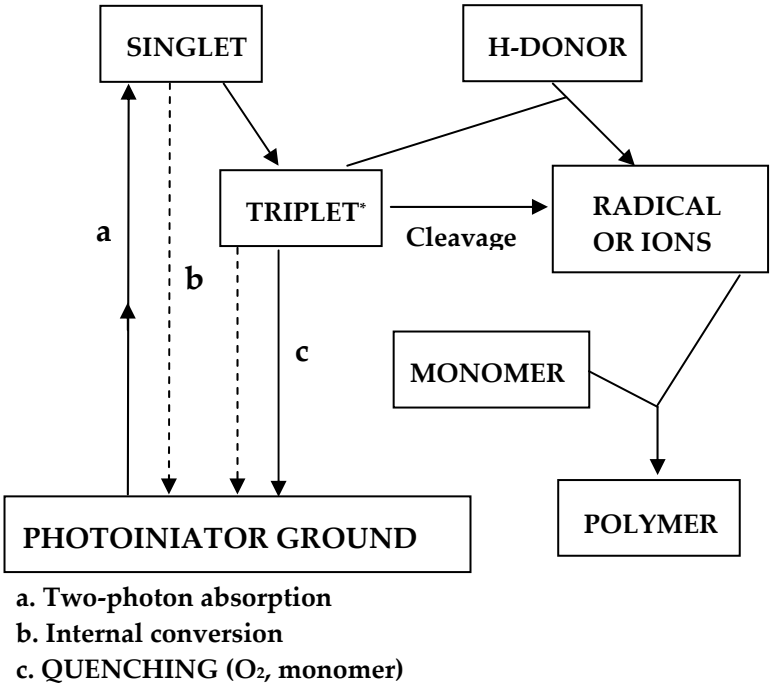

Fig. 1.8 Mechanism of photopolymerization.

(B) Photochemical process

The free radicals initiate the polymerization of AA/BSA which forms a polyacrylamide network. This process occurs via a mechanism known as free radical polymerisation. Free radical polymerization consists of three separate steps: initiation, propagation and termination [4].

The initiation:

Initiation takes place when the free radical initiator attaches to the monomer by addition across the C-C double bond. Figure 1.9 shows such chemical reaction taking place [4].

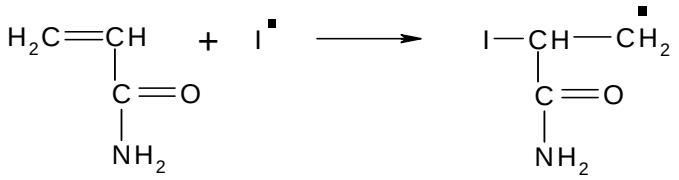

Fig. 1.9 Addition across the carbon-carbon double bond.

While bond formation, in order to attach itself to the monomer, the free radical uses its own unpaired electron and a π electron from C-C bond. This leaves one of the carbons with an unpaired electron therefore the monomer becomes free radical.

The propagation:

Propagation occurs when the new radical attaches itself to another monomer by addition across the double bond by the same method as above. The second monomer now becomes a radical and in this way a polymer grows. Figure 1.10 shows such reaction taking place [4].

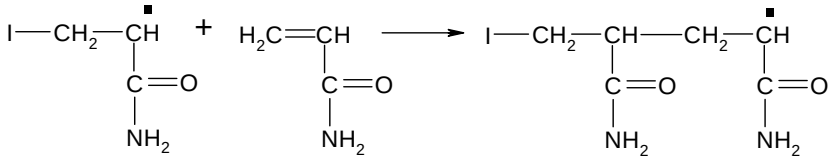

Fig.1.10 The propagation step.

Termination:

After initiation and propagation, the newly formed chain will continue to grow until it is stopped by a termination reaction. This process can arise by two reactions known

as disproportonation or combination [4]. Disproportonation takes place when a hydrogen is abstracted from one propagating chain by another. The hydrogen reacts with the free radical and the original double bond is reformed. This process results in two separate chains as illustrated in the figure 1.11:

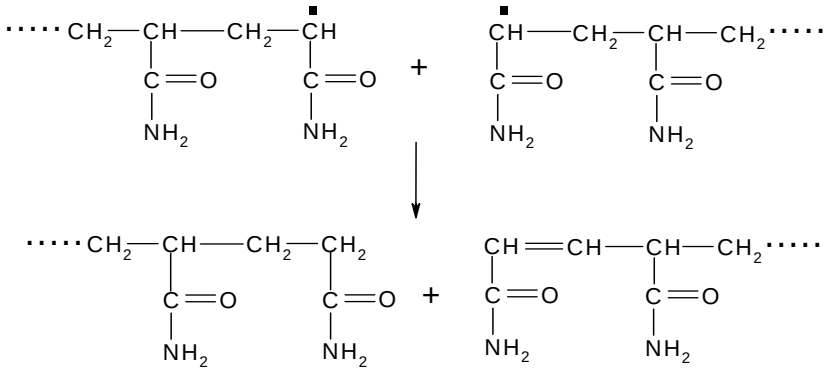

Fig.1.11 Two separate chains formed.

The second method of termination is combination, this consist when the radicals at the ends of two propagating react forming one long chain (fig. 1.12) [4]

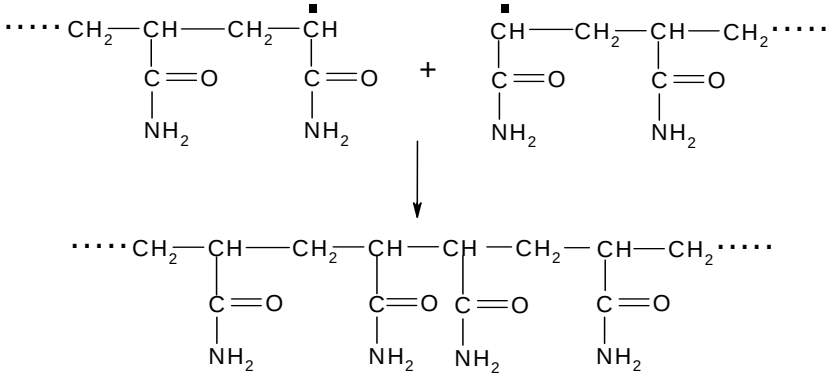

Fig.1.12 Two propagating chains react forming one long chain.

On polymerization each carbon double bond is converted into a carbon single bond lowering the molar refractivity from approximately 4.16 cm^3 to 2.15 cm^3. This lowers the refractive index of the medium, besides an increase of the density occurs which leads to an increase in the refractive index. The combination of these two processes results in a higher refractive index in polymerised regions compared to non-polymerised regions so that a refractive index modulation exists between exposed and unexposed areas [4]. Figure 1.13 emphasizes the whole process taking place towards photopolymerization leading to refractive index modulation caused by monomer diffusion from the dark areas to the bright areas [44].

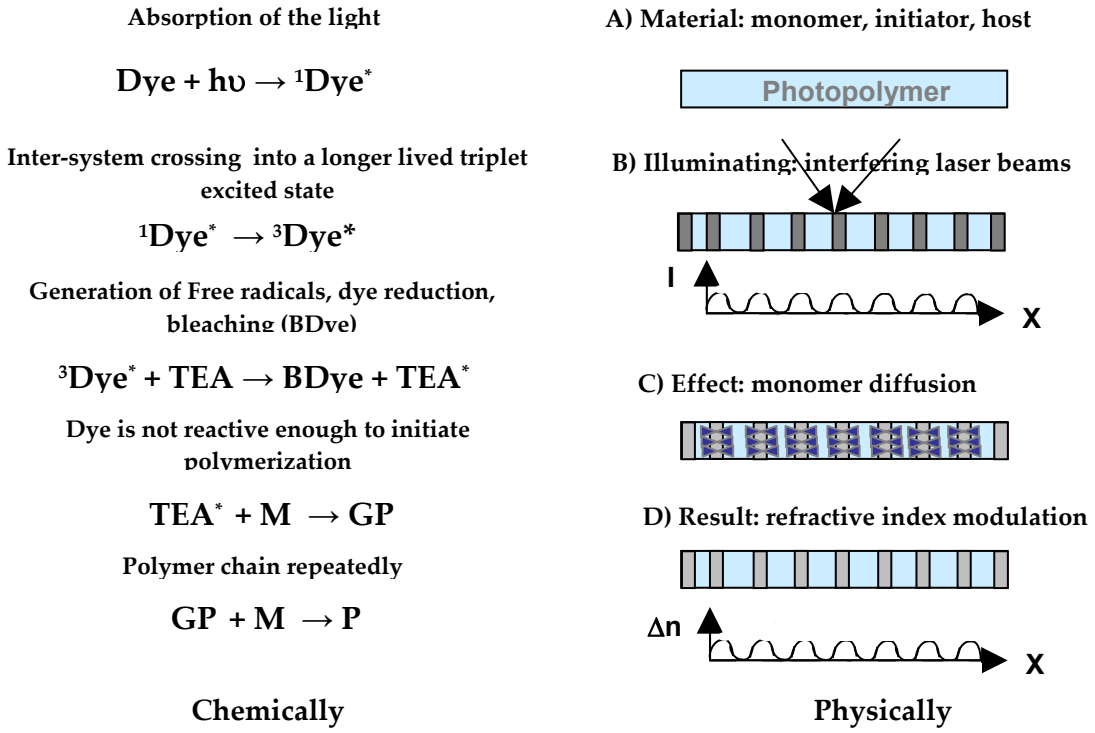

Fig. 1.13 Process of photopolymerization.

1.6 Monomer Diffusion

As discussed in the previous section, monomer diffusion is an important process which leads to the refractive index modulation through polymerization of brightly illuminated portion of the photopolymer films. This also leads to a change in localized density of the recording film. A density increase in these essentially incompressible materials must occur by mass transport [45]. During exposure contiguous volume elements, undergoing relatively slow and relatively fast polymerization, are established in the recording material by the spatial variation of light intensity in the holographic interference pattern [45]. Density increase in the rapidly polymerization volume elements require material influx from the surrounding volumes. Spatial variations in polymerization rates produce monomer concentration gradients that also drive monomer diffusion [6]. These two effects combine to produce spatial segregation of the various components of the photopolymer system. If the components have different refractive indices their spatial segregation will make a significant contribution to the required refractive index modulation.

During exposure monomer diffuses into bright regions as a result of the concentration gradient induced by the depletion of these compounds. This will create a difference in the density (as well in the refractive index) between bright and dark regions. Figure 1.10 illustrates the principles of the diffusion model that is able to depict the interaction among free-monomer diffusion, photopolymerization, and

grating formation during holographic exposure. In the figure 1.14, two coherent waves of intensities I_1 and I_2 interfere in the material, creating an illumination pattern as [45]:

$$I_{(x)} = I_o\left[1 + m\cos(K_g x\right] \qquad (20)$$

in which Kg is the grating wave number, $I_0 = I_1 + I_2$ is the average recording intensity, and m is the beam intensity modulation:

$$m = \frac{2\sqrt{I_1 I_2}}{I_o} \leq 1 \qquad (21)$$

The concentration of free monomers in the material is initially spatially uniform. The interference pattern initiates the polymerization of these free monomers. In the proximity of the bright fringes this photopolymerization is more intense, causing the concentration of created polymeric molecules to be higher [45]. At the same time, the consumption of free monomers owing to this photopolymerization results in a free monomer concentration [M](x,t) that also varies in time and space (Fig. 1.14).

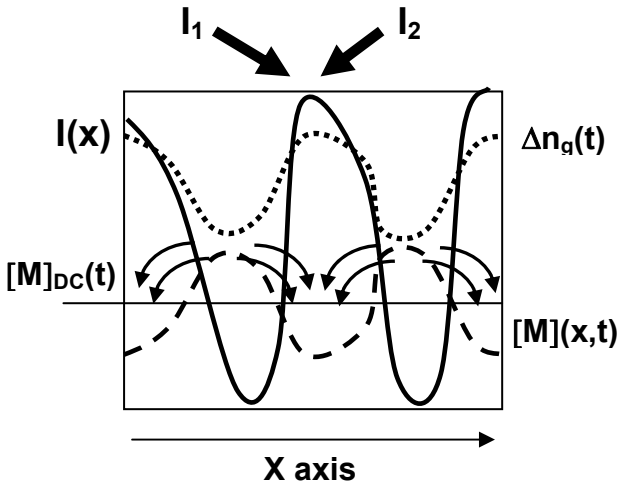

Fig. 1.14 Model of the interaction between monomer diffusion and grating formation during holographic exposure in photopolymers. $I(x)$ (solid curve) is the recording intensity. [M](x, t), indicated by the dashed curve, is

the free-monomer concentration, with a dc term $[M]_{DC}(t)$ (solid line) and $[M]_1(t)$ as its modulation term (not shown). Because the monomer consumption is higher along the illumination peaks, the free-monomer concentration is 180° out of phase with the refractive-index modulation $\Delta n_g(t)$ (dotted curve) caused by free-monomer photopolymerization. Free-monomer diffusion tends to cancel the free-monomer concentration gradient.

Because their consumption is more rapid where the intensity peaks are located, we assume and approximate the spatial concentration of the free monomers as sinusoidal with a phase shift of 180° relative to the intensity pattern [45], which gives

$$[M](x,t) = [M]_{DC}(t) - [M]_1(t)\cos(K_g x) \qquad (22)$$

where $[M]_1(t)$ is the amplitude of the harmonic term of the free-monomer concentration and $[M]_{DC}(t)$ indicates the dc term of the free-monomer concentration (Fig. 1.14). At the same time, free-monomer diffusion tends to level out this free-monomer gradient, moving free monomers from the dark regions, where polymerization is less effective [local minima of $I(x)$ and local maxima of $[M]$ (x, t), to the bright regions [local maxima of $I(x)$ and local maxima of the refractive index], where the free-monomer depletion is more intense (curved arrows in Fig. 1.10). The resultant variation in material density (owing to Photopolymerization and monomer diffusion) causes a spatial variation in the index of refraction [45].

1.7 Holographic recording

There are various possible ways to record information through formation of holographic slant gratings in a photopolymer film [3]. The laser interferometry is

commonly used set-up for holographic recording. Principally, an object beam and a reference beam are superimposed on the recording material where interference fringes create dark and bright zones. This can be done in two different ways; when both the object and the reference beam intersect the recording film from the same side or they are made to approach the recording film from the opposite side [3]. Figure 1.15 shows the possible way of information storage using either of the geometries. When the recording experiments use the set-up where object and reference beam traverse the sample from the same side volume transmission gratings are formed. In the other case when these two beams traverse the recording film by opposite direction, reflection gratings are recorded.

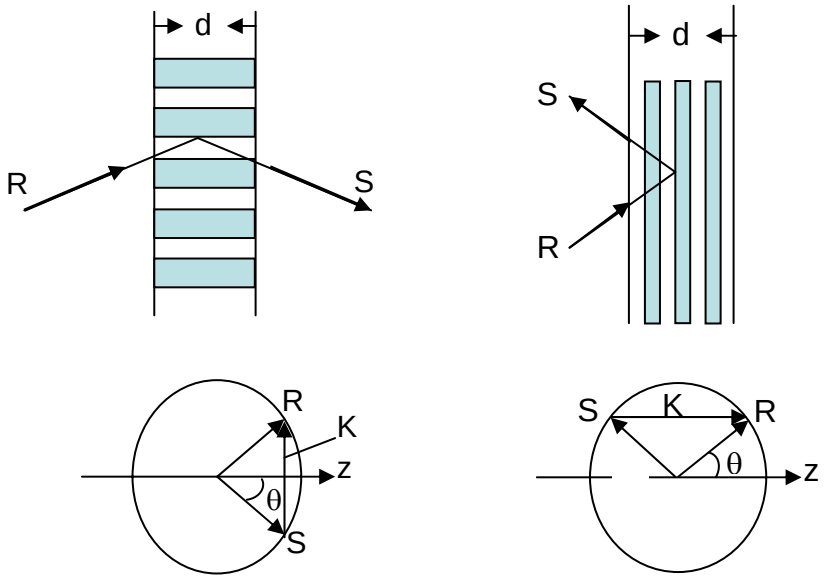

Fig. 1.15 Recording of volume phase gratings in photopolymer layers using transmission geometry; both the reference (R) and the object beam intersect the sensitive layer from the same side, and in reflection geometry; the object and the reference beam intersect the sensitive layer from the opposite sides.

1.8 Kogelnik's two-wave coupled wave theory

When analysing the diffraction efficiency of light by formation of such volume gratings, it is necessary to take into account the fact that the amplitude of the diffracted wave increases progressively, while that of the incident wave decreases, as they propagate through the grating [4] . This is explained through the coupled wave approach of Kogelnik [46].

This theory considers the efficiency with which thick holograms can diffract incident light and the angular and wavelength dependence of this diffraction efficiency as the incident light deviates from the Bragg condition. It yields an equation, which may be used to relate the diffraction efficiency,η of the grating to a number of grating parameters [46]. For lossless unslanted transmission geometry grating, replayed on-Bragg angle with TE polarised light, it can be shown that η can be expressed as

$$\eta = \frac{I_D}{I_{IN}} = \sin^2 \frac{d\,\pi\, n_1}{\lambda \cos\theta} \qquad (23)$$

I_D is the intensity of the diffracted beam; I_{In} is the input intensity, d, represents grating thickness, θ_B and λ are the Bragg angle and wavelength of incidence inside the grating. In the case of photopolymer, n_1 the refractive index modulation of the perfect sinusoidal grating is assumed linearly proportional to the first harmonic of the recorded polymer spatial distribution [46]. Increasing exposure increases this modulation up to some saturation value. Changing the composition of the material varies its ability to capture the exposing pattern.

References

[1]. Science & Vie. 102-105. April 2006.

[2]. P. Hariharan, *Optical holography – Principles, Techniques and Applications*, 2 nd ed. (Cambridge University Press, Cambridge, UK). (1996).

[3]. H.J. Caufield, *Handbook of optical holography*, (1979).

[4]. J.R. Lawrence, F.T. O'Neill and J.T. Sheridan. "Photopolymer holographic recording material". Optic 112. No. 10 449-463, (2001).

[5]. G. Saxby. *Practical holography*. Third edition. Institute of physics publishing Bristol and Philadelphia. Oip Publishing Ltd, 2004.

[6]. F. del Monte, O. Martinez, J. A. Rodrigo, M.L. Calvo and P. Cheben, "A volume holographic sol-gel material with large enhancement of dynamic range by incorporation of high refractive index species. Adv. Mat. 18, 2014-2017, (2006).

[7]. H. Sherif, I. Naydenova, S. Martin, C. McGinn and V. Toal, "Characterization of an acrylamide-based photopolymer for data storage utilizing holographic angular multiplexing", J. Opt. A: Pure Appl. Opt. **7**, 255-260 (2005).

[8]. C. Sanchez, M.J. Escuti, C Van Heesch, C. W.M. Bastiaansen, D. J. Broer, J. loos and R. Nussbaumer, "TiO_2 nanoparticle-Photopolymer composites for volume holographic Recording", Adv.Funct. Mater **15**, 1623-1629 (2005).

[9]. J. V. Kelly, M. R. Gleeson, C. E. Close, F. T. O'Neill and J.T. Sheridan, "Temporal response and first order volume changes during grating formation in photopolymer", J. Appl. Phys. 99, 113105-1-7, (2006).

[10]. S. Blaya, L. Carretero, R. Mallavia, A. Fimia, R.F. Madrigal, M. Ulibarrena and D. Levy, "Optimization of an acrylamide-based dry film used for holographic recording", Appl. Opt. 37, No. 32, 7604-7609, (1998).

[11]. - J. Ashely, M.-P. Bernal, G.W. Burr, H. Coufal, H. Guenther, J.A. Hoffnagle, C.M. Jefferson, B. Marcus, R.M. Macfarlane, R.M. Shelby and G.T. Sincerbox. Holographic data storage. IBM J. Res. Develop. 44. No.3. 341-368, (2000).

[12]. S. C. Burden, J. A. Arns and W. S. Colburn, “Volume-phase holographic gratings and their potential for astronomical applications”, for SPIE use.

[13]. L. Shour-Jun, L. Guo-Dong, H Q-Shen, W. Min-Xian, J. Guo-Fan, S. Meng-Quan, W. Taro and W. Fei-Peng, “Holographic grating formation in dry photopolymer film with shrinkage”, Chin. Phys. 13, No. 9, 1428-1431, (2004).

[14]. J. T. Gallo and C.M. Veber, “Model for the effects of material shrinkage on volume holograms”, Appl. Opt. 33, No. 29, 6797-6804, (1994).

[15]. J. Qi, M. DeSarkar, G.T. Warren, and G.P. Crawford, “In situ shrinkage measurement of holographic polymer dispersed liquid crystals”, J. Appl. Phys. 91, No. 8, 4795-4800, (2002)

[16]. S. Wu and E. Glytsis, “Characteristics of DuPont photopolymers for slanted holographic grating formations” J. Opt. Soc. Am. B. 21, No. 10, 1722- 1731(2004).

[17] DH. Close et al, “Hologram recording on photopolymer materials”, Appl. Phys. Lett. 14, 159-160, (1969).

[18] JA. Jenney, “Holographic recording in photopolymers”, J. Opt. Soc. Am. 6à, 1155-1161, (1970).

[19] JA. Jenney, “Nonlinearities of photopolymer holographic recording materials”, Appl. Opt. 11, 1371-1381, (1970).

[20] S. Sugawara, K. Murase, T. Kitayama, “Holographic recording by dye-sensitized photopolymerization of acrylamide”, Appl. Opt. 14, 378-382, (1975).

[21] N. Sadlej and B. Smolinska, “Stable photo-sensitive polymer layers for holography”, Opt. Laser Technol, 175-179, August 1975.

[22] MJ. Jeudy and JJ. Robillard, “Spectral photosensitization of a variable index material for recording phase holograms with high efficiency”, opt. Commum. 13, 25-28, (1975).

[23] S. Calixto, “Dry polmer for holographic recording”, Appl. Opt. 26, 3904-3909, (1987).

[24] A. Fimia, N. Lopez and F. Mateos, “Acrylamide photopolymers for use in real time holography: improving energetic sensitivity”, Proc. SPIE 1732, 105-109, (1992).

[25] A. Fimia et al, "Elimination of oxygen inhibition in photopolymer systems used as holographic recording materials", J. Mod. Opt. 40, 699-706, (1993).

[26] S. Martin, P. Leclere, Y. Benotte, V. Toal and Y. Lion, "Characterisation of an acrylamide-based dry photopolymer holographic recording material", Opt. Eng. 33, 3942-3946, (1994).

[27] V. Weiss, E. Millul and A. Friesen, "Photopolymeric holographic recording media: in-situ and real-time characterisation", Proc. SPIE. 2688, 11-21, (1996).

[28] S. Blaya et al., "Highly sensitive photopolymerisable dry film for use in real time holography", Appl. Phys. Lett. 75, 1628-1630, (1998).

[29] F. Zhao, E. Frietmann and X. Li, "Novel type of red sensitive photopolymer system for optical storage", Proc. SPIE. 3468, 317-321, (1998).

[30] C. Neipp, A. Beléndez, S. Gallego, M. Ortuño, I. Pascual and J.T. Sheridan, "Angular responses of the first and second diffracted orders in transmisión diffraction effciciency grating recorded on photopolymer material", Opt. Expr., Vol. 11, No. 16, 1835-1843, (2003).

[31] W. S. Kim, H-S. Chang, Y-C. Jeong, Y-M. Lee, J-K. Park, C-W. Shin, N-Kim and H-J. Tak, "A new phase-stable photopolymer with high diffraction efficiency based on modified PMMA", Optics Commu. 249, 65–71, (2005)

[32] Y-Ch. Jeong, S. Lee, and J-K Park, "Holographic diffraction gratings with enhanced sensitivity based on epoxy-resin photopolymers", Opt. Expr. Vol. 15, No. 4, 1497-1504, (2007).

[33] R. Jallapuram, I. Naydenova, S.Martin, R. Howard, V. Toal, S. Frohmann, S. Orlic, H. J. Eichler, "Acrylamide-based photopolymer for microholographic data storage", Opt.l Mater. 28, 1329–1333, (2006.)

[34]. K. H. Dietz, "Dry film photoresist components and their function (Part A). Tech talk. Fine line in highfield (P. 1-2). (2003).

[35]. S. Blaya, L. Carretero, R.F. Madrigal, A. Fimia, "Optimization of a photopolymerizable holographic recording material on polyvinylalcohol using angular responses", Opt. Mat. 23, 529-538, (2003).

[36]. H. Coufal. and G. Sincerbox. *Holographic Data Storage*. Springer Series in optical sciences. (2003).

[37]. S. Gallego, M. Ortuño, C. Neipp, C. Garcia, A. Beléndez and I. Pascual, "Temporal evolution of angular response of a holographic diffraction grating in PVA/Acrylamide photopolymer", Opt. Express. 11, No. 2, 181-190, (2003).

[38]. C. García, I. Pascual, A. Fimia, "Diffraction efficiency and signal-to-noise ratio of diffuse-object holograms in real time in polyvinyl alcohol photopolymers," Appl. Opt. **38**, 5548-5551 (1999)

[39]. L. Carretero, S. Blaya, and A. Fimia, "Acrylamide-N,N'methylenebisacryamide silica glass holographic recording material", Opt. Express, 12, No.8, 1780-1787, (2004).

[40]. S. Gallego, M. Ortuño, A. Márquez, C. Neipp, C. García, A. Beléndez, I. Pascual, "Formación de un holograma en un fotopolímero basado en PVA/Acrilamida Hologram formation in PVA/Acrylamide based photopolymer", Óptica pura y aplicada. 37, 61-66, (2004).

[41]. H. Yao, M. Huang, Z. Chen, L. Hu and F. Gan, "Optimization of two-monomer-based photopolymer used for holographic recording". Mat. Lett. 56, 3–8. (2002).

[42]. M. Ortuño, S. Gallego, C. García, C. Neipp, A. Belendez and I. Pascual, "Optimization of a 1 mm thick PVA/acrylamide recording material to obtain holographic memories: method of preparation and holographic properties". Appl. Phys. B. 76, 851-857. (2003).

[43]. R.T. Ingwall and D. Waldman, Holographic data storage. (Eds: H.J Coufal, D. Psaltis, G.T. Sincerbox). Springer, Berlin, (2000).

[44]. Zilker, S. "Holographic Data Storage-The Materials Challenge". ChemPhysChem. 3, 333–334. (2002).

[45]. S. Piazzolla and B. K. Jenkins, "First-Harmonic diffusion model for holographic grating formation in photopolymers", J. Opt. Soc. Am. B. 17, No. 7, 1147-1157, (2000).

[46]. H. Kogelnik, Bell Syst. Tech. J. **48**, 2909 (1969).

2

Chapter 2
Acrylamide based photopolymers for red region volume holographic recording

2.1. Introduction

Photopolymers are promising candidate for data storage as large amount of data can be stored through formation of volume holographic gratings with large sensitivity and at low cost without any post processing treatment. As described in the previous chapter, a photosensitizer is a crucial component of photopolymer system where it has an important role to start the polymerization process under illumination. Therefore it is an elemental factor responsible for generation of the radicals by photoreduction. Besides it will determine the zone of absorption therefore the wavelength to be used for recording and reading the grating [1].

In present chapter, we study acrylamide based photopolymer system with red photosensitizing dye methylene blue. This previously studied photopolymer is used for optimization of all the active components of our photopolymer system.

2.2 Preparation of photopolymer films

Photopolymers were prepared by combining methylene blue photosensitizer as radical generator (Aldrich) at different proportions. Acrylamide (Aldrich) was used as monomer, N,N'-methylenebisacrylamide (Fluka) was employed as cross-linking monomer, triethanolamine (Aldrich) used as initiator and all dissolved in a poly(vinyl alcohol) (Aldrich) solution at 10% w/v (80% hydrolyzed. Mol. Wt. 9000-10000). All the reagents were used without further purification. In the case of monomers, both were used in most of the experiments without further purification. In order to study the effect of purification, these monomers were purified by recrystallization in order to compare to the experiments using them just as we received. Thick photoactive layers were prepared in dark to avoid polymerization of acrylamide by drop casting the final solution on pre cleaned glass plates (2 x 2.5 cm) which were then left to dry for 2 days. The average film thickness measured using a DEKTAK 6M profilometer was 34 μm. Several Solutions were prepared with fixed concentration of Methylene Blue in order to achieve absorbance of around 0.2. A further increase in absorbance value of the sensitizing dye may result in over sensitivity induced intensity modulation inside the recording medium.

Table 2.1 illustrates a short description and the role of the present photo polymeric system and its components used in our studies.

Material	Function	Description
Polyvinyl alcohol	Binder	Allows to obtain dry photopolymer layers.
Triethanolamine	Initiator (electron donor)	Produces electron transfer reactions with the dye. Reduces layer surface precipitation
Acrylamide	Monomer	High reaction rate, High solubility in water.
N,N′-methylenebisacrylamide or N,N′-dimethylacrylamide	Cross-linking monomer	Cross-linking agent. Improves recorded grating life.
Methylene Blue	Dye	Determines absorption range for record wavelength.

Fig. 2.1 shows the chemical structure of the photosensitizer: methylene blue. We measured the spectral response of this material by recording its absorption spectra in water solution at different concentration as well as mix in pre-polymer film.

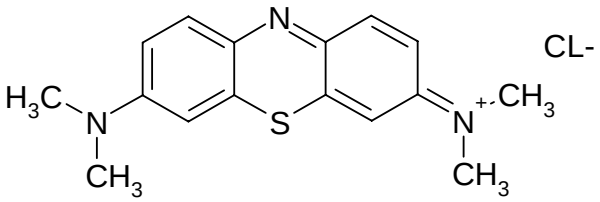

Fig. 2.1 Chemical structure of Methylene Blue.

The spectral evolution of methylene blue in water solution at different concentration was measured. We observed two bands of absorption in the spectra for each

concentration, the main band of absorption was found at 661 nm and the other at 610 nm, this band is believed to be related to the formation of dimeric forms (these forms are involved in a polymerization termination reaction, producing a decrease in the overall rate of polymerization) [2]. We detect that by increasing the concentration of MB (see fig. 2.2a) the absorbance of second peak (610 nm) started to augment until it has almost the same absorbance as the main absorption peak. For the case of higher concentration, as is shown in fig 2.2b, the absorbance of both bands has almost the same absorbance value but further increase in the concentration reveals that the side band becomes higher than the main band showing the formation of dimers.

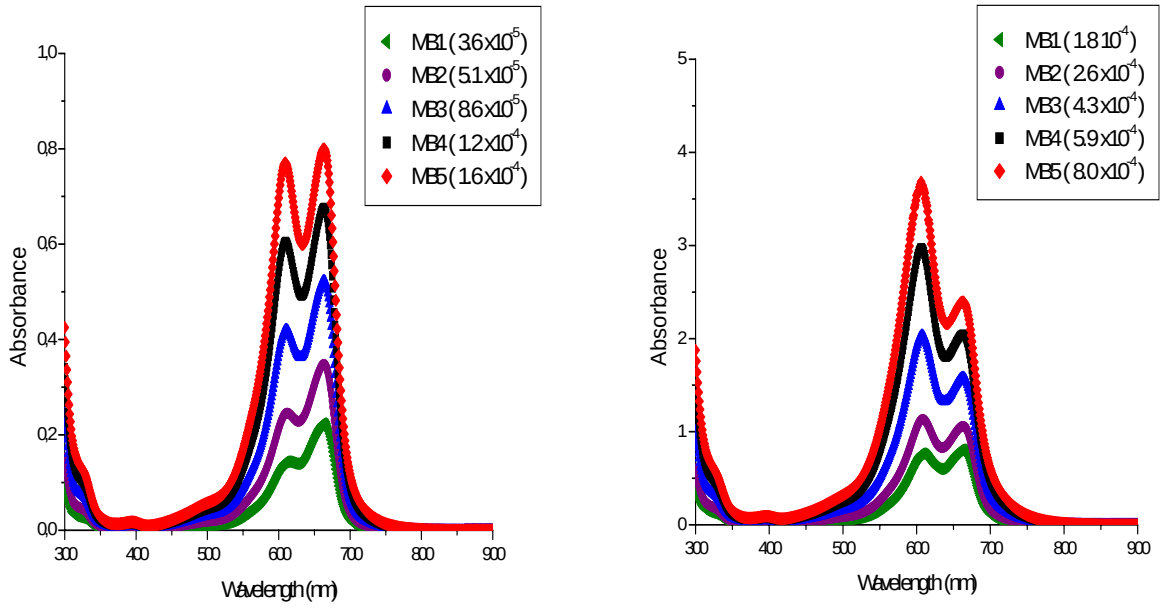

(a) Concentration in 2.5 ml. (b) Concentration in 25 ml.

Fig. 2.2 UV/Vis spectra measured in 2.5 ml and 25 ml of MB1-MB5.

We checked the individual absorption influence of other components over the MB before the final recording. Figure 2.3 shows the fairly nominal response of AA monomer and TEA initiator over the wide spectral regions. We found that the PVA and BSA are totally transparent as well in the region of writing and reading wavelengths.

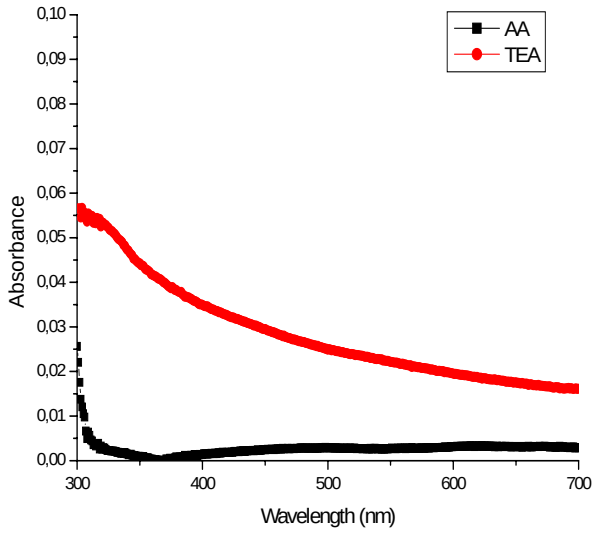

Fig. 2.3 UV/Vis spectra of monomer (AA) and initiator (TEA)

2.2.1 Optimization of the photosensitizer

As we mentioned above, radicals are generated by a photoreduction reaction of the dye. An increase of the dye concentration up to certain limit can improve the performance of the recording material due to the high absorption of the light can be produced before the light traverse all the material. In table 2.2, the composition of the photopolymer using methylene blue is presented. The concentration of MB was tuned to obtain the maximum diffraction efficiency while keeping the AA, BSA and

TEA concentration constant. This helps us to understand the effect of the sensitizing dye in the photopolymer recording medium.

Table 2.2 Composition of the photopolymers.

MB photopolymer	[MB] (M)	[Acrylamide] (M)	[BSA] (M)	[TEA] (M)
1	3.6×10^{-5}	0.452	0.052	0.605
2	5.15×10^{-5}	0.452	0.052	0.605
3	8.16×10^{-5}	0.452	0.052	0.605
4	1.20×10^{-4}	0.452	0.052	0.605
5	1.61×10^{-4}	0.452	0.052	0.605

Fig. 2.4. shows the UV-Vis spectra, before recording, of the photopolymer layers using methylene blue as photosensitizer. We can observe an expected increase in the absorption for photopolymer films as the concentration of MB increases. Photopolymer layers with MB3-5 shows higher absorption compared to the rest of the materials. This shows that a moderate increase in the concentration of MB can lead to obtain higher photo sensitivities at recording wavelength.

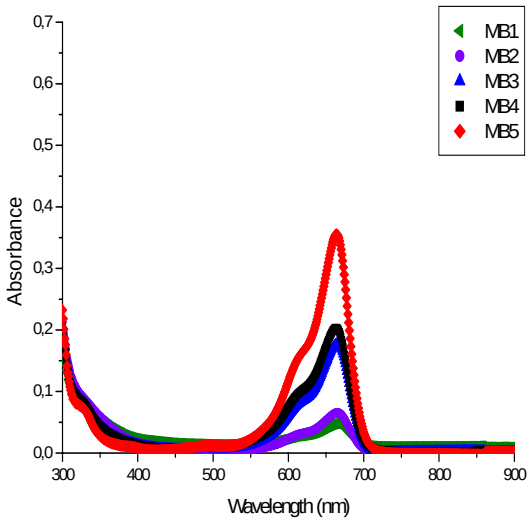

Fig. 2.4 UV-Vis spectra of MB1-5 films with a thickness of 34 μm.

2.3 Holographic recording : Experimental set-up

The recording of holographic gratings in methylene blue sensitized photopolymer was performed in transmission interference geometry. The set-up used for transmission geometry recording is described in Fig 2.5. Here, for transmission phase grating formation, two mutually coherent writing beams from a He-Ne laser at 632.8 nm were used as recording wavelength. Both the recording and reference beams interfere the sample from the same side giving particular fringe spacing. A low intensity (2.1 mW/cm^2) frequency doubled Nd:YAG laser beam (532 nm) placed at Bragg angle was used to read-out the evolution of the gratings in real time as the photosensitizer is insensible in this wavelength, this avoids unwanted polymerization after recording.

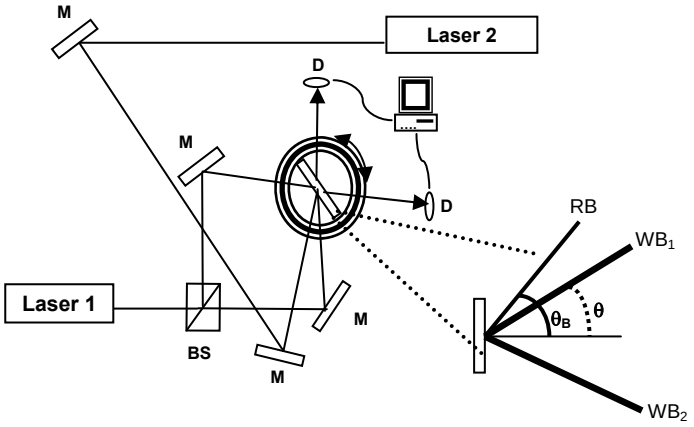

Fig. 2.5 Experimental Set up used for recording holographic gratings in transmission geometry. Laser 1 and 2 used for writing (He-Ne) and reading (frequency doubled Nd:YAG) the gratings respectively. M: Mirrors, BS: Beams splitter, D: detectors. Close-up of beams approaching the photopolymer film; RB: reading beam, $WB_{1\text{-}2}$: writing beams, θ is half angle between the two beams and θ_B is the Bragg's angle.

The diffraction efficiency is of the phase gratings created in the bulk of the recording medium as because of selective polymerization is one important measure of the quality of the recording medium. Neglecting the loss mechanisms such as absorption and scattering at the surface of the recording layer, ideally, an diffraction efficiency of 100% is desired from a photopolymer recording medium, which can be experimentally measured by following relation $\eta = \frac{I_D}{I_D + I_T}$ (1)

where I_D and I_T are diffracted and transmitted intensities.

2.4 Experimental results.

Fig. 2.6, shows the evolution of diffraction efficiency as a function of exposure time for photopolymer MB3-5 at maximum intensity of 166 mW/cm^2. As we can observe in fig; 2.6, all photopolymers show the same trend of evolution, the diffraction efficiency increases and saturates during recording time. No initial delay in the diffraction efficiency growth was observed.

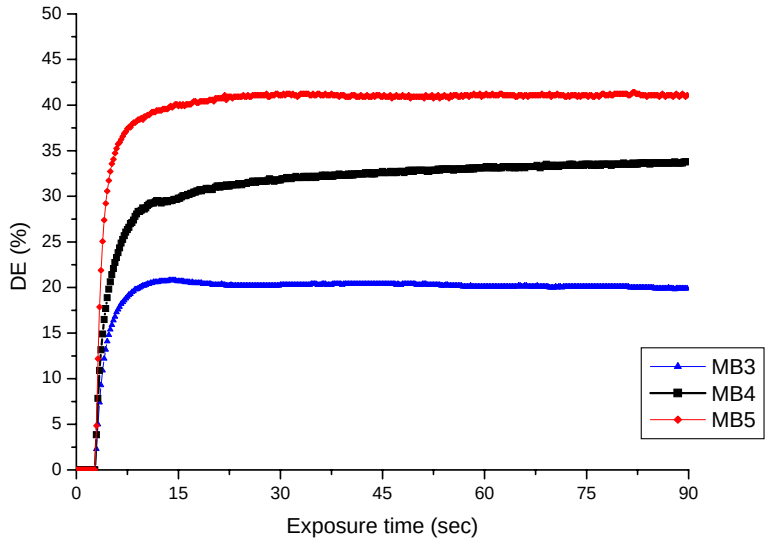

Fig. 2.6 Diffraction efficiency as a function of Methylene Blue concentration.

The maximum diffraction efficiency achieved was 40% using the highest concentration of methylene blue of 1.61x10^{-4} M. For the measurements of red holographic gratings (HG) in the transmission geometry, we use the angle between the beams using the set up described in Fig. 2.6.

The pitch of the grating was calculated using the relation described in chapter 1 [3];

$$\Lambda = \frac{\lambda}{2 \sin \theta} \qquad (2)$$

where λ is recording wavelength (633 nm) and θ is the half-angle (34^{o})between the recording beams inside the material. The grating period; Λ of the MB sensitized photopolymer is about 0.565 μm. This also gives the Bragg angle for reconstruction of the stored information at reading wavelength. In our case the reading beam is 532 nm where MB doesn't show significant absorption. Hence at 532 nm the Bragg angle θ_B is 28°.

Once the diffraction efficiency is measured, the refractive index modulation can be calculated using the Kogelnik's coupled wave theory as illustrated in eq. 3 used for the diffraction efficiency under Bragg condition [4].

$$\eta = \sin^2\left(\frac{\pi \Delta n d}{\lambda \cos\theta}\right) \qquad (3)$$

where λ is the wavelength of reconstruction beam, θ is the reconstruction angle, d is the sample thickness and η is the diffraction efficiency.

The calculated refractive index modulation Δn in the RB sensitized photopolymer, using the above formula, is 2 × 10^{-3}. The spatial frequency of such transmission gratings is calculated using the relation; SF= 1/Λ, where Λ is the grating period. Hence for a grating period of 0.565 μm, we get a spatial frequency of 1767 lines/mm in our present photopolymer system. This further confirms the formation of volume

gratings and demonstrates the potential capability of this recording medium for high density storage.

The Sensitivity [3] of the MB sensitized material is calculated following the relation:

$$Sensitivity\,(S) = \frac{\sqrt{\eta}}{I\,t\,d} \quad \text{(cm/J)} \qquad (4)$$

where η is the diffraction efficiency, I is the incident intensity in mW/cm^2, t is the exposure time and d is the thickness of the material. For the equally thick films (34 μm) and at constant intensity and exposure time (fig 2.6), we do see the difference in the sensitivity of the MB3-5 recording medium. This is primarily because of the high diffraction efficiency from the higher concentration of the MB in the recording layers. Hence an optimum concentration of the sensitizing dye is an important factor for the development of any photopolymer system.

In table 2.3 the detailed parameters from the diffraction efficiencies for the three photopolymers (MB3-5) after 2.5 sec of exposure are presented. In the case of MB1-2 the diffraction efficiencies were not shown due to their negligible values, this can be explained due to the low concentration of methylene blue to start the polymerization.

Table 2.3 Transmission grating parameters of photopolymer MB3-5.

MB photopolymer	**DE (%)**	**Sensitivity (cm/J)**	**RIM**	**Thickness (μm)**
3	15.4	270	1.72×10^{-3}	35
4	20.6	312	2×10^{-3}	35
5	32.7	394	2.59×10^{-3}	35

The rise in the concentration leads to an increase in the diffraction efficiency. This raise in the efficiency represents higher sensitivities and refraction index modulation as well. As we can see in table 2.3 the sensitivities increased as high as 394 cm/J for the MB5 photopolymer. As well this favoured the increase of the refractive index modulation by increasing the concentration from $1.72x10^{-3}$ to $2.59x10^{-3}$ for the case of MB3 and MB5, for the lower and higher concentration respectively.

2.4.1 Angular Selectivity

Angular responses of the stored diffraction gratings were performed by mounting the recorded samples on a computer-controlled rotary stage with a resolution of 0.1°. From the angular responses, the effect of methylene blue concentration can be obtained. Fig. 2.7 corresponds to the angular selectivity curves obtained immediately after exposure is presented for photopolymer MB3-5 using different concentrations. In all the cases practically moderate symmetrical responses with reference to the zero order diffracted beam are shown. It was noticed that the FWHM increased by increasing the concentration [5] of the dye achieving a 0.41° and 0.59° for MB3 and MB5 respectively. It is important to mention that the first diffracted order besides the zero order is clearly observable. As the Bragg angle was detuned, the diffraction efficiency in all cases diminished, but it did not get to zero before it grew again [6]. The appearance of only the first diffracted order (apart from the zero one) indicates the formation of thick holograms.

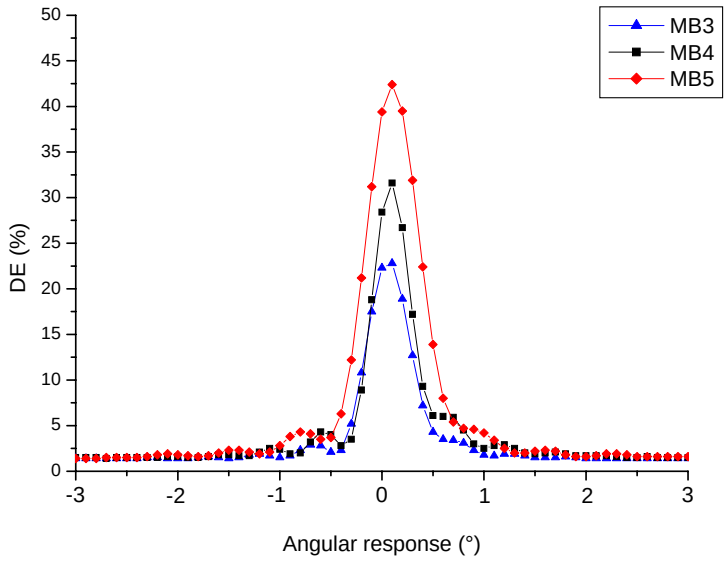

Fig. 2.7 Angular selectivity of the diffraction efficiency of a holographic grating

After exposure and photo polymerization, we study the morphological variation in the recording layer. Morphological characterization was carried out by using a Microscope at 60X magnification Nachet objective from Nachet Company connected with a CCD camera Pulnix (TM-6CN) to visualize the image. Fig. 2.8 shows the wide range microscope image of the holographic gratings created in methylene blue photopolymers. The clearly visible grating lines can be seen with good uniformity of the grating period. In the central part of the image we can see a irregular pattern, which may appear because of the localized variation in the thickness of the recording film leading to non-uniform surface.

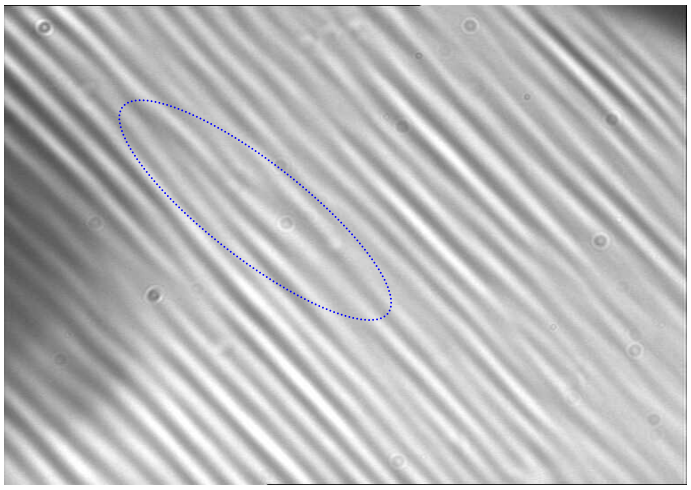

Fig. 2.8 Microscope image of grating patterns of a methylene blue photopolymer layer.

Experiments with further increase in MB concentration beyond MB5 suffered from the loss in DE primarily [2] because of the intense absorption due to the higher sensitivity of MB at the recording wavelength and resulted in deep blue coloured recording films. A deep coloured recording film should be avoided for recording as it can significantly increase the intensity of the transmitted beam during recording [7]. Therefore there is always a trade-off between the maximum sensitivity and the concentration of the dye.

2.5 Conclusion

In this chapter we presented the studies on the development and characterization of Methylene Blue sensitized photopolymer suitable for information storage. The optimum dye concentration is shown to influence the maximum diffraction efficiency, which reaches 40%, and also modulates the sensitivity of the recording medium. A high spatial frequency of 1767 lines/mm is experimentally measured by our experimental set-up. It must be noticed that the low diffraction efficiency of 40% is primarily because of the high spatial frequency recording. The results presented here will be used as guideline in order to develop different dye sensitized photopolymer systems. The effect of other active components such as BSA, TEA and AA monomer will be presented in next chapter with an emphasis on further increase in the diffraction efficiency and spatial frequency.

References

[1]. S. Blaya, L. Carretero, R. Mallavia, A. Fimia, R.F. Madrigal, M. Ulibarrena and D. Levy, "Optimization of an acrylamide-based dry film used for holographic recording", Appl. Opt. 37, No. 32, 7604-7609, (1998).

[2]. M. Ortuño, S. Gallego, C. García, C. Neipp, A. Belendez and I. Pascual, "Optimization of a 1 mm thick PVA/acrylamide recording material to obtain holographic memories: method of preparation and holographic properties". Appl. Phys. B. 76, 851-857. (2003).

[3]. H. Kogelnik, Bell Syst. Tech. J. 48, 2909 (1969).

[4]. H.J. Caufield, *Handbook of optical holography*, (1979).

[5]. S. Blaya, L. Carretero, R.F. Madrigal, A. Fimia, "Optimization of a photopolymerizable holographic recording material on polyvinylalcohol using angular responses", Opt. Mat. 23, 529-538, (2003).

[6]. C. Sanchez, M.J. Escuti, C Van Heesch, C. W.M. Bastiaansen, D. J. Broer, J. loos and R. Nussbaumer, "TiO_2 nanoparticle-Photopolymer composites for volume holographic Recording", Adv.Funct. Mater **15**, 1623-1629 (2005).

[7]. H. Sherif, I. Naydenova, S. Martin, C. McGinn and V. Toal, "Characterization of an acrylamide-based photopolymer for data storage utilizing holographic angular multiplexing", J. Opt. A: Pure Appl. Opt. **7**, 255-260 (2005).

3

Chapter 3
Photopolymers for green region volume phase holographic recording

3.1 Introduction

In last chapter we described formation of volume transmission gratings recorded using a red sensitizing dye with high spatial frequency close to 1800 lines/mm. For high capacity storage and better fidelity, high spatial frequency with high diffraction efficiency is desired [1]. High spatial frequency can be achieved in photopolymers either by tuning the dye sensitivity towards lower wavelength regime or recording the reflection phase gratings [2]. In this chapter we present studies towards achieving high diffraction efficiency and high spatial frequency by using green sensitizing dyes such as Rose Bengal, Erythrosin B, Acridine Orange and Eosin. We use transmission as well as reflection geometry for volume phase gratings. For in-depth understanding of the photopolymerization process and its limitations, in each case, detailed analysis is performed using additional characterizations such as DSC, TGA, CV and FTIR. We also study the effect of cross linking agent (with Acridine Orange) n,n'-methylenbisacrylamide (BSA) by replacing it for n,n-dimethylacrylamide (DMAA). The effect of the different dye on the shrinkage using is also studied. In the

first half of this chapter we present our studies on the photopolymers recording performed in transmission geometry. In the final part , we describe the reflection geometry for holographic recording using the same photopolymers studied in the first part.

I. Volume transmission gratings

3.2 Rose Bengal photopolymer

Rose Bengal has been widely used as photosensitizer in photopolymers for holographic gratings recording. The chemical structure of rose Bengal is shown in fig 3.1.

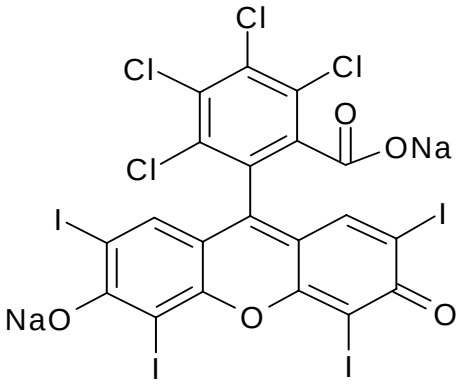

Fig. 3.1 Chemical structure of Rose Bengal.

Before the selection of the writing and reading beam, it is required to characterize the absorbance profile of the RB. We first recorded the UV-Vis absorption spectrum of Rose Bengal (obtained from Aldrich) and its reduction properties by electro-chemical measurements (CV). Figure 3.2 shows the absorption profile of rose Bengal dissolved in water.

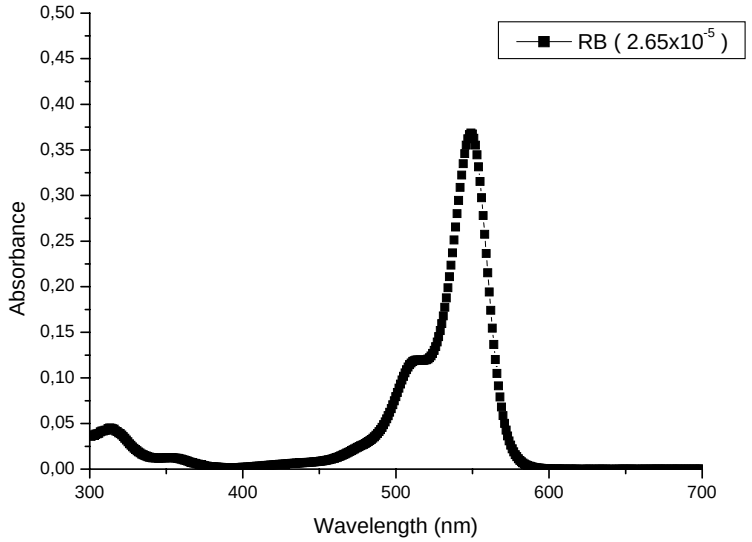

Fig. 3.2 Absorption spectrum of RB at $2.65x10^{-5}$ M of concentration in water solution.

The cyclic voltammogram (CV) were recorded in order to try to understand the limitations of the dyes as an electron acceptor and the role of the dye in the photopolymerization process. The CV scans were performed at dye concentration 0.76mM in CH_2Cl_2 using TBAP (O.1M) as the supporting electrolyte, Fc/Fc^+ as the reference, platinum wires as counter and working electrodes at a scan rate of 200 mV/s. The cyclic voltammograms (CV) of RB are shown in fig 3.3. CVs were recorded at varying reduction range in order to have more information about its role as electron acceptor in the photoreduction reaction that will suffer in the photopolymerization.

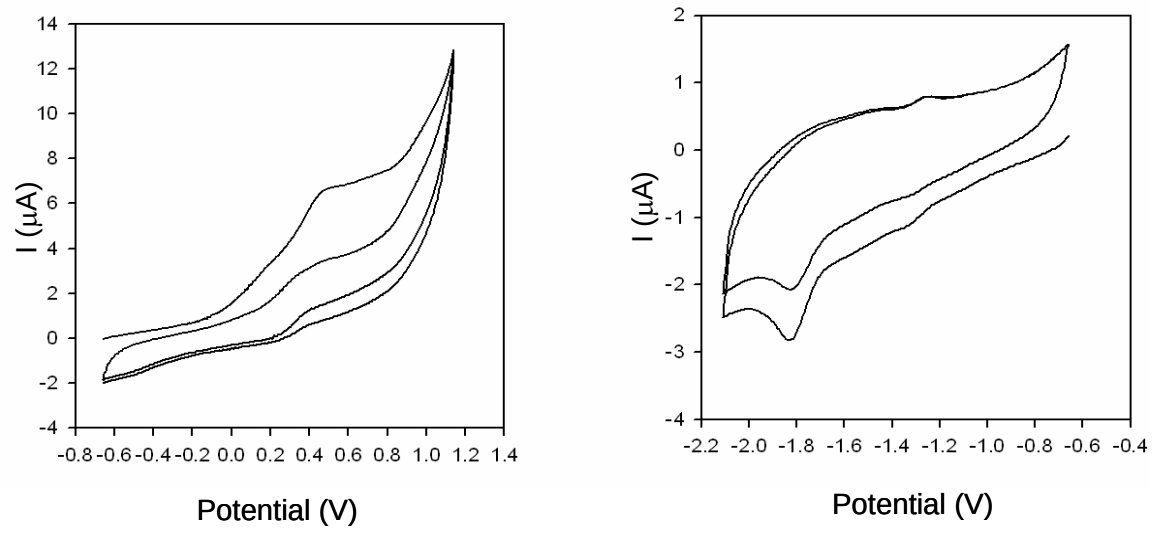

Fig. 3.3 Cyclic voltammogram of Rose Bengal

In the lower scan scale we don't see any reduction but a reduction peak appears at –1.8eV. This confirms the suitability of rose Bengal as an acceptor though the acceptor strength appears limited.

Preliminarily, for optimization of the RB recording material, we investigated a series of photopolymers keeping a similar monomer concentration (AA), fixing the initiator concentration and the photosensitizer concentration (in order to produce films with an absorbance close to 0.2) while varying the cross-linking monomer (BSA). In table 3.1 the composition of the pre-polymer solutions using RB as photosensitizer varying the BSA content is shown. All the reactants were dissolved in a PVA solution at 10% wt/v.

Table 3.1 Compositions of RB photopolymers with various amounts of BSA.

RB photopolymer	[RB] (M)	[Acrylamide] (M)	[BSA] (M)	[TEA] (M)	DE (%)
1	2.88×10^{-5}	0.38	0.028	0.605	43.4
2	2.88×10^{-5}	0.36	0.041	0.605	81.1
3	2.88×10^{-5}	0.37	0.051	0.605	95.3
4	2.88×10^{-5}	0.30	0.060	0.605	56.7
5	2.88×10^{-5}	0.36	0.065	0.605	35.7
6	2.88×10^{-5}	0.30	0.078	0.605	Precipitation

Fig. 3.4 shows the absorption spectrum profile of 27μm Rose Bengal thick film. The absorption is confined in the range of 500 and 600 nm, locating the maximum peak around 560 nm with a small shoulder at 523 nm. For balance absorption through out the film, we formulated the absorbance value near or lower than 0.2 to avoid high optical density. At high optical density much light can be absorbed by the dye before it can travel far inside the film.

To characterize performance of RB photopolymers, transmission and reflection gratings were recorded. The experimental set up used for transmission geometry recording is described earlier in chapter 2.

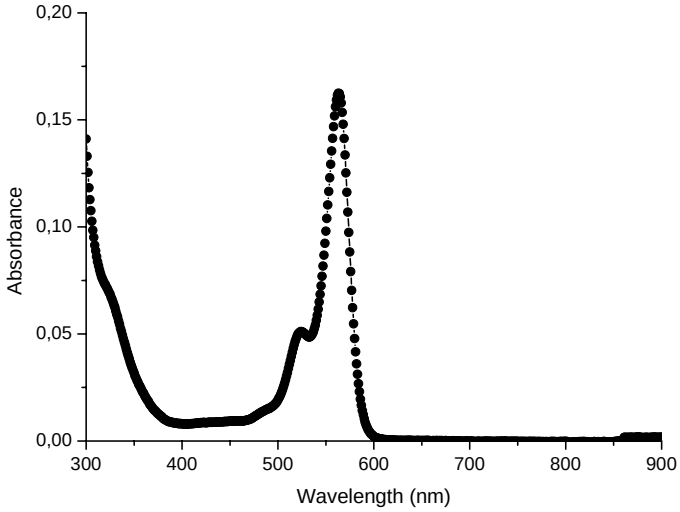

Fig 3.4 Absorption spectrum of Rose Bengal film at 2.88×10^{-5} of RB concentration.

In the table 3.2 the parameters used for the characterization are illustrated.

Table 3.2 Transmission geometry parameters used to evaluate the RB photopolymers where θ/2 is the half-angle between the interference beams; WB and RB are the writing and reading beam respectively; Λ is the fringe period; θ_B(T,E) are the theoretical and experimental Bragg angle and I is the recording intensity.

Photo-Polymer	θ/2 (°)	**WB (nm)**	**RB (nm)**	**Λ (μm)**	**SF (lines/mm)**	**I (mW/cm²)**	**θ_B (°)**
RB	30	514.5	633	0.5145	1943	200	37.94 (T) 37.09 (E)

Firstly, six different samples were prepared with varying monomer ratio using the same dye concentration. Experimentally measured results from all the samples indicate the formation of stables grating surfaces. Diffraction efficiency remains stable during the whole exposure time as no significant decrease was observed. As

summarized in table 3.2, optimal diffraction efficiency was 95.3 % at spatial frequency nearly 2000 lines/mm. This reveals that the formulations **3** and **2** are the best recipe among all others under study. Fig. 3.5 represents the dependence of diffraction efficiencies of photopolymers **1-6** on BSA content at constant concentration of Rose Bengal sensitizer.

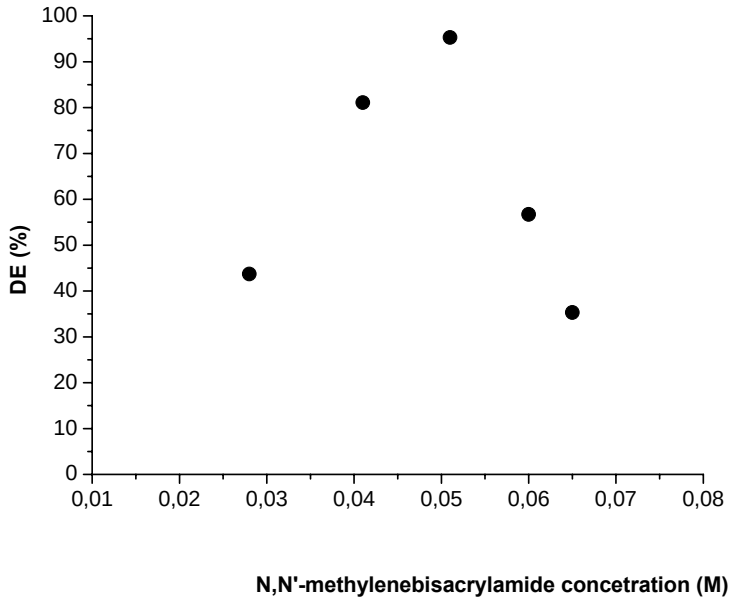

Fig. 3.5 Diffraction efficiency as a function of N,N′methylenebisacrylamide concentration (M)

We see a weak dependence of DE with AA content, which confirms that the AA content can be slightly increased up to 0.37 M in 5ml solution. A strong dependence of BSA content suggests that it should not be more than 0.051M to obtain satisfactory results. High BSA content (around 0.0778 M/5 ml of solution) resulted in precipitation during drying of the films and hence no measurement was possible on photopolymer 6 [3].

In an effort to achieve higher diffraction efficiency, the monomers (AA and BSA) were purified by a simple recrystallization process. It is a technique used to purify solids. A material termed impure is a mixture of two or more components from which only one component is desired [4]. The other components are impurities. Thus recrystallization and other methods of purification are methods of separations. There are steps to the recrystallization such as: choosing a solvent, adding hot solvent until compound dissolves, adding decolorizing charcoal if coloured impurities are present, filtering the resulting solution while it is still hot, cooling the solution and obtaining crystals, suction filtration to isolate the compound and drying the crystals that were isolated.

The Recrystallization of Acrylamide and N,N'-methylenebisacrylamide as outlined in the following process: 20 grams of acrylamide in 28 mL of anhydrous ethanol was magnetically stirred and heated at 30° for 15 min until the acrylamide was totally dissolved. For the case of n,n'-methylenebisacrylamide, 1.4 grams of n,n'-methylenebisacrylamide in 50 mL of anhydrous ethanol was magnetically stirred and heated at 30° for two hrs until it was dissolved. The procedure for isolate the purified crystals was the same for both recrystallization. The mixture was first filtered and then the filtrate was refrigerated for 24 hrs. The solution with newly formed crystals was filtered. The crystals were collected and then put to dry in desiccators until all the solvent content had evaporated. The recovery yield of acrylamide and n,n'-methylenebisacrylamide were 27.85% and 32.5% respectively.

Table 3.3 compares the use of purified monomers (AA and BSA) over non-treated ones for one kind of photopolymer maintaining the same formulation for both cases.

Table 3.3 Composition of pre-polymer syrups for RB photopolymer using non-purified and purified monomers.

RB photopolymer	[RB] (M)	[Acrylamide] (M)	[BSA] (M)	[TEA] (M)	DE (%)
7 (non purified)	2.88×10^{-5}	0.33	0.051	0.605	50
7 (purified)	2.88×10^{-5}	0.33	0.051	0.605	60

In Fig 3.6 the evolution of the diffraction efficiency growth during an exposure time of 60 sec and a intensity of 200 mW/cm^2 as function of the RB content for the two photopolymers with monomers (AA and BSA) used as we received and treated (purified by recrystallization). The growth in both materials is different, for untreated monomers the diffraction efficiency increased and reached its maximum value (saturate one) and then stabilized. For the treated ones, the diffraction efficiency increased to 65% which then undergoes a small decrease to 60% and then stabilizes. Comparing the use of purified monomers in the photopolymeric layer over without treatment we observed an average increase in the DE of 10%.

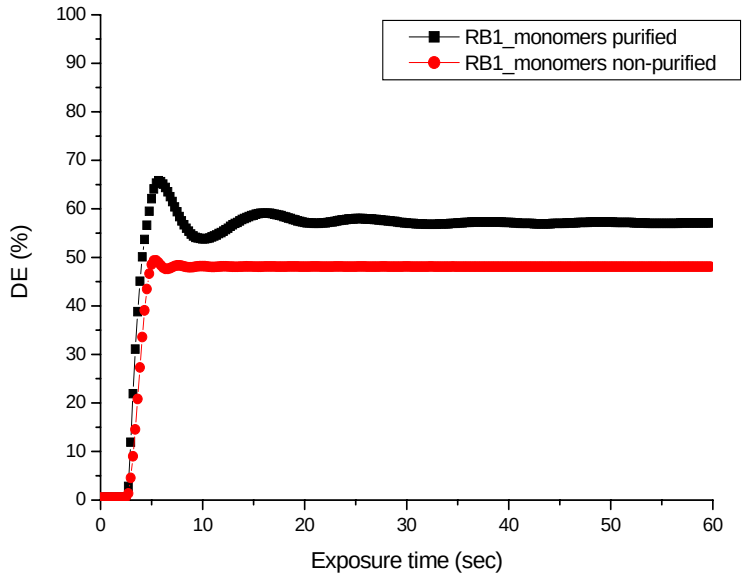

Fig. 3.6 Diffraction efficiency as a function of monomer purified and non-purified.

In figure 3.7, the two angular scans of the gratings created in photopolymer with purified and non purified monomer (AA and BSA) are represented. The first curve (squares) is obtained for the layer with purified monomers and the second curve is obtained for the layer with non-purified ones. We observed almost identical angular width. That occurs because when their effective optical thickness is the same; in the other words the two diffraction gratings recorded have the same effective thickness. After the first side lobe (apart from the zero diffracted order) the subsequent lobes almost vanished.

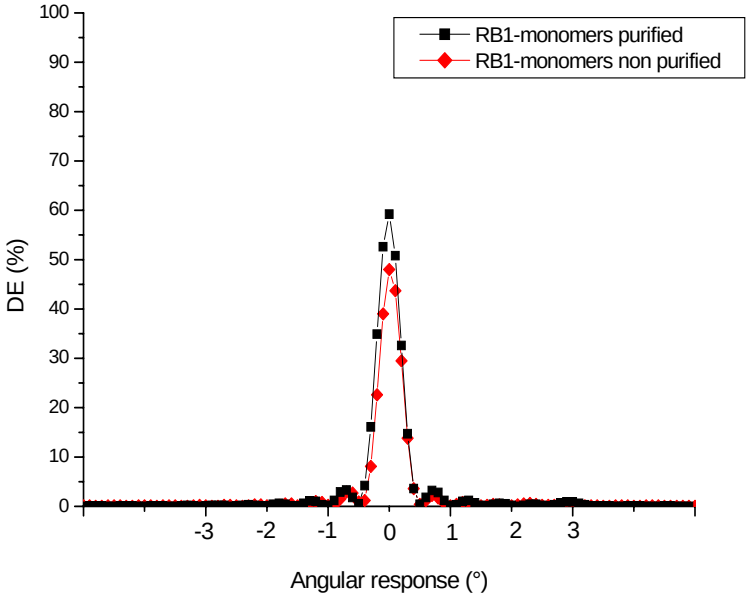

Fig. 3.7 Angular scan around the first Bragg angle is plotted for two layers with non-treated and treated monomers.

These studies show that the purity of components significantly affects the diffraction efficiency of gratings stored in the photopolymers. We therefore used all individual components for our studies at highest possible purity.

One of the significant factors in the diffraction efficiency and the energetic is the relative quantity of dye [5]. DE and Sensitivity can be increased by augmenting the dye concentration but also can be deteriorated by its excess because of additional energy is needed to bleach the extra sensitizer [6]. In an attempt to optimize our best formulation previously described (RB3) keeping constant the triethanolamine content and BSA content, raising the monomer concentration (AA) in order to try to increase the DE due to more acrylamide conversions will be converted into polymer but varying the RB content in a range to obtain films with low optical density. In table 3.4

the concentrations of components for the different photopolymers varying the RB content are shown.

Table 3.4 Components of the pre-polymer solution with various amount of RB.

RB photopolymer	[RB] (M)	[Acrylamide] (M)	[BSA] (M)	[TEA] (M)
8	$2.66x10^{-5}$	0.452	0.052	0.605
9	$3.47x10^{-5}$	0.452	0.052	0.605
10	$4.47x10^{-5}$	0.452	0.052	0.605

In fig. 3.8, the UV/Vis absorption spectra of the RB8-10 photopolymers fabricated are presented. Here we ensured that the absorbance of the three materials remains lower than 0.2.

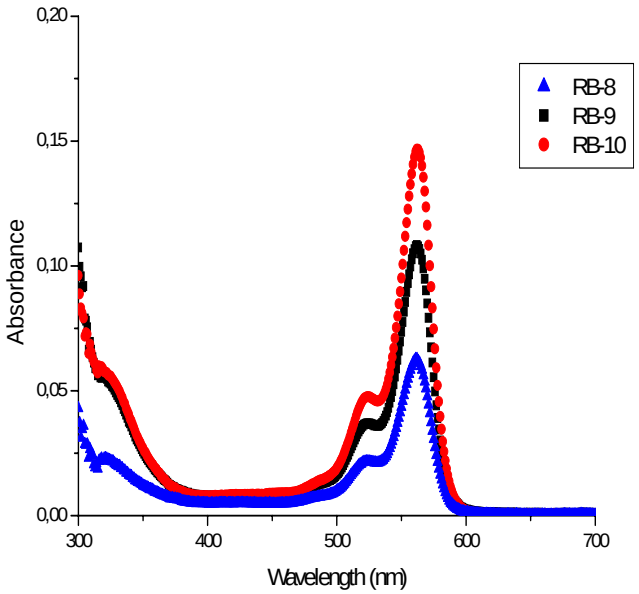

Fig. 3.8 UV/Vis spectra of RB8-10 unexposed layers.

To study the optimum behaviour of the RB photopolymeric layers as holographic recording media, we recorded diffraction gratings using the same holographic set up by increasing the angle between the two intersecting beams described earlier. Though the illumination intensity was decreased by 50 mW/cm^2, we would like to emphasize that by a slight change in the recording angle can lead to substantial increase in spatial frequency as we observed increase in spatial frequency by 200 lines/mm and a decrease of the grating period compared to the previous results using RB as photosensitizer.

Thus the spatial frequency of the grating recorded was changed by varying the angle between the two symmetric exposing beams. This was achieved in practice by changing the distance from the plate to the plane mirrors and overlapping the beams on the plate. In this way, gratings with spatial frequencies from 1943 up to 2173 lines/mm could be recorded. In the table 3.5 the new parameters for the RB photopolymers are illustrated.

Table 3.5 Parameters for recording holographic grating in RB8-10 photopolymers where θ/2 is the half-angle between the interference beams; WB and RB are the writing and reading beam respectively; Λ is the fringe period; θ_B(T,E) are the theoretical and experimental Bragg angle and I is the recording intensity.

Photo-polymer	θ/2 (°)	**WB (nm)**	**RB (nm)**	**Λ (μm)**	**SF (lines/mm)**	**I (mW/cm^2)**	**θ_B (°)**
RB	34	514.5	633	0.46	2173	153.3	43.4 (T) 42.6 (E)

Fig 3.9 shows the evolution of the diffraction efficiency during exposure time of 90 sec for RB8-10 photopolymers. The diffraction efficiency growth can be seen to follow the same pattern for all three photopolymers. The efficiency increases immediately, without any delay and reaches close to 100% which then suffers a fall of almost 20% and stabilizes subsequently over the exposure time. Thus we observed a significant increasing in the diffraction efficiency by increasing the RB content.

The diffraction efficiency was defined as I_D/I_D+I_T where I_D and I_T are the diffracted and transmitted light intensities respectively.

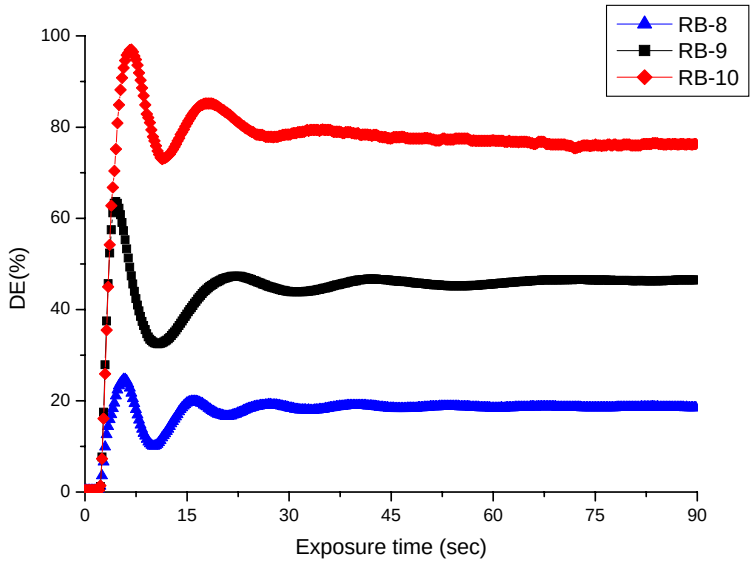

Fig. 3.9 Evolution of diffraction efficiency during time for photopolymers containing RB as photosensitizer.

Table 3.6, summarizes some optical properties for photopolymer RB(8-10). The refractive index modulation, sensitivities were previously defined at the beginning of the chapter 2. We observed by increasing the RB content, the diffraction efficiency

increased as well as the sensitivity. As evident in the table, the response time was reduced to achieve maximum diffraction efficiency by increasing the amount of photosensitizer producing higher sensitivities [7]. The increase of the DE represents an increase on the RIM from $1.75x10^{-3}$ to $3.76x10^{-3}$ for the lowest and highest RB content.

Table 3.6 Optical parameters of RB8-10 photopolymers after **1.587 sec** of exposure.

RB photopolymer	DE (%)	Sensitivity (cm/J)	RIM	Thickness (μm)
8	17	470.76	$1.75x10^{-3}$	36
9	57.5	865.82	$3.54x10^{-3}$	36
10	62.8	904.84	$3.76x10^{-3}$	36

We can see that the angular response of the diffraction efficiency as a function of the reconstructing angle using a He-Ne probe beam. The samples were positioned on a computer-controlled rotary stage with a resolution of 0.1°. We can only see the first diffracted order in the angular response, which indicates formation of thick holographic gratings in this photopolymer [8].

In figure 3.10, the diffraction efficiency around the first Bragg's angle replay is plotted for photopolymer RB(8-10). It was observed in the angular selectivity curves when the concentration of photoinitiator varied, the symmetrical responses with reference to Bragg's angle are obtained. Low variations are observed, which are not significant because these differences are order of magnitude lower than the measurement errors. In this figure it can be seen that the first lobes increases with the

higher RB content. Prominently we can appreciate the fact that in the case with lower RB content these lobes are almost vanished and the principal lobe width remained constant.

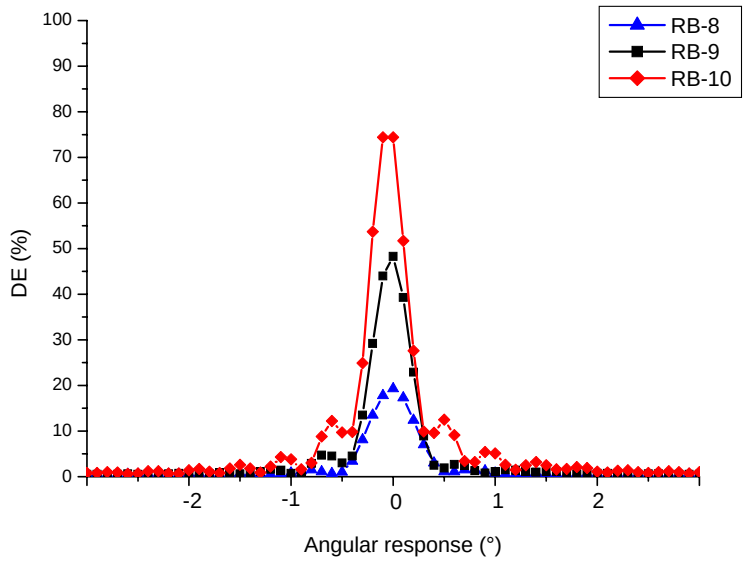

Fig. 3.10 Angular response of diffraction efficiency for photopolymer RB(8-10).

In order to understand the photo induced chemical changes in the composition, and their influence on the DE response of RB 8-10, if any, we measured their FT-IR spectra. FT-IR measurements are illustrated, in Fig. 3.11, for photopolymers RB(8-10).We essentially do not see any significant shift in the features from RB 8-10.This means that the higher DE for RB10 comes primarily because of its increased sensitivity caused by the higher dye content.

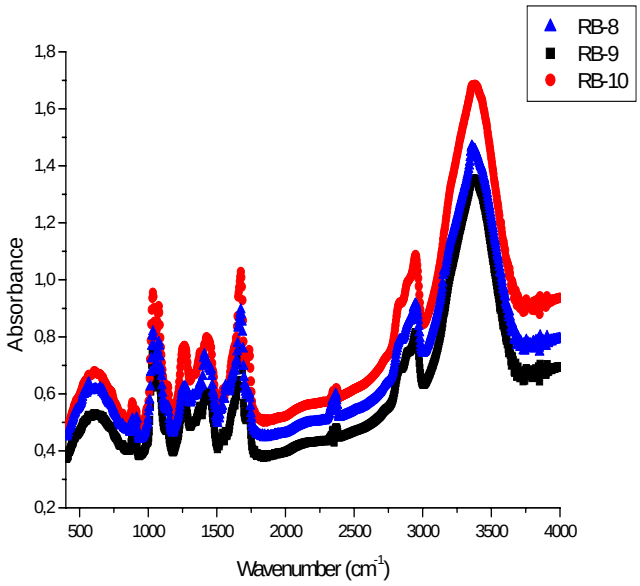

Fig. 3.11 FTIR spectra of RB-8-10 polymerized photopolymers.

After recording, we looked at the film surface using a microscope. The microscopic images shown in figure 3.12 reveal the formation of gratings with a regular grating period. The fringe spacing thus probed was close to 0.46 μm which confirms the formation of gratings with a spatial frequency higher than 2000 lines/mm.

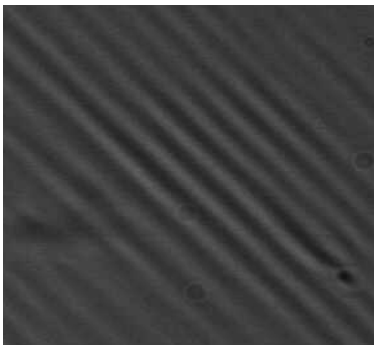

Fig. 3.12 Microscope image of RB photopolymer

3.3 Erythrosin B photopolymer

Erythrosin B is a widely studied photosensitizer and it has been used in photopolymer for holographic data storage [9,10]. The chemical structure of the erythrosin B is illustrated in fig. 3.13.

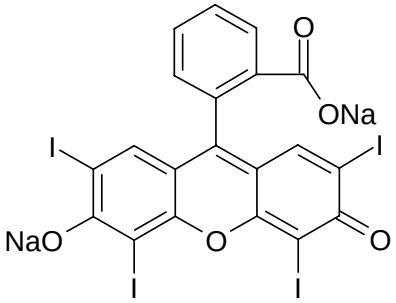

Fig. 3.13 Chemical structure of Erythrosin B.

The cyclic voltammogram of erythrosine B is shown in fig 3.14. The recording parameters are described earlier. The CV study provides more information on the behaviour of the dye as an electron acceptor compared to the rest of photosensitizer used for green holographic recording. We can easily distinguish the reduction peak at -1.1 eV which confirms the electron accepting nature of this dye.

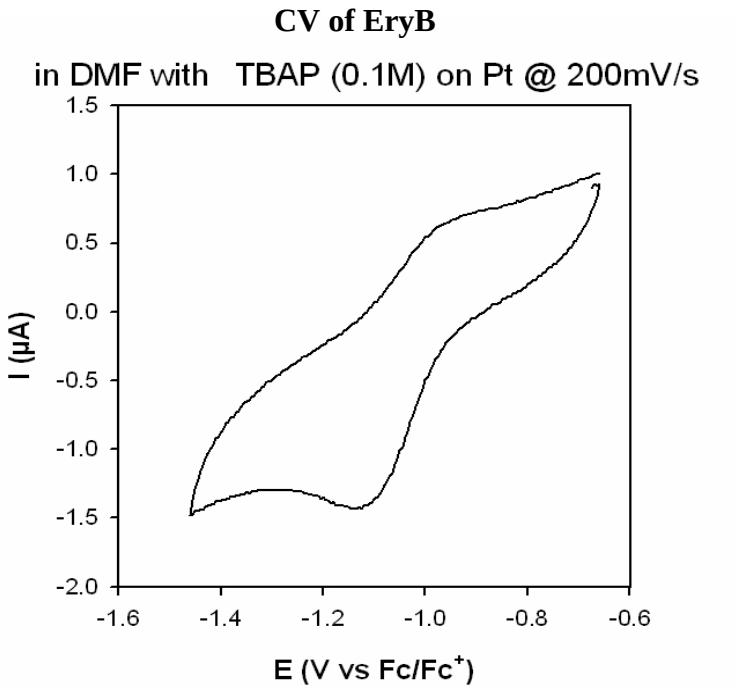

Fig. 3.14 Cyclic voltammograms of Erythrosin B.

In fig 3.15 the UV-Vis spectra of the erythrosin B in water solution (in 2.5 and 25 ml of water solution) are shown. All the solutions present have absorption band at 526 nm with a small shoulder located at 490 nm that grows with the concentration. Four photopolymers were fabricated to study the effect of erythrosine B as photosensitizer in photopolymer suitable for holographic recording medium. The PVA solution at 10% wt/v dissolved in water again forms the matrix and is used to prepare the mixture of AA, BMA (monomers) and photopolymerization initiator system (TEA, EryB). In table 3.7, the concentrations of components are illustrated.

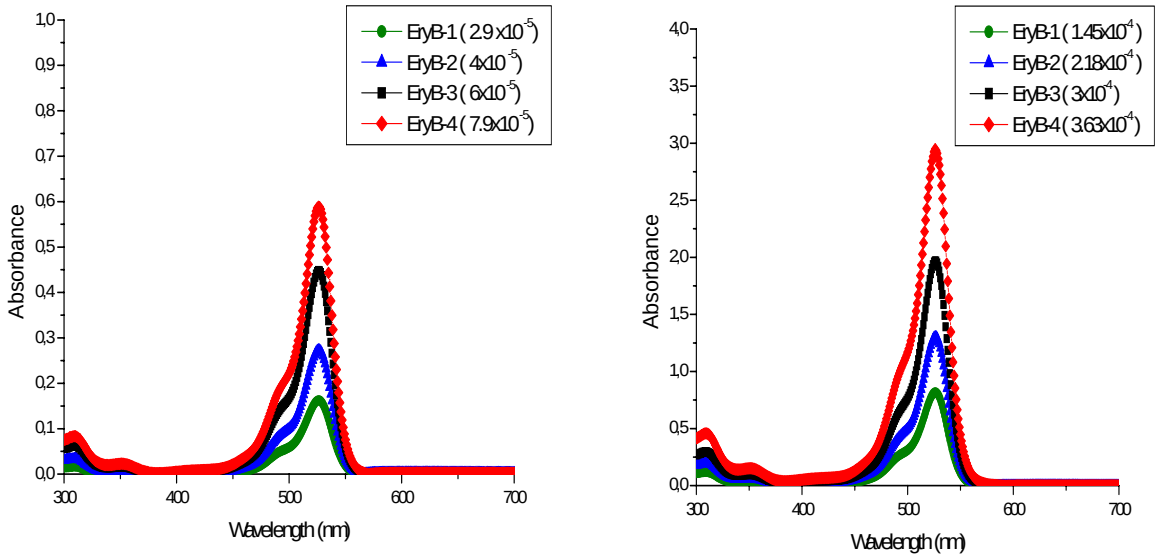

2.5ml 25ml

Fig. 3.15 UV/Vis spectra of EryB-1-4.

Table 3.7 Concentration and components for different EryB photopolymeric layers.

EryB photopolymer	[EryB] (M)	[Acrylamide] (M)	[BSA] (M)	[TEA] (M)
1	2.92×10^{-5}	0.452	0.052	0.605
2	4.03×10^{-5}	0.452	0.052	0.605
3	6.02×10^{-5}	0.452	0.052	0.605
4	7.94×10^{-5}	0.452	0.052	0.605

Fig. 3.16 shows the UV-Vis absorption spectra of different films using Erythrosin B as dye. The principal absorption band shows a red shift to 535 nm. The appearance of the band at 500 nm is more clear and sharper for the EryB-3 film compared to the rest of the materials.

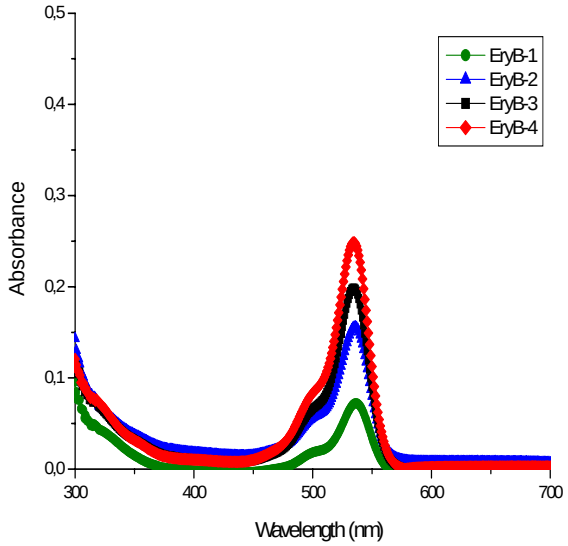

Fig. 3.16 UV/Vis spectra of EryB-1-4 photopolymeric layers with the same thickness of 34 μm.

For the characterization of the performance of the EryB photopolymers, gratings were recorded using the previously described transmission set up. In the table 3.8, the parameters used for the creating the gratings in this kind of material are shown. As usual the diffraction efficiency was defined as the ratio between the diffracted and the sum of diffracted and transmitted intensities.

Table 3.8 Parameters for gratings recording in EryB photopolymers.

Photo-polymer	θ/2 (°)	**WB (nm)**	**RB (nm)**	**Λ (μm)**	**SF (lines/mm)**	**I (mW/cm²)**	**θ_B (°)**
EryB	34	514.5	633	0.46	2173	153.3	43.47 (T) 41.89 (E)

where $\theta/2$ is the half-angle between the interference beams; WB and RB are the writing and reading beam respectively; Λ is the fringe period; $\theta_B(T,E)$ are the theoretical and experimental Bragg angle and I is the recording intensity.

Fig. 3.17 shows the temporal traces of diffraction efficiency for the photopolymers using different dye concentrations as function of exposure time. The materials were expose for 90 sec to create the gratings. We observe the same pattern for the growth of diffraction efficiency shown in RB photopolymer, the efficiency value reaches its maximum value first and a decrease of approximately 20% follows which then stabilizes the response. Here again we found that the diffraction efficiency increases by increasing the dye concentration up to certain limit (from EryB-1 up to EryB-3) which then decreases as in the case of EryB-4. The reason for this is the possible competitive polymerization mechanism that is produced when high concentrations of the dye are used because the dye forms dimeric forms [11], which is involved in a polymerization termination reaction, resulting in a decrease in the overall rate of polymerization.

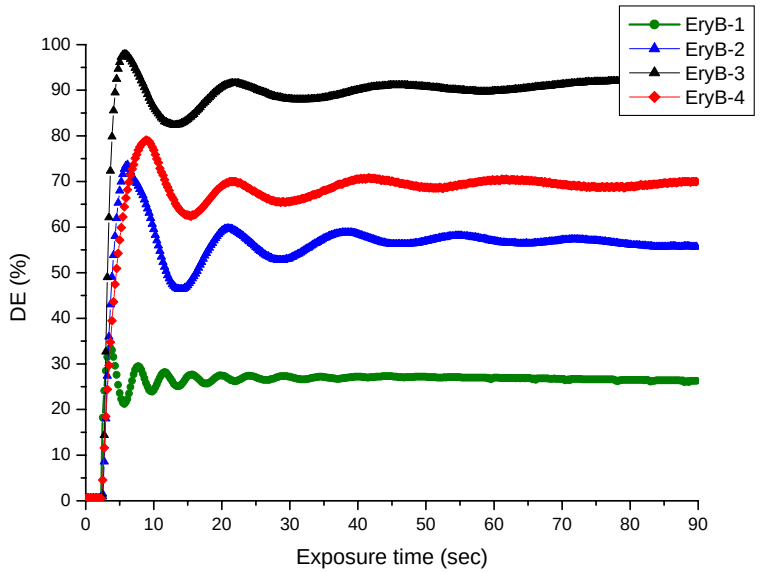

Fig. 3.17 Diffraction efficiency during exposure time at different EryB concentration.

After those dye molecules participating in the polymerization have been consumed, the dimeric molecules of the dye will decompose; the monomers in the material will polymerize perfectly as long as the exposure time is long enough [11]. The decomposition process of the dimeric dye influences the polymerization rate, leading to the decrease in the sensitivity of the material [11,12]. The presence of the formation of dimeric forms by increasing in the Erythrosine B concentration produces the apparition of a band at 490–510 nm [11]. Another explanation can be reached because of the lower molecular weight of grating polymer that results from the fast termination rate because of the existence of a larger quantity of photosensitizer, which in turn diminishes the modulation of the refractive index modulation [6].

The angular response half-width was obtained by scanning the diffraction efficiency as a function of the angular deviation from Bragg angle condition for photopolymers exhibiting different concentration of Erythrosin B [13]. In figure 3.18, it was observed by increasing the photosensitizer concentration the principal lobe width remains constant. The uplifted satellite peaks (first diffracted order) increases by augmenting the dye concentration, in the case of EryB-1 this peaks are almost vanished. The FWHM for the EryB photopolymer was found to be around to 0.48°.

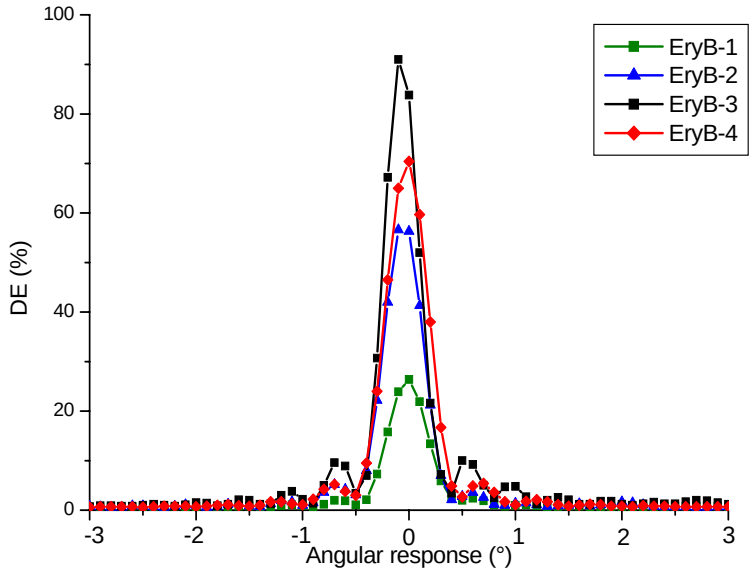

Fig. 3.18 The experimental angular scan around the Bragg angle is plotted for all photopolymer at different concentration of erythrosine B.

In table 3.9, we found the sensitivity increases when the concentration was augmented. It is easy to understand that the more the dye molecules, meaning more photons being absorbed, and the more the excited states of the dye, the easier the

triethanolamine is excited and the quicker is the polymerization rate of the acrylamide. The sensitivity of the material decreases with increasing concentration of Erythrosine B when it is greater than $6.02x10^{-5}$ M [11]. Elevated concentration, larger than $6.02x10^{-5}$ M for erythrosine B as dye origins a reduction in the sensitivity of the material. A possible explanation is the existence of competitive polymerization mechanism when high dye concentration is used due to the formation of dimeric forms which is involved in polymeric termination reaction resulting in a decrease in the polymerization rate. In a photopolymer, the index modulation is proportional to the concentration of the monomer reacted [11]. The refractive index modulation as the sensitivity increased by the dye concentration is raised up to $6.02x10^{-5}$ M. This increase in the content feature in the RIM an improvement from $2.39x10^{-3}$ for EryB-1 up to $5.16x10^{-3}$ for the EryB-3, and a decrease to $3.16x10^{-3}$ for EryB-4, exhibiting the same trend observed in the sensitivity.

Table 3.9 Optical parameters for photopolymer containing Erythrosin B after 1.818 sec.

EryB photopolymer	DE (%)	Sensitivity (cm/J)	RIM	Thickness (μm)
1	29.6	542.26	$2.39x10^{-3}$	36
2	58.0	759.07	$3.60x10^{-3}$	36
3	89.4	942.39	$5.16x10^{-3}$	36
4	47.4	686.85	$3.16x10^{-3}$	36

Intensity plays an essential role in the formation of the diffraction gratings due to the fact that it produces a significant increase in the rate of photopolymerization [14].

The behaviour has been represented in Fig. 3.19, where the temporal variation in diffraction efficiency is shown for different intensities. The kinetics of photopolymerization and the diffraction efficiency increase in the rate when intensity is increased [15]. We observed by increasing the intensity that the efficiency is augmented. It can be seen that at the moment of illumination, the diffraction efficiency of the photopolymer was comparative to the exposure time, but after awhile say after 3 sec, the efficiency got to its maximum value; then the diffraction efficiency decreased and subsequently stabilize with increasing exposure time. This tendency was more intense in the case of higher intensities.

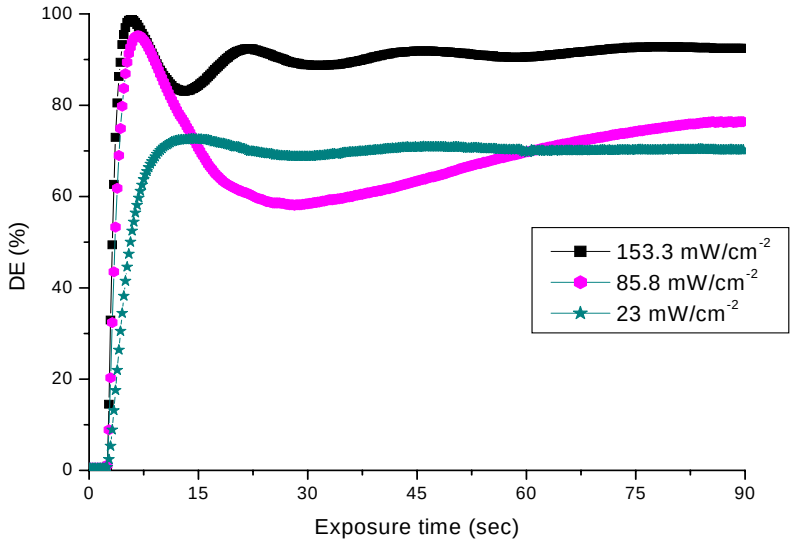

Fig. 3.19 Effect of different intensity on the diffraction efficiency during exposure time for the photopolymer EryB-3.

Table 3.10 Optical parameters for photopolymer containing Erythrosin B-3 after 1.818 sec.

Intensity (mW/cm^2)	**DE (%)**	**Sensitivity (cm/J)**	**RIM**	**Thickness (μm)**
153.3	89.4	942.3	$5.16x10^{-3}$	36
85.84	74.9	1541.2	$4.35x10^{-3}$	36
23	30.5	3668.8	$2.43x10^{-3}$	36

As summarized in above table, we can see that by decreasing the intensity the RIM decreases from $5.16x10^{-3}$ (for the less dye content photopolymer) to $2.43x10^{-3}$ for the photopolymer with higher dye content.

In figure 3.20 the angular response of the gratings stored in EryB-3 photopolymer at different intensities is presented. As it is seen there is no divergence in the half-width of their angular selection responses. The first diffracted order was more clearly resolved for the cases of higher intensities compared to the low ones.

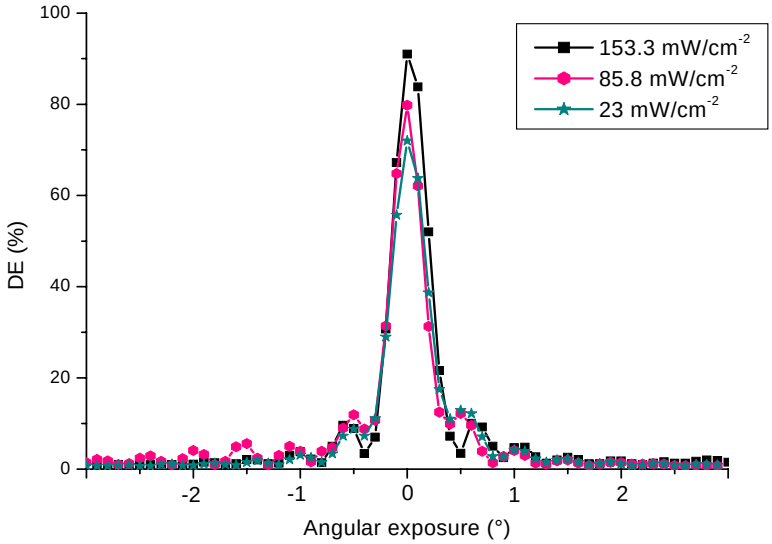

Fig. 3.20 Angular response as function of diffraction efficiency for photopolymer EryB-3 at different intensities.

We previously mentioned that diffusion has a vital effect on the amount of photopolymerization of acrylamide. Diffusion process can be influenced by both chain flexibility of photopolymer and also by mobility of the monomers [16]. Here we analyzed the chain flexibility of photopolymers by measuring the glass transition temperature (Tg) of the photopolymer. The Tg was seen to increase, in figure 3.21, with the increasing dye concentration, meaning the photopolymer becomes more rigid. Generally the diffusion of acrylamide in the material for photopolymerization would be more difficult for photopolymer with higher Tg, resulting in a decrease of diffraction efficiency [17].

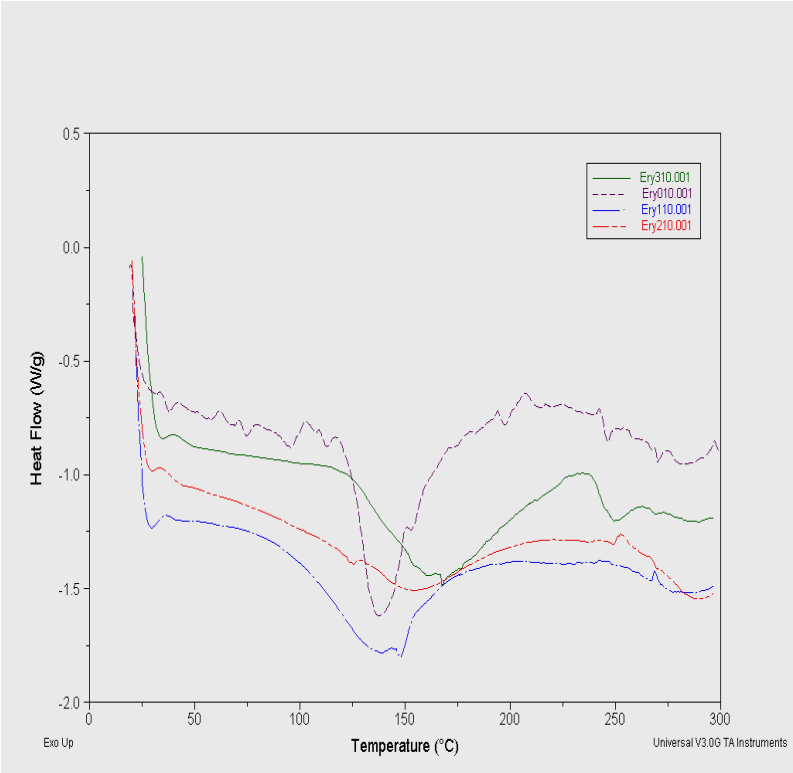

Fig. 3.21 DSC thermogram of the Erythrosin B-1-4 films.

Also it is believed that the mobility of polymerized polymer chains can be reduced and this can lead to a reduction of free volume change and thus to the volume shrinkage of recorded gratings. In our case by increasing the dye content, the diffraction efficiency increased, featuring higher Tg higher diffraction efficiency can be achieved [7]. One possible explanation is by increasing the concentration of the dye, the chain length can decrease acting as a retarder due to the polymer chains initiated inside the brought regions can continue growing to the adjacent dark regions leading to a smearing of the RIM. If the chain length could be shortened then the chain growth should decrease [18].

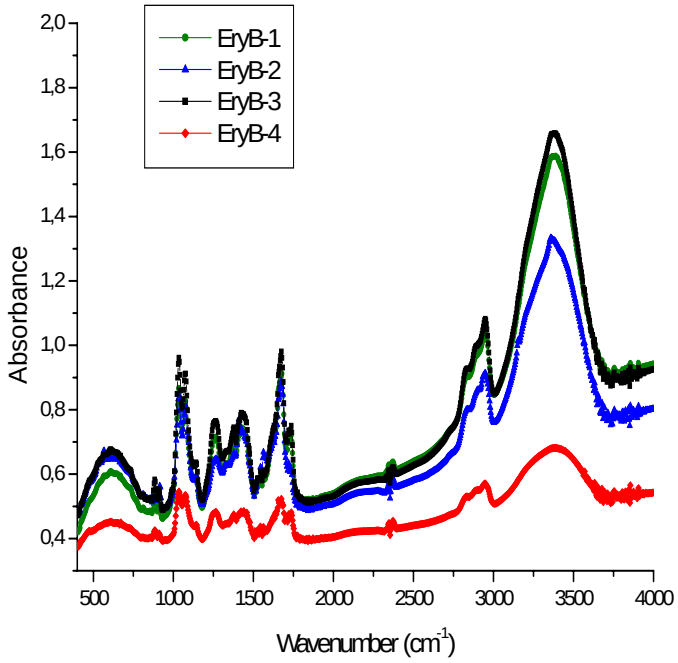

Fig. 3.22 FTIR spectra of EryB-1-4 polymerized films.

We also confirmed from the results of FT-IR measurements in figure 3.22 that the characteristic peak intensity of acrylamide (1670cm-1 C=O stretch, 1605cm-1 NH2 deformation in amide) does not change in all formulations are shown in fig. 3.22, indicating that the deterioration in the optical properties for Ery4 compared to Ery3 is mainly affected by the relative content of dye.

The physical confirmation of the gratings formation created by interference pattern can be seen in fig. 3.23 with a grating period close to 0.46 μm.

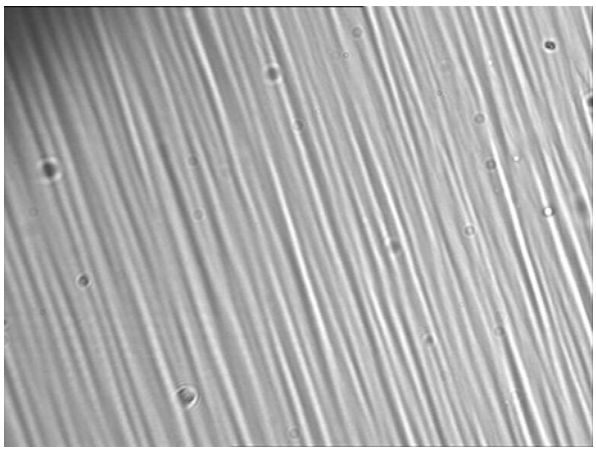

Fig. 3.23 Microscope image of the Erythrosin B photopolymer layer.

3.4 Eosin photopolymer

Eosin is a material commonly used in medicine to heal the skin injuries. Yellowish eosin is a similar component that has been widely used in photopolymer for holographic data storage purposes [19-22]. The eosin used in our experiments was obtained from the Gifrer Company-France as a solution of eosin aqueous at 2% v/v. No chemical structure is presented here due to the confidentiality imposed from this vendor. We first measured the spectral response of the eosin. Fig 3.24 shows the optical absorption measurements of eosin in water solution at different concentration. The main absorption band is located at 530 nm of wavelength which starts from 475 nm and extends up to 530 nm.

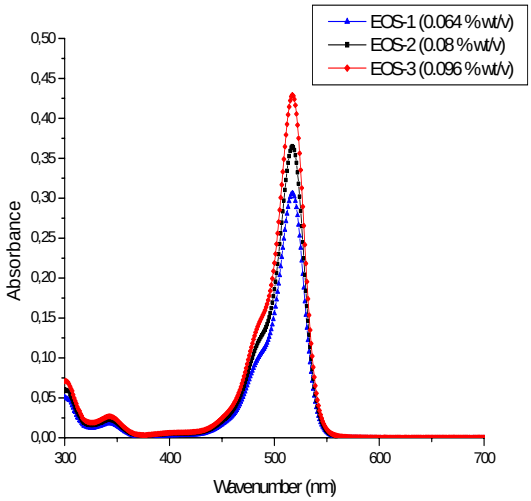

Fig. 3.24a UV/Vis spectra of Eosin 1-3 in 2.5 ml water solution.

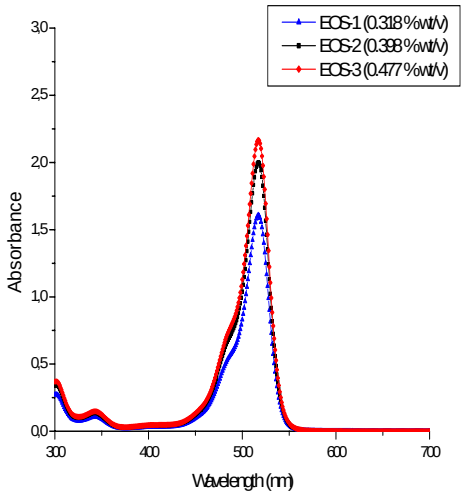

Fig. 3.24b UV/Vis spectra of Eosin 1-3 in 25 ml water solution.

For the realization of potential of eosin as photosensitizer in acrylamide based photopolymer, three different compositions were formulated to study its effect as a recording media. All the components used (AA, BSA, TEA and eosin) were dissolved in a PVA solution at 10% wt/v in a composition shown in table 3.11. Fig. 3.25 shows the absorption spectra of 35 μm thick films using eosin as photosensitizer at different concentration before photopolymerization. The main band of absorption suffered a red shift from 517 nm to 530 nm of wavelength making it suitable for green holographic recording.

Table 3.11 Concentration and components of the different layers compositions.

Eosin photopolymer	[Eosin] (% v/v)	[Acrylamide] (M)	[BSA] (M)	[TEA] (M)
1	0.064	0.452	0.052	0.605
2	0.080	0.452	0.052	0.605
3	0.096	0.452	0.052	0.605

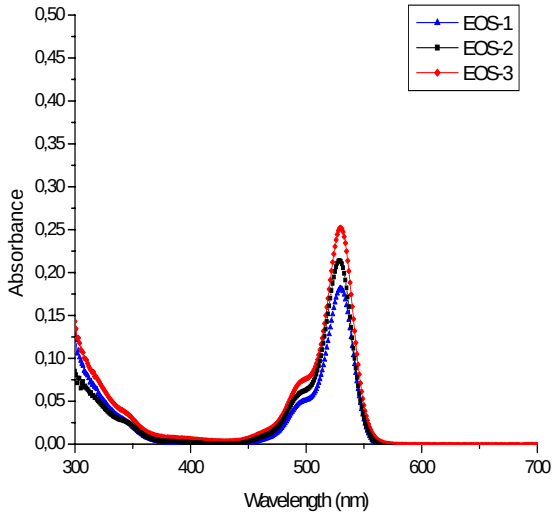

Fig. 3.25 UV/Vis spectra of 35 μm thick Eosin (1-3) layers.

The grating parameters generated using eosin based photopolymer is shown in the table 3.12, using the previously described experimental set up and the diffraction efficiency is defined as the ratio between the diffracted and the sum of diffracted and transmitted intensities.

Table 3.12 Parameters for grating recording using eosin as photosensitizer.

Photo-polymer	θ/2 (°)	**WB (nm)**	**RB (nm)**	**Λ (μm)**	**SF (lines/mm)**	**I (mW/cm²)**	**θ_B (°)**
Eos	34	514.5	633	0.46	2173	153.3	43.4 (T) 42.2 (E)

where θ/2 is the half-angle between the interference beams; WB and RB are the writing and reading beam respectively; Λ is the fringe period; θ_B(T,E) are the theoretical and experimental Bragg angle and I is the recording intensity.

In the fig. 3.26, the diffraction efficiency of the gratings created in this medium during the exposure time of 90 sec is presented. It can be observed through the graph that the evolution for EOS-1-3 pursues the same performance; the efficiency grows reaching their maximum value and then stabilizes after approximately 10 sec of exposure but for EOS-2 the dynamics of the efficiency was different, after 12 sec it decreased drastically to 25% then increase to its maximum and stabilized. The diffraction efficiency was observed to decrease slightly by increasing the eosin concentration. Similar to and as was the case with acridine orange, this trend can be elucidated for the possibility of competitive polymerization mechanism arising produced when high concentrations of eosin are used [11,12].

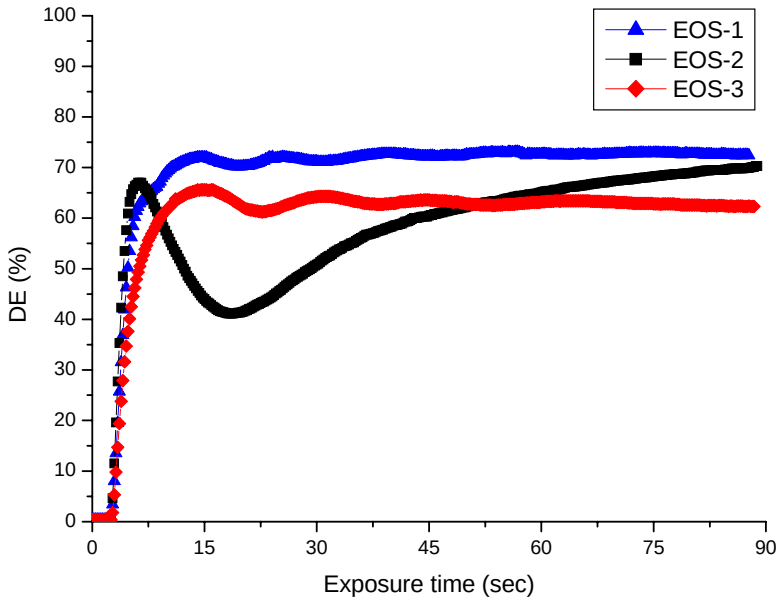

Fig. 3.26 Evolution of diffraction efficiency during exposure time at different concentration for eosin photopolymers.

Once the diffraction efficiency for the different material varying the dye content was obtained, the sensitivity and RIM were calculated. In table 3.13, the optical parameters are presented for eosin photopolymers. We observed that by increasing the dye content the sensitivity and RIM suffered a slightly increase first and then decreased in the same way. The slight increase in the sensitivity and RIM can be due to more molecules of dye capable to initiate the polymer chain turning in a faster process and then the faintly reduction can be explained by the fact that an excess of photosensitizer raises the requirement of more energy for bleaching [6,12].

Table 3.13 Optical parameters of photopolymers with eosin as photosensitizer after 2.5 sec of exposure.

Eosin photopolymer	**DE (%)**	**Sensitivity (cm/J)**	**RIM**	**Thickness (μm)**
1	53.5	545.28	3.498×10^{-3}	35
2	63.2	592.69	3.919×10^{-3}	35
3	40.1	472.11	2.924×10^{-3}	35

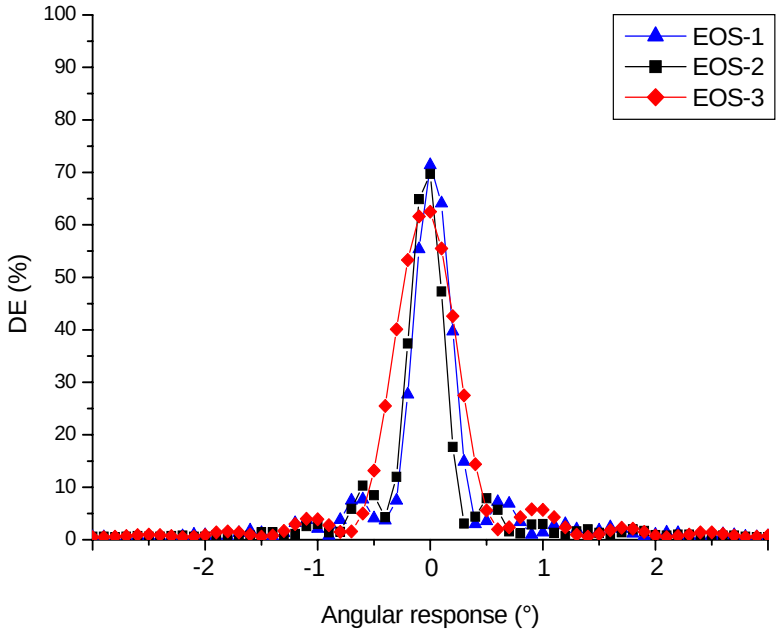

Fig. 3.27 Diffraction efficiency as a function of the Bragg angle for eosin photopolymers.

The angular scans around the Bragg angle condition as a function of the diffraction efficiency are plotted in fig. 3.27 for all the three-eosin photopolymers. The narrowing of the principal lobe can be easily observed when the dye concentration becomes higher. The FWHM for EOS-1-2 is similar in value ~0.45°, while for EOS-3 it turns into almost 1°. The first lobes corresponding to first diffracted beam are well defined (visible) for all the three photopolymers.

In fig. 3.28 (a), the FT-IR measurement was carried out to comprehend our previous results. The appearance of specific interaction between AA and TEA can be contributed to the decrease in the amount of AA into the polymer through a photoreaction where the interaction of hydroxyl group of TEA enables the hydrogen bonded to the amide group of AA. This can result in a reduction of the AA mobility

inducing a decrease in the DE. Given that higher is the dye concentration greater is the band of absorption of AA located at 1670 cm^{-1} indicating the smaller value of the intensity band of AA was observed for the photopolymer EOS-1 which reports the maximum value of efficiency among all the material representing a higher extent of acrylamide turned into photopolymer [16].

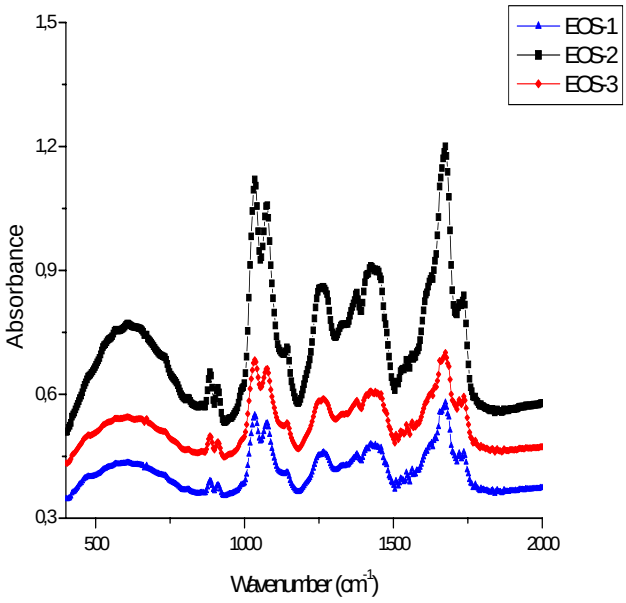

Fig. 3.28a spectra of Eosin 1-3 photopolymeric layers.

The DSC analysis illustrated in fig 3.28 (b) elucidates the explanation of our results. The Tg measured for all three photopolymers using eosin doesn't vary significantly representing the diffusion of the monomer among photopolymers was similar. This effect is in accordance with our results about similar DE values for all other materials.

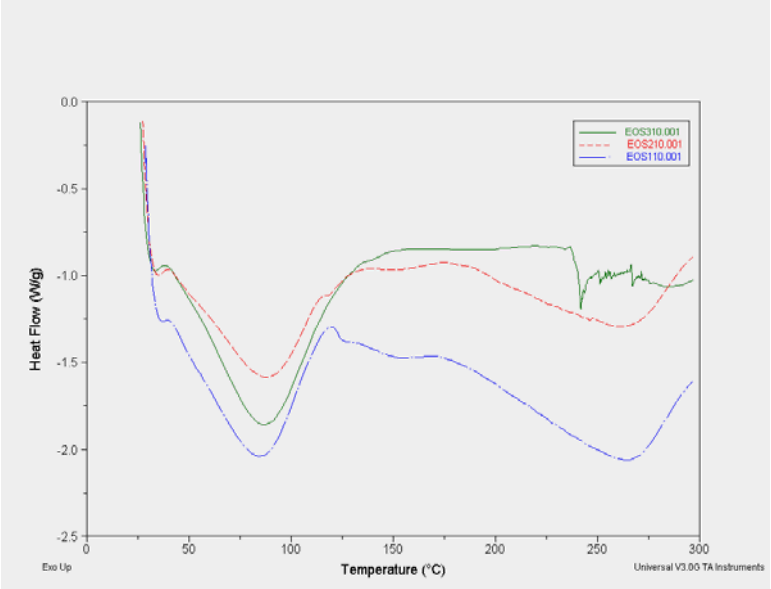

Fig. 3.28b DSC thermogram of the eosin (1-3) photopolymers.

The construction of holographic gratings using interference exposure is shown in fig. 3.29. The image of the well-defined grating with an identical period of 0.46 μm was obtained using microscope imaging at a magnification of 60.

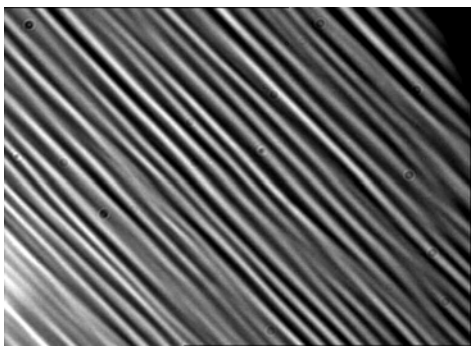

Fig. 3.29 Microscope image of holographic grating using eosin photopolymers.

3.5 Acridine Orange photopolymer

Acridine orange (AO) has been used to stain the DNA [23]. There is not information about its use as photosensitizer in photopolymers. In fig 3.30 the chemical structure of acridine orange is shown.

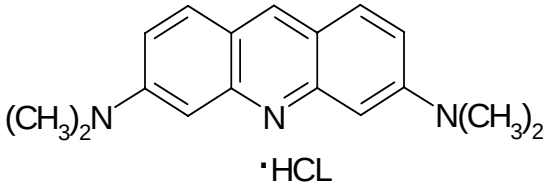

Fig. 3.30 Chemical structure of acridine orange.

In fig. 3.31 the absorption spectra of the acridine orange measured in water solution at different concentration are shown. AO absorbs in the range between 450 nm and 515 nm presenting two main bands around 470 and 492 nm respectively. The first band increases while the second band diminished by augmenting the AO concentration.

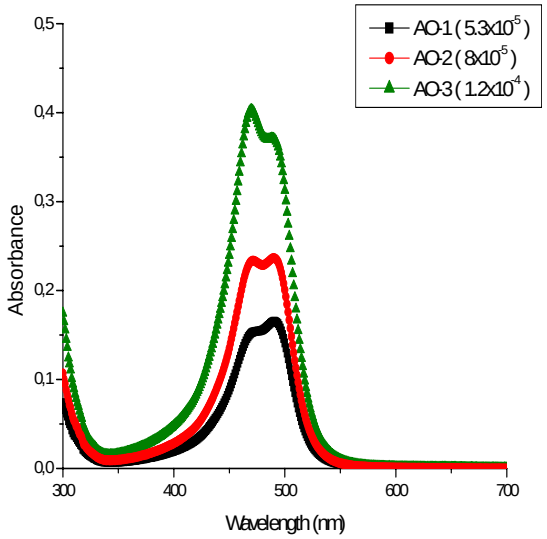

Fig. 3.31a UV/Vis spectra of acridine orange (AO1-3) in 2.5 ml water solution.

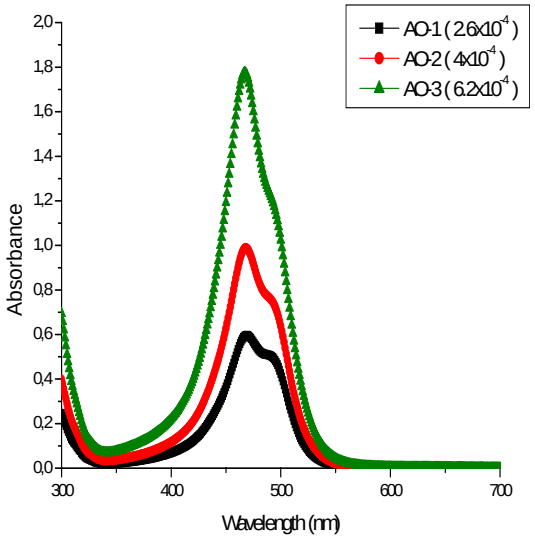

Fig. 3.31b UV/Vis spectra of the acridine orange (AO1-3) in 25 ml water solution.

A series of photopolymers were fabricated using acridine orange as photosensitizer in acrylamide based photopolymer. The photopolymers were made by combining all the monomers (AA, BSA), initiator (TEA) dissolved in a PVA matrix solution at 10% wt/v using the compositions shown in table 3.14 Keeping constant all the material but varying the AO content.

Table 3.14 Composition of AO pre-polymer solutions.

AO photopolymer	[AO] (M)	[Acrylamide] (M)	[BSA] (M)	[TEA] (M)
1	5.32×10^{-5}	0.452	0.052	0.605
2	7.99×10^{-5}	0.452	0.052	0.605
3	1.25×10^{-4}	0.452	0.052	0.605
4	1.99×10^{-4}	0.452	0.052	0.605

As shown in the fig 3.32, the absorption spectra in dried film reveals the acridine orange can be used as photosensitizer for green holographic recording as the maximum absorption band was found to be at 492 nm. The second band observed at 469 nm in the previous measurements in water solution has a small contribution.

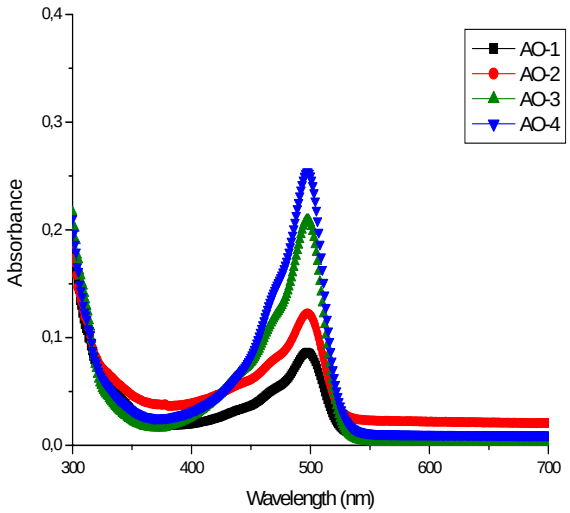

Fig. 3.32 UV/Vis spectra of acridine orange photopolymers (AO-1-4).

In order to characterize the performance of the material, we used the basic transmission setup to record holographic gratings described previously. The transmission grating parameters used are shown in table 3.15.

Table 3.15 Parameters used for gratings recording using AO.

Photo-polymer	θ/2 (°)	**WB (nm)**	**RB (nm)**	**Λ (μm)**	**SF (lines/mm)**	**I (mW/cm²)**	**θ_B (°)**
AO	34	514.5	633	0.46	2173	166	43.4 (T) 42.3 (E)

where θ/2 is the half-angle between the interference beams; WB and RB are the writing and reading beam respectively; Λ is the fringe period; θ_B(T,E) are the theoretical and experimental Bragg angle and I is the recording intensity.

The evolution of the diffraction efficiency as a function of exposure time was monitored in fig. 3.33. The development of the efficiency in photopolymers (AO2-4) follows the same tendency; it augments to its maximum value then decreases and becomes stable during the elongated exposure. In the case of AO-1 it increases up to saturation and then stabilizes during illumination. The behaviour of the diffraction efficiency increases by increasing the dye content up to certain limits, 7.99×10^{-5} M of AO concentration, a further increase comes with a decrease in the efficiency. As evident in the fig 3.33, it increases notably from AO-1 to AO-2 then suffers a slight decrease as the dye continues increasing (the case of AO-3-4). This can be supported through the manifestation of a small band at 470 nm in the absorption spectra for the cases of AO3-4 (fig 3.34) that can lead to possible formation of dimmers [17]. We can thus summarize saying that the DE grows in AO1-2 remarkably and then decreases faintly and then remains almost constant with the increase in the dye concentration during the exposure time.

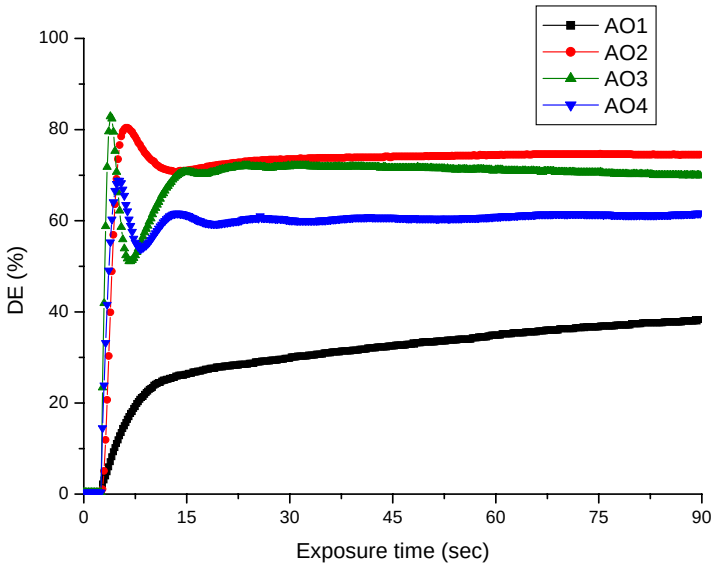

Fig. 3.33 Growth of diffraction efficiency during exposure time at different concentration of acridine orange.

In table 3.16, it was found that the photopolymer sensitivity increases significantly from AO1 to AO3. If we continue increasing the dye concentration its variation is negligible, increasing slightly from AO-2 to AO-3 then decays insignificantly. The trend is that the sensitivity of the material decreases with concentrations of AO greater than 7.99×10^{-5} M. The reason for this is the possible competitive polymerization mechanism that is produced when high concentrations of AO are used [11]. In the case of RIM, an important grating parameter, it is proportional to the diffraction efficiency, which experiences a significant increase from 1.40×10^{-3} to 4.13×10^{-3} for the AO-1 and AO-3 respectively, for further concentrations it decreases with a slightly lower value than photopolymer AO-3.

Table 3.16 Optical parameters of photopolymers AO1-4.

AO photopolymer	DE (%)	Sensitivity (cm/J)	RIM	Thickness (μm)
1	11.1	245.3	1.40×10^{-3}	36
2	69.2	612.5	4.06×10^{-3}	36
3	70.7	619.1	4.13×10^{-3}	36
4	68.1	607.7	4.01×10^{-3}	36

The angular response of the four photopolymers using different AO content as a function of diffraction efficiency was measured by rotating the photopolymer from the position satisfying the Bragg condition; as is shown in fig. 3.34. In the case of high dye content, the photopolymer AO2-4, there is no significant differences in their angular widths, but in the case of AO1 (the photopolymer with less dye content) the angular width is narrower than the rest [24]. The side lobe (first diffracted order) was visible for all photopolymers apart from the zero diffracted order representing the formation of thick holograms.

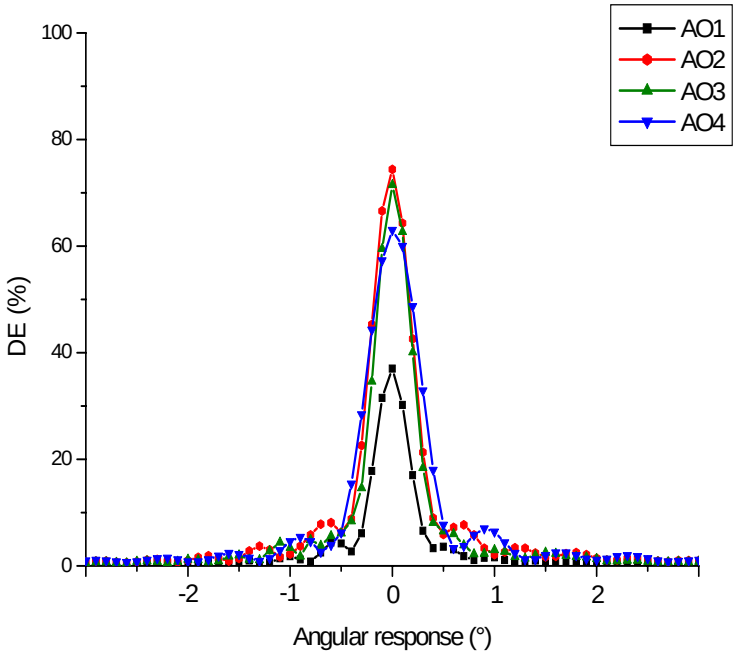

Fig. 3.34 Angular Selectivity of diffraction efficiency of photopolymers AO-1-4.

We observed that the diffraction efficiency as well as the sensitivity started to decrease slightly after photopolymer AO3. This could be because a decrease in the relative content of photopolymerisable acrylamide or the specific interaction between AA and TEA for AO3-4. As for the interaction, the hydroxyl group of TEA is able to be hydrogen bonded to the amide group of acrylamide. This fact may lead to limit the acrylamide to move freely (diffusion) resulting in a decline of diffraction efficiency as well as the sensitivity. Figure 3.35 shows the DSC measurements on the photopolymers containing AO 1-4 .

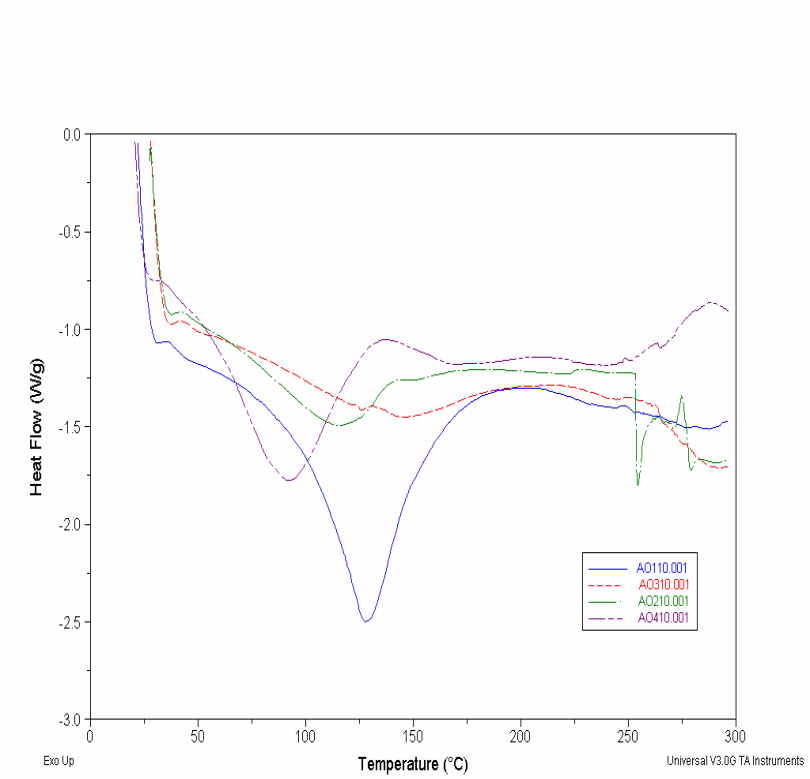

Fig. 3.35 DSC thermogram of the acridine orange photopolymers (AO-1-4).

According to fig. 3.36, using FT-IR measurement we could observe that the peak intensity of acrylamide (1670cm^{-1} C=O stretch, 1605cm^{-1} NH2 deformation in amide) does not change significantly in all AO photopolymers, indicating thus, the deterioration in the optical properties for AO3-4 compared to AO1-2 is mainly affected by the relative content of AA.

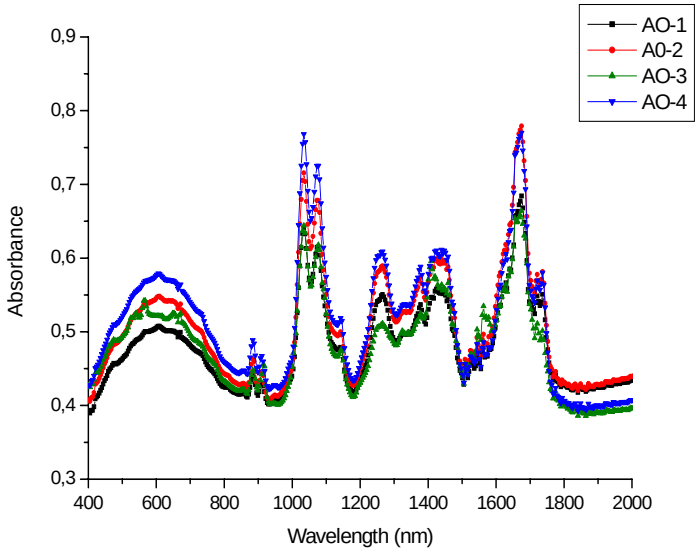

Fig. 3.36 FTIR spectra of the polymerized acridine orange photopolymers (AO-1-4).

The signature of volume grating formation by interference pattern in AO photopolymers can be seen in the fig. 3.37, a microscope image using 60x of magnification.

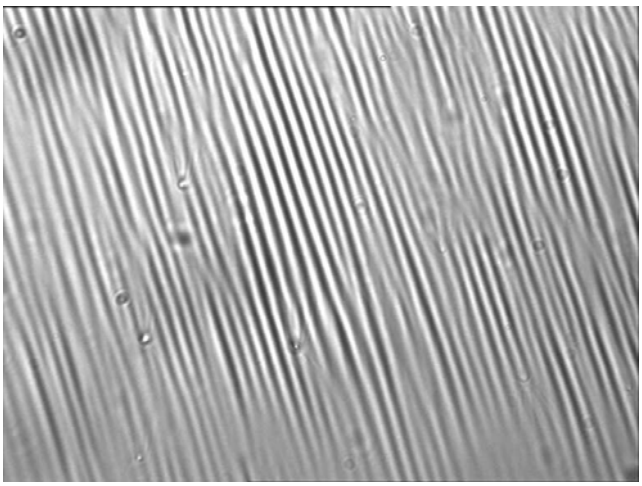

Fig. 3.37 Microscope image of an acridine orange photopolymer.

3.6 Effect of BSA in Photopolymer

As an important step was the study of the effect of BSA in the photopolymer formulations by replacing this cross-linker agent to n,n-dimethylacrylamide (DMAA). Also the inclusion of this new component makes it possible to use high concentrations of AA with less risk of surface crystallization during exposure time, it also facilitates the homogenization of the chemical species of the recording material by favouring their diffusion [25].

In the table 3.17 the composition for the experiment replacing BSA for DMAA is shown. Using the same DMAA content used

Table 3.17 Composition for the first experiment using DMAA as cross-linker agent in AO photopolymer.

Photopolymer	**[AO] (M)**	**[Acrylamide] (M)**	**[DMAA] (M)**	**[TEA] (M)**
AO-DMAA	1.99×10^{-4}	0.33	0.052	0.605

In fig. 3.38, we observed the effect of the inclusion of DMAA in our photopolymer. The evolution of the diffraction efficiency during exposure time differs from the previous experiments. The efficiency decays rapidly after reaching saturation reaching to values almost close to zero. This decay is more pronounced by increasing the thickness, as it can be observed in the fig 3.38b, as the thickness augments the response time to reach zero is smaller meaning the diffraction decays faster at higher

thickness of the material. As can be seen the diffraction efficiency increases until it reaches a maximum of nearly 10%. However when the exposure continues to increase the diffraction efficiency drops almost to zero. The shape of this curve suggests that the photopolymer exhibits over-modulation effects [26]. A higher DE is reached outside the Bragg condition and when this condition is fulfilled the DE drops to zero. This is due to the fact that when the Bragg condition is fulfilled the DE is determined by the function $\sin^2(\nu)$ [26]. At this point, over-modulation of the index occurs and this can be explained mainly by polymerization of the monomer in the bright zones. In other words, the refractive index modulation is so great that ν takes on a value greater than $\pi/2$. This means that the diffraction efficiency at the Bragg condition begins to decrease (since the diffraction efficiency at the Bragg angle is governed by the function $\sin 2\nu$, whereas it increases at the lateral lobes [26].

Very high values of RIM are necessary to obtain a value of $\nu=\pi$ however such values were obtained in our materials due to the fact that a high acrylamide concentration (~0.43 M) was used thereby enabling us to observe the non-linear behaviour of this material which is known as the overmodulation effect [27]. In this way we were able to observe that the DE decreases rapidly after reaching its maximum value not because of the grating is destroyed but the index modulation is too high.

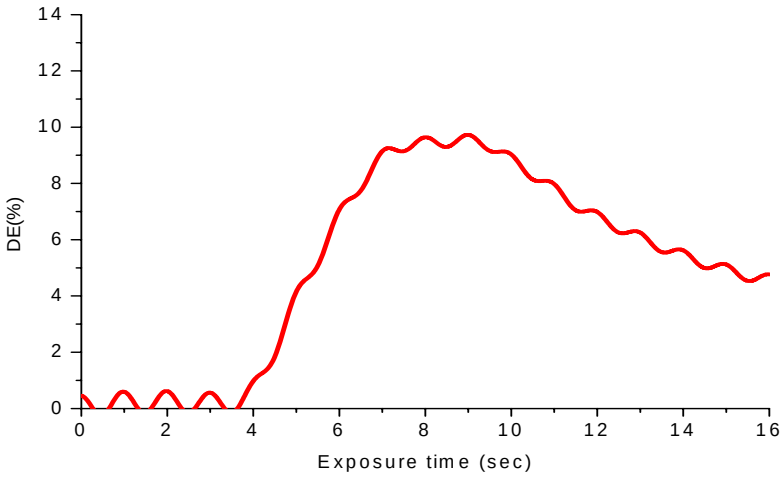

DE ≈ 9% for a 15 μm thick film.

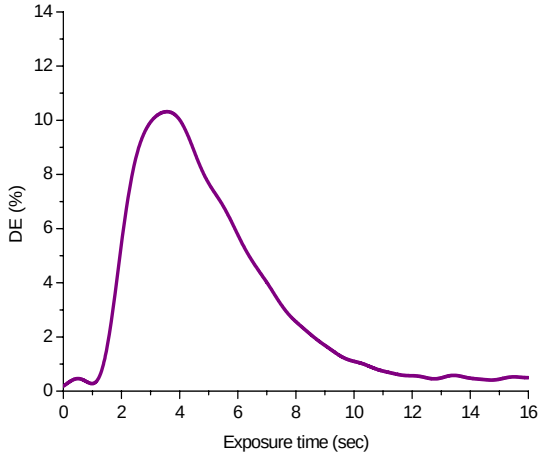

DE ≈ 10.3 % for a 77 μm thick film.

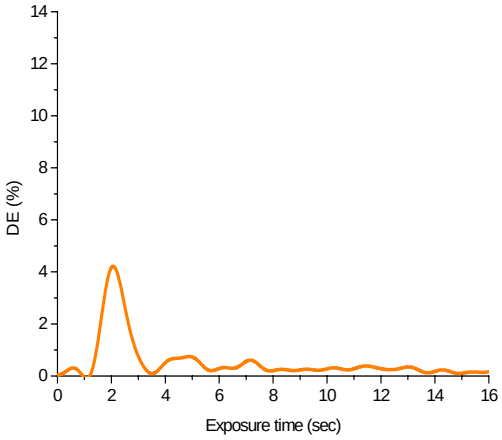

DE ≈ 4.3% for a 96 μm thick film.

Fig. 3.38 Diffraction efficiency as a function of time for photopolymer AO-4 using DMAA as cross-linking monomer for different thickness.

In an attempt to improve our previous results using DMAA as second monomer, an optimization of the composition of the components of the pre-polymer syrup was carried out. For these experiments, photopolymers using BSA and DMAA as cross-linker agents were fabricated. The DMMA concentration used here was increased in

50% compare to the first experiments. In table 3.18, the composition of the components used in this section is shown.

Table 3.18 Composition of the photopolymer comparing different cross-linker agents.

AO photopolymer	[AO] (M)	[Acrylamide] (M)	[Cross-linker] (M)	[TEA] (M)
4-B	1.99×10^{-4}	0.452	0.052 (BSA)	0.605
4-D	1.99×10^{-4}	0.452	0.078 (DMAA)	0.605

In fig. 3.39, the UV-Vis absorption spectrum for photopolymer using different cross-linker monomers is presented. It could be observed not significant differences between their spectra. Both photopolymers exhibits the same absorption peak at 500 nm of wavelength.

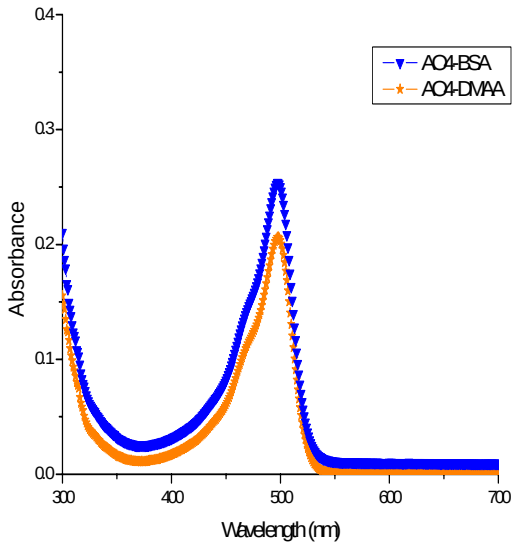

Fig. 3.39 UV/Vis spectra of acridine orange photopolymer AO-4 using different cross-linking monomers (BSA and DMAA).

Fig. 3.40 shows the performance of diffraction efficiency as a function of exposure time when a holographic diffraction grating is stored on the AO4 photopolymer layers using two types of cross-linker agents. The formation of gratings was recorded using the set up and parameters used in the first experiments using AO as photosensitizer. It can be seen that the diffraction efficiency increases and reaches their maximum values of 60 and 50% for AO4-B and AO4-D respectively and then stabilizes. We observed the grating formation for the case of AO4-D was stable for the whole time period of 90 sec compared to the previous results. The diffraction efficiency for material with DMAA remains stable longer by increasing the DMAA content.

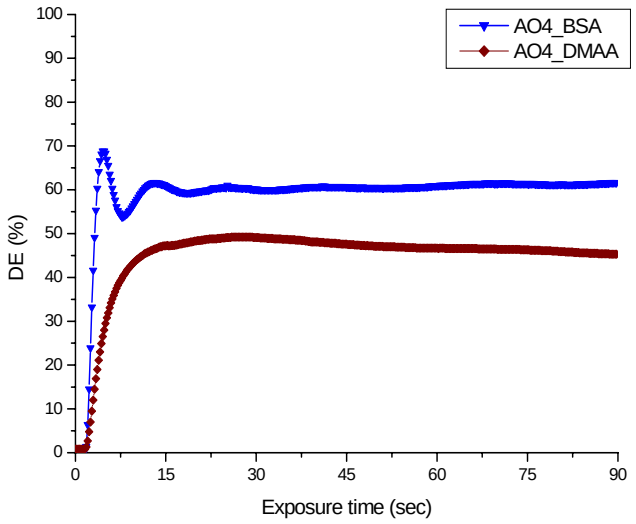

Fig. 3.40 Diffraction efficiency as a function of time for photopolymer AO-4 using different cross-linking monomers (BSA and DMAA).

In table 3.19, the optical parameters obtained by the comparison between BSA and DMAA as alternative monomer is exhibited. We observed, by replacing the BSA for

DMAA the diffraction efficiency, sensitivity and RIM decreases by almost 50% despite the concentration of DMAA over BSA was higher.

Table 3.19 Optical parameters of photopolymers AO4 using different cross-linking agents after 2.273 sec.

AO photopolymer	DE (%)	Sensitivity (cm/J)	RIM	Thickness (μm)
4 (BSA)	68.1	607.7	$4.01x10^{-3}$	36
4 (DMAA)	28.0	389.6	$2.31x10^{-3}$	36

The temporal evolution of the angular response as a function of diffraction efficiency is shown in fig. 3.41. The angular response for both materials was after recorded 3 min after exposure was finished. At this point, the over-modulation effect occurs, we observed that the diffraction efficiency for AO4-D decays by 50% of its original value obtained during exposure while the efficiency for A04-B remains the same. No difference was observed in the angular width by replacing BSA for DMAA but the satellite peaks (first diffracted order) for AO4-D are almost vanished compare to AO4-B are clearly resolved. It was foreseen that if we continued to measure the angular response for AO4-D at different times the efficiency was going to reach zero due to this effect [25].

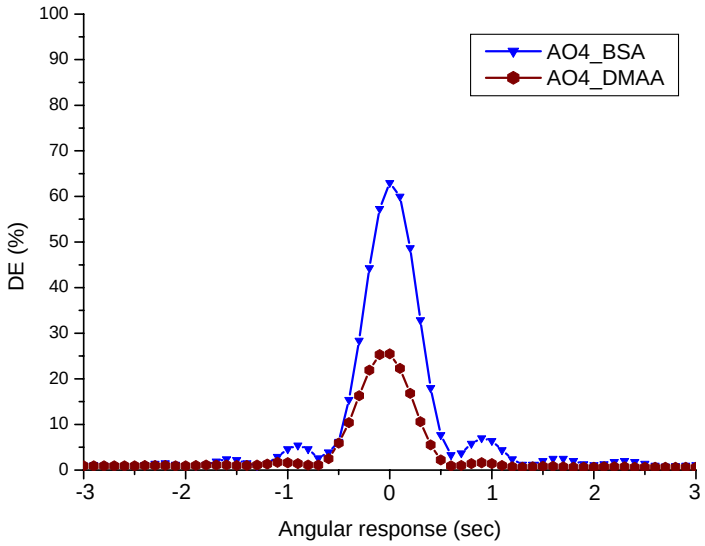

Fig. 3.41 Angular Selectivity of diffraction efficiency for photopolymer AO-4 using different cross-linking monomers (BSA and DMAA).

In fig. 3.42 the DSC thermogram and FT-IR measurements were carried out to try to understand this effect. The Tg value for the AO4-D is higher than the one obtained with AO4-B representing that the material becomes more rigid and the diffusion is more difficult leading to a decrease in DE and RIM as well [16].

Specific interactions between AA and TEA can reduce the mobility of AA affecting the diffusion process that an important effect on the photopolymerization of AA resulting in a decrease of both diffraction efficiency and energetic sensitivity for AO4-D [16]. It was illustrated from the results of FT-IR measurements that the characteristic peak intensity of acrylamide (1670cm-1 C=O stretch) are smaller in the of AO4-B compare to AO4-D meaning more acrylamide was converted to polymer in the case of the photopolymer using BSA as cross-linker agent.

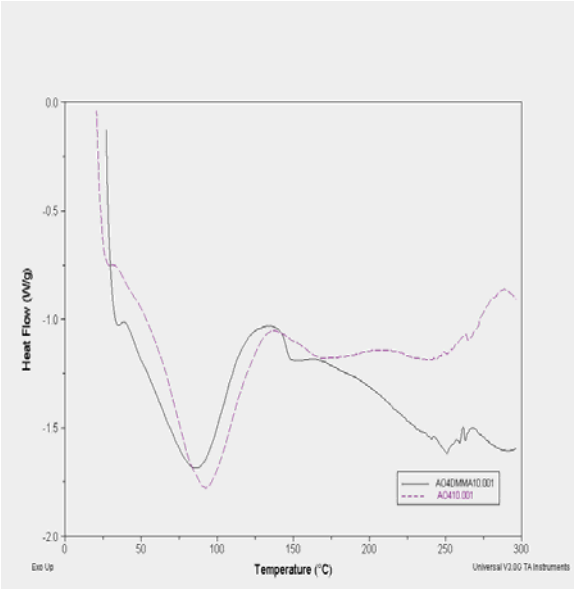

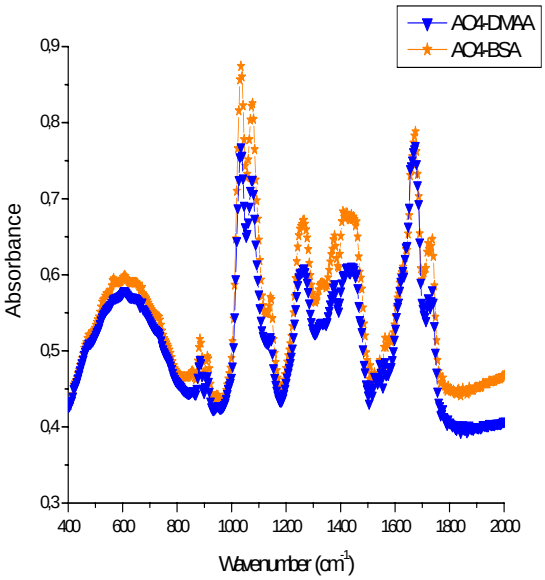

Fig. 3.42a DSC thermogram of the acridine orange photopolymer AO-4 using BSA and DMAA as cross-linking monomers.

Fig. 3.42b FTIR spectra of the polymerized acridine orange photopolymer (AO-4-BSA-DMAA).

We successfully explored here that by adding DMAA to the composition of the photopolymer, it is possible to control certain properties of the polymer film, once it is dry. As a consequence, it can be said that if DMAA is not used it is possible to preserve the stored gratings for longer time by replacing it for BSA, but this is not the case if DMAA is used [26,27].

II. Reflection volume phase gratings

By comparing the results presented in the last section to those obtained in chapter 2 with a red sensitizing dye, we experienced that the volume phase transmission gratings can be stocked in photopolymers with even higher spatial frequency as the wavelength of the recording beam is lowered from red to green. We also observed by rotating the sample, parallel to the intersecting beams, the recording process can lead to achieve an improved grating quality with even higher spatial frequency. Although this process has limitations (Reflection holograms are formed of fringes, the plane of which is parallel to the plane of the emulsion. These fringes are more difficult to record than those of the transmission gratings: they are more sensitive to shrinkage effects due to the polymerization reaction) [28] and its not always possible to use this step as an advantage, we can still expect a further increase in the capacity of the same recording media just by changing the recording geometry from transmission to reflection. Reflection recording geometry allows the stockage of the optical information through bulk of the recording material hence the whole thickness of the recording media can be used to store the induced gratings. In coming sections we study the photopolymer compositions already explored in section I with an aim to further enhance the storage capacity of the green sensitized photopolymers.

3.7 Reflection experimental set-up

We first describe the experimental set-up used for the grating formation using this new geometry. Figure 3.43 depicts the set-up used for recording the reflection phase gratings in our studies. Distinct from the previously used transmission set-up, the two Ar-ion laser beams, B1 and B2, here propagate from the opposite directions and overlap in the film, S [29]. The beams propagate at 3° and 6° with respect to the film normal, so that beam 1*R*, reflected by the film surface and does not coincide with transmitted beam 2. Two quarter-wave plates convert the linear polarization of the beams to right circular polarization. As the beams are counter propagating, however, their electric vectors rotate in opposite senses, and the intensity of the resulting light that induces the holographic modulation in the sample is constant.

The gratings were written using a line from an Argon ion laser that was split into two beams using a 50:50 cubic beam splitter and recombined at an angle of 30° with respect to the normal from the opposite sides of the sample. Sample was mounted on a rotary stage. For writing, the samples were tilted 3° in order to separate the reflection of the glass and distinguish the diffracted and transmitted beams. The gratings were probed with the same laser at the same writing wavelength at low intensity for further unwanted polymerization.

The sample plane is set slightly tilted from the equal-phase plane of the interference field of the two beams, such that the part of beam 2 that is reflected by the sample surface does not hit detector D, which is used to record only the light in the direction

of beam 1. The two beams make a crossing angle of 30° and therefore form an interference modulation of particular period with its equal-phase plane approximately parallel to the surface of the sample. Thus the two beams split from an Argon-ion laser interfere at the sample area. Beam 2 is vertically polarized (perpendicular to the plane of the optical table). The beams hit the film at almost the same angle, so the planes with equal phase differences are almost parallel to the film surface.

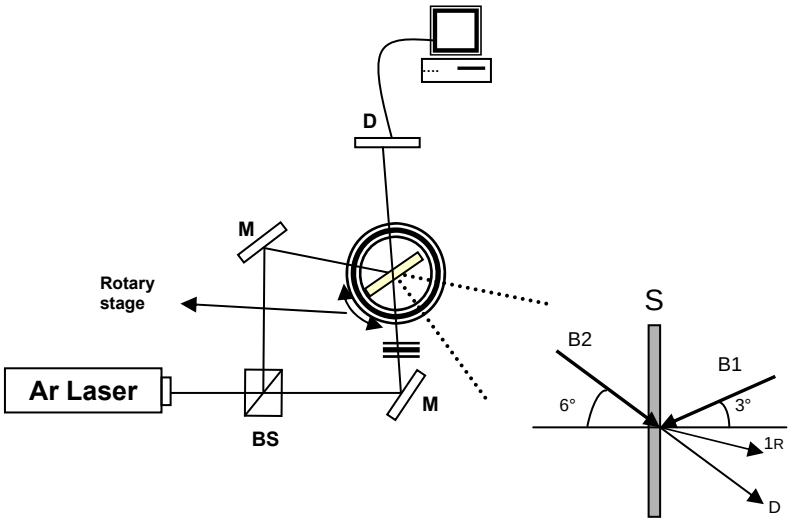

Fig. 3.43 Experimental set up used in reflection experiments.
M: mirrors, BS: beam splitter, D: detector.

The Diffraction efficiency in reflection geometry is defined [30-32] as :

$$\eta_r = \tanh^2\left(\frac{\pi\,\Delta n\,L}{\lambda}\right) \approx \left(\frac{\pi\,\Delta n\,L}{\lambda}\right)^2 \qquad (1)$$

$$\text{and} \quad L = \frac{2\pi w^2}{\lambda} \qquad (2)$$

where L is the length of the grating, Δn is the refractive index modulation, λ is the wavelength and w is the radius of the laser beam.

The fringe spacing for reflection geometry is defined [33,34] as:

$$\Lambda = \frac{\lambda}{2n\cos\theta_{\text{int}}} \qquad (3)$$

Where θ_{int} is the internal angle of the beam with respect to the surface normal and n is the refractive index of the composite. The $\theta_{c\text{-}int}$ is the complementary angle inside the sample and is calculated according to Snell's Law. It is defined as:

$$n \text{ x } \sin\theta_{c\text{-}int} = n \text{ x } \sin(\theta_{c\text{-}ext})$$

$$\theta_{\text{int}} = \frac{n_{ext} \; x \; \theta_{ext}}{n_{\text{int}}}$$

In the following figures we observed that the first increase of the signal when the laser is switch on should correspond to the transmitted beam (no grating formation), then the signal is raised, this could be due to the development of holographic reflection, meaning the grating formation [29].

3.8 RB photopolymer for reflection holographic gratings recording

A set of three photopolymers using Rose Bengal as a dye were fabricated in order to record reflection holographic gratings. The mixture of the components early described (AA, BSA, TEA, RB) were dissolved in a PVA solution at 10% wt/v. An optimization of the acrylamide (by increasing its content) was carried out in this kind

of photopolymer. In table 3.20, the composition of the component is shown. The thickness of this photopolymer was 27 μm.

Table 3.20 Composition of the components for reflection gratings in different photopolymers.

Photopolymer	AA (M)	TEA (M)	BSA (M)	Dye (M)
3a	3.7×10^{-1}	0.602	0.052	2.88×10^{-5} (RB)
3b	4.05×10^{-1}	0.602	0.052	2.88×10^{-5} (RB)
3c	4.33×10^{-1}	0.602	0.052	2.88×10^{-5} (RB)
3d	4.05×10^{-1}	0.602	0.052	0.064%v/v Eosin)

To illustrate the performance of RB photopolymers for recording holographic reflection data storage, gratings were recorded using the reflection geometry set up described. In the table 3.21 the parameters used for the characterization are illustrated.

Table 3.21 Reflection geometry parameters used to evaluate the RB and Eosin photopolymers.

Photo-polymer	θ/2 (°)	WB (nm)	RB (nm)	Λ (μm)	SF (lines/mm)	I (mW/cm^2)	θ (°)
RB	30	514.5	514.5	0.210	4761	153.3	33.0 (I) 35.5 (F)
Eosin	30	514.5	514.5	0.210	4761	153.3	33.0 (I) 37.0 (F)

where θ/2 is the half-angle between the interference beams; WB and RB are the writing and reading beam respectively; Λ is the fringe period; θ (I,F) are the initial and final reading angle (before and after shrinkage) and I is the recording intensity.

Figure 3.44 represents the angular selectivity of transmission gratings with previously obtained 95% diffraction efficiency. It was recorded in our photopolymer RB-3 under 1943 lines/mm spatial frequency, written at 514.5 nm and probed at 633 nm using a He-Neon laser. Using the same material, reflection gratings were recorded with a diffraction efficiency of 6.8% under 4800 lines/mm spatial frequency (see fig 3.44b).

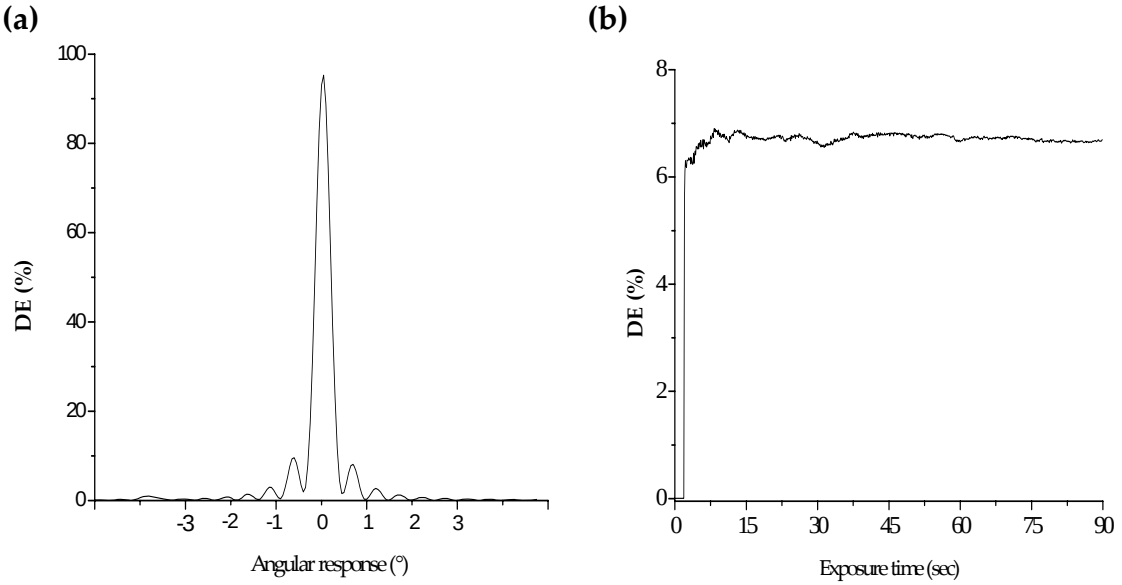

Fig. 3.44 (a) Evolution of diffraction efficiency during time for RB_3a film.
(b) Angular selectivity as a function of diffraction efficiency for RB-3b film.

In order to increase the diffraction efficiency, the monomer concentration must be optimized, due to the fact that the index modulation is proportional to the concentration of the reacted monomer [11]. Table 3.21 shows the effect of increasing

the **AA** concentration by 14 % compared to the first concentration used. This lead us to increase the efficiency from around 6.8 % to 12.33 %, showing that a higher **AA** concentration can significantly raise the efficiency. Although still avoiding precipitation in the film. Figures 3.45 (a, b) represent the influence of **AA** concentration on diffraction efficiencies as a function of exposure time. We limited further increase in **AA** concentration in order to avoid precipitation.

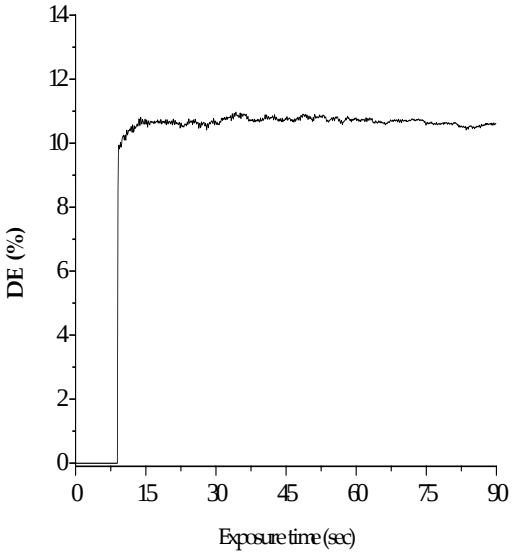

Fig. 3.45a Evolution of diffraction efficiency during time for RB-3b film.

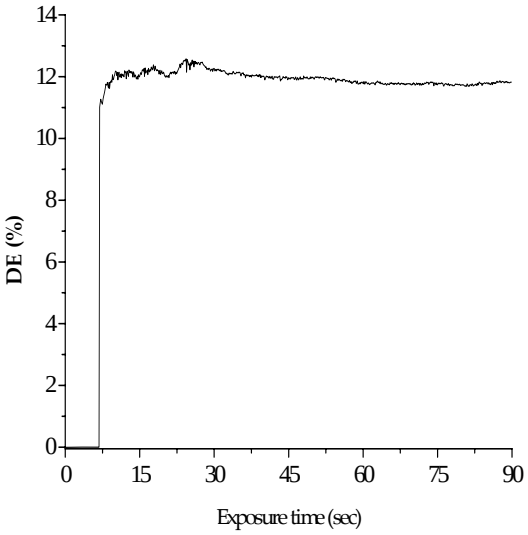

Fig. 3.45b Evolution of diffraction efficiency during time for RB-3c film.

3.8.1 Effect of photosensitizer.

Photosensitizer has a crucial role in photopolymeric systems. As discussed in chapter 1, after the photoreduction of the sensitizing dye, the radicals are produced. We studied the effect of photosensitizers on DE by changing Rose Bengal to Eosin at

unchanged concentration for all other components. Figure 3.46 represents the diffraction efficiency obtained when eosin was the dye. We notice that diffraction efficiency raised to 17% at similar concentration (2.88 $x10^{-5}$ M) just by changing the dye. An enhancement of almost 5% comes due to the fact that Eosin has a higher yield of triplet excited states than Rose Bengal [34]. This provides ample time for **AA** to react with the dye which further increasing the amount of polymerization and thus finally increasing DE because of the increased sensitivity.

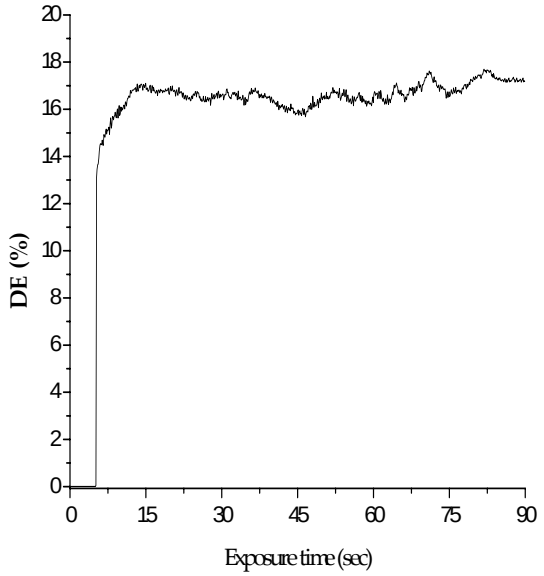

Fig. 3.46 Diffraction efficiency as function of exposure time recorded in reflection geometry using Eosin film.

3.8.2 Sensitivity

The sensitivity of the recording material is defined as:

$$S = \frac{\eta^{1/2}}{I \times \tau \times d} \qquad (6)$$

where τ: exposure time to reach maximum efficiency, d: thickness of the material, P: power of each beam and A: illuminated area in the recording material.

We observed that **AA** concentration has a direct effect on the overall sensitivity of the recording material. As discussed in section 3.1, by increasing the concentration of **AA** one can observe further increase in sensitivity. Sensitivity calculated using equation (6) shows that increasing the **AA** concentration by 20% remarkably increases the sensitivity of our films. Figure 3.47 presents the evolution of sensitivity and DE as a function of **AA** concentration. Table 3.22 summarizes the change in sensitivity and DE with respect to the concentration of **AA** with Rose Bengal as the sensitizer.

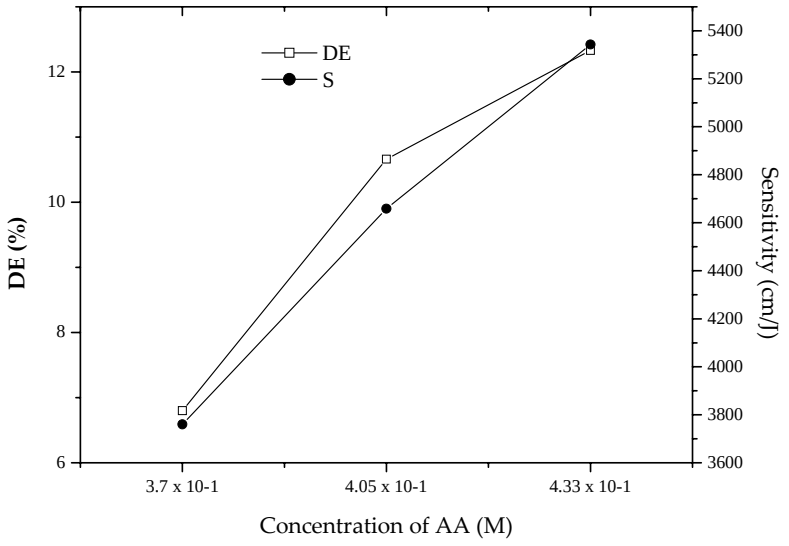

Fig. 3.47 Effect of AA concentration on sensitivity (filled circles) and diffraction efficiency (open squares) using Rose Bengal .

Table 3.22 Sensitivity as a function of AA concentration using Rose Bengal as sensitizer. DE values are also given.

Photopolymer	DE (%)	Sensitivity (cm/J)
3a	6.8	3760.11
3b	10.66	4658.79
3c	12.33	5342.51

Sensitivity remains high even after changing the photosensitizing dye. Although significant increase in DE was observed using Eosin based films, almost similar sensitivity of Eosin based films (see table 3.23) suggests that **AA** basically defines the sensitivity in such films.

Table 3.23 Effect of photosensitizing dye on recording parameters for RB and Eosin film.

Dye	Diffraction Efficiency (%)	Sensitivity (cm/J)
RB	10.66	4658.79
Eosin	16.98 ≅ 17	5785.83

3.8.3 Shrinkage

High sensitivity of our recording media caused relatively high shrinkage observed while re-reading the stored gratings. Shrinkage is a common phenomenon in photopolymer based recording media which comes into picture because of the swelling or shrinking of the film under illumination of the writing beam [35]. This means that the read-out angle varies from the recording one (Bragg's angle).This

variation results in a change of the grating period due to the partial change in the thickness or index of the film causing an alteration of the readout beam angle to achieve maximum diffraction efficiency. The fractional change in the thickness was calculated by relation defined in chapter 1. Irrespective of the **AA** concentration we observed the same shrinkage of ~ 10% for films containing Rose Bengal. Whereas the films with Eosin suffered relatively higher shrinkage of ~ 16% compare to the Rose Bengal one at constant film thickness of 27 μm. Our immediate interest is to avoid shrinkage in our films by controlling undesired diffusion of the monomer.

3.8.4 Effect of the exposure time on the diffraction efficiency

In order to study the effect of recording exposure in the diffraction efficiency, a experiment varying the exposure time was performed using RB photopolymers. Decreasing the cross-linker monomer (BSA) content in photopolymer RB-3 by 12.5 % and varying the exposure time the efficiency reflection gratings were recorded. The reactant composition used in the photopolymer is illustrated in the table 3.24.

Table 3.24 Composition of the pre-polymer solution (5 ml).

Photopolymer	**AA (M)**	**BSA (M)**	**TEA (M)**	**RB (M)**
3a	3.7×10^{-1}	4.5×10^{-2}	0.605	2.8×10^{-5}

In fig 3.48 the evolution of the diffraction efficiency varying the recording exposure time is shown. An improvement in the efficiency was observed by increasing the exposure time, from 8.94% to 12.23% for 20 and 40 seconds respectively. An explanation of this trend is at longer exposure time the density of the photons in a given period of time will be lesser so the concentration of radicals will be smaller resulting in a termination rate so a single radical can live longer causing the polymerization of more acrylamide molecules.

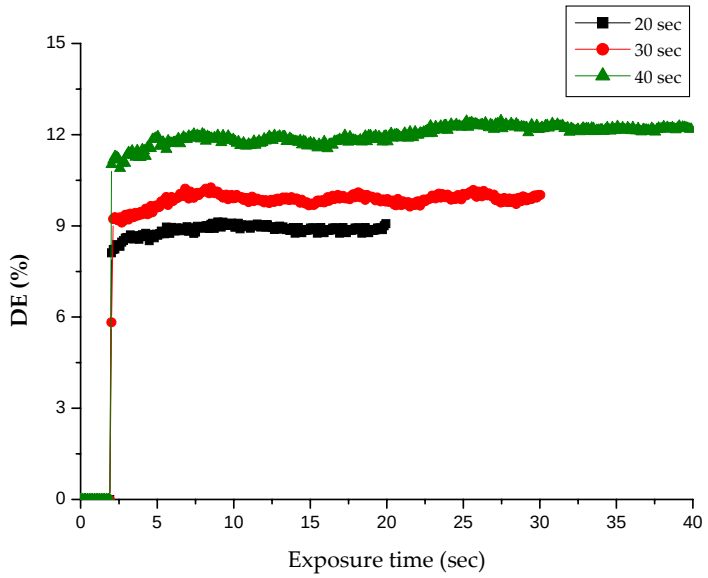

Fig. 3.48 Diffraction efficiency as function of exposure time using Rose bengal film varying the exposure time.

3.9. Acridine orange for reflection geometry

We obtained diffraction efficiency as high 7.3% when AO was used as a sensitizing dye in AA based photopolymer. Table 3.26 represents the value obtained for diffraction efficiency and sensitivity of the acridine orange photopolymer experimental conditions are summarized in table 3.27.

Table 3.26 Acridine orange photopolymer in reflection geometry

Photopolymer	**AA (M)**	**BSA (M)**	**TEA (M)**	**AO (M)**	**DE (%)**
AO	4.05×10^{-1}	4.5×10^{-2}	0.605	7.99×10^{-5}	7.30

To characterize the AO photopolymers as material to create reflection holographic gratings we recorded using the same set up used previously. In table 3.27 the parameters used for the recording are illustrated.

Table 3.27 Reflection geometry parameters used to evaluate the AO photopolymers.

Photo-polymer	**θ/2 (°)**	**WB (nm)**	**RB (nm)**	**Λ (μm)**	**SF (lines/mm)**	**I (mW/cm²)**	**θ (°)**
AO	30	514.5	514.5	0.210	4761	153.3	33.0 (I) 37.0 (F)

where θ/2 is the half-angle between the interference beams; WB and RB are the writing and reading beam respectively; Λ is the fringe period; θ (I,F) are the initial and final reading angle (before and after shrinkage) and I is the recording intensity.

Figure 3.49 represents the efficiency using the pre-established formulation shown in table 3.26 using acridine orange as photosensitizer at a particular concentration in order to achieve absorbance of 0.15. We observed the diffraction efficiency value achieved with acridine orange as photosenstizer was lower compare to the one obtained with Rose Bengal and eosin.

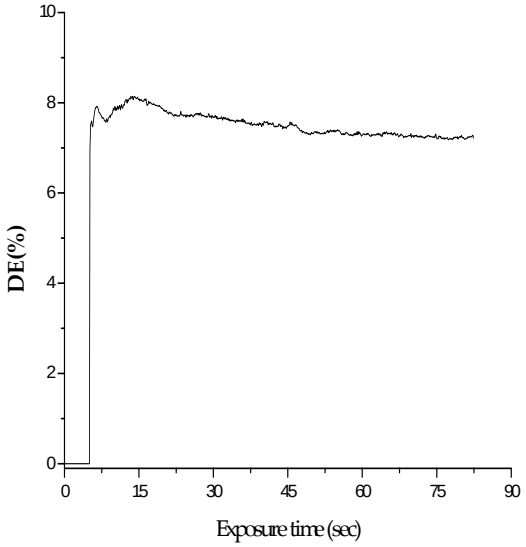

Fig. 3.49 Diffraction efficiency as function of exposure time recorded in reflection geometry using Acridine orange.

3.10 Conclusion

In this chapter we first explored the suitability of green wavelength recording for holographic data storage through formation of volume phase gratings using both the transmission and reflection recording geometries. Effect of material purity, at optimum conditions shows a significant effect on the recording parameters. Dynamics of grating formation and characterization are probed using various supporting characterizations which helped us to optimize the whole photopolymer system. Grating periods thus stored in photopolymers with Rose bengal, Eosin, Acridine orange etc dyes have shown high diffraction efficiencies close to 95%. We demonstrated the increase of spatial frequency from 1900 lines/mm to close to 2200 lines/mm just by slight change in recording parameters. The effect of shrinkage after recording is probed through recording the angular response of the stored gratings in the thick polymer films.

A further capacity enhancement was achieved using the reflection geometry recording. Volume grating formation in the photopolymer studied in reflection geometry is demonstrated with the same sensitizing dyes where spatial frequency exceeds 4760 lines/mm.

References

[1]. F. del Monte, O. Martinez, J. A. Rodrigo, M.L. Calvo and P. Cheben, "A volume holographic sol-gel material with large enhancement of dynamic range by incorporation of high refractive index species. Adv. Mat. 18, 2014-2017, (2006).

[2]. H.J. Caufield, *Handbook of optical holography*, (1979).

[3]. H. Sherif, I. Naydenova, S. Martin, C. McGinn and V. Toal, "Characterization of an acrylamide-based photopolymer for data storage utilizing holographic angular multiplexing", J. Opt. A: Pure Appl. Opt. **7**, 255-260 (2005).

[4]. http://en.wikipedia.org/wiki/Recrystallization

[5]. M. Ortuño, S. Gallego, C. García, C. Neipp, A. Belendez and I. Pascual, "Optimization of a 1 mm thick PVA/acrylamide recording material to obtain holographic memories: method of preparation and holographic properties". Appl. Phys. B. 76, 851-857. (2003).

[6]. Y-Ch. Jeong, S. Lee, and J-K. Park," Holographic diffraction gratings with enhanced sensitivity based on epoxy-resin photopolymers", Opt. Express. 15, No.4, 1497-1504, (2007).

[7]. J.R. Lawrence, F.T. O'Neill and J.T. Sheridan. "Photopolymer holographic recording material". Optic 112. No. 10 449-463, (2001).

[8]. C. Sanchez, M.J. Escuti, C Van Heesch, C. W.M. Bastiaansen, D. J. Broer, J. loos and R. Nussbaumer, "TiO_2 nanoparticle-Photopolymer composites for volume holographic Recording", Adv.Funct. Mater **15**, 1623-1629 (2005).

[9]. H. Yao, M. Huang, Z. Chen, L. Hu and F. Gan, "Optimization of two-monomer-based photopolymer used for holographic recording". Mat. Lett. 56, 3–8. (2002).

[10]. I. Naydenova, E. Mihaylova, S. Martin, V. Toal," Holographic patterning of acrylamide–based photopolymer surface", Opt. Express. 13, No. 13, 4878-4889, (2005).

[11]. M.A. khodorkovskii, S.V. Murashov, T.O. Artamonova, A.L. Shakmin, A.A. Belaeva and D.Yu. Davydov, " Fullerene films highly reistant to laser ablation", Technical Phys. 49, No. 2, 258-262 (2004).

[12]. S. Blaya, L. Carretero, R. Mallavia, A. Fimia, R.F. Madrigal, M. Ulibarrena and D. Levy, "Optimization of an acrylamide-based dry film used for holographic recording", Appl. Opt. 37, No. 32, 7604-7609, (1998).

[13]. S. Gallego, M. Ortuño, C. Neipp, A. Marquez and A. Beléndez and I. Pascual, "Maximum effective optical thickness of the gratings recorded in photopolymers", Proc. of SPIE Vol. 5827 (SPIE, Bellingham, WA), 107-117. (2005).

[14]. S. Piazzolla and B. K. Jenkins, "First-Harmonic diffusion model for holographic grating formation in photopolymers", J. Opt. Soc. Am. B. 17, No. 7, 1147-1157, (2000).

[15]. V. Moreau, Y. Renotte and Y. lion, "Characteriztion of Dupont photopolymer: determination of kinetic parameters in a diffusion model", Appl. Opt. 10, 3427-3435 (2002).

[16]. W. S. Kim, Y-Ch. Jeong, J-K Park, Ch-W. Shin, N-K, "Diffraction efficiency behavior of photopolymer based on P(MMA-co-MAA) copolymer matrix", Opt. Mat. 29, 1736–1740, (2007).

[17]. W.S. kim, H-S. Chang, Y-C. Jeong,Y-M Lee, J-K. Park, C-W Shin, N. Kim and H-J. Tak, "A new phase-stable photopolymer with high diffraction efficiency based on modified PMMA", Opt. Comm. 249, 65-71 (2005).

[18]. S. Blaya, L. Carretero, R.F. Madrigal, M. Ulibarrena, P. Acebal and A. Fimia, "Photopolerization model for holographic gratings formation in photopolymers", Appl. Phys. B. 77, 639-662, (2003).

[19]. C. Garcia, I. Pascual, A. Costela, I. Garcia-Moreno, C. Gomez, A. Fimia, and R. Sastre, "Hologram recording in polyvinyl alcohol_acrylamide photopolymers by means of pulsed laser exposure" Appl. Opt. 41, No. 14, 2613-2610, (2002).

[20]. S. Gallego, M. Ortuño, C. Neipp, A. Márquez and A. Beléndez, I. Pascual, J. V. Kelly and J. T. Sheridan, "Physical and effective optical thickness of holographic

diffraction gratings recorded in photopolymers", Opt. Express. 13, No. 6 1939-1947, (2005).

[21]. S. Gallego, M. Ortuño, C. Neipp, A. Márquez, A. Beléndez and I. Pascual, "Characterization of polyvinyl alcohol_acrylamide holographic memories with a first-harmonic diffusion model", App. Opt. 44, No.29, 6205- 6210, (2005).

[22]. E. Fernández, C. García, I. Pascual, M. Ortuño, S. Gallego, and A. Beléndez, "Optimization of a thick polyvinyl alcohol–acrylamide photopolymer for data storage using a combination of angular and peristrophic holographic multiplexing", Appl. Opt. 45, No.29, 7661-7666, (2005).

[23]. M.K. Dutt, "Aqueous solution of acridine orange in the staining of DNA-aldehyde", Cellular and Mol Life Sci. 30, No. 6, 667-669, (1974).

[24]. S. Blaya, L. Carretero, R.F. Madrigal, A. Fimia, "Optimization of a photopolymerizable holographic recording material on polyvinylalcohol using angular responses", Opt. Mat. 23, 529-538, (2003).

[25]. S. Gallego, M. Ortuño, C. Neipp, C. García, A. Beléndez and I. Pascual, "Temporal evolution of the angular response of a holographic diffraction grating in PVA/acrylamide photopolymer", Opt. Express. 11, No. 2, 181-190, (2003).

[26]. S. Gallego, M. Ortuño, C. Neipp, C; Garcia, A. Beléndez and I. Pascual, " Overmodulation effects in volume holograms recorded on photopolymers", Opt. Comm. 215, 263-269, (2003).

[27]. N. Suzuki and Y. Tomita, "Diffraction properties of volume holograms recorded in SiO_2 nanoparticle-dispersed methacrylate photopolymer films", Jpn. J. Appl. Phys. 42, L927-L929 Part 2 No. 8A, (2003).

[28]. Y. Defosse, C. Cam and D. J. Lougnot, "Use of a self-developing polymer material for volume reflection hologram recording", Pure Appl. Opt. **2** 437-40. (1993).

[29]. L. Nikolova, T. Todorov, V. Dragostinova, T. Petrova, and N. Tomova, "Polarization reflection holographic gratings in azobenzene-containing gelatine films", Opt. Lett. 27, No. 2, 92-94, (2002).

[30]. H. Kogelnik, Bell Syst. Tech. J. 48, 2909 (1969).

[31]. R. Jallapuran, I. Naydenova, S. Martin, R. Howard, V. Toal, S. Frohmann, S. Orlic and H. J. Eichler, "Acrylamide-based photopolymer for microholographic data storage", Opt. Mat. 28, 1329-1333, (2006).

[32]. P. Hariharan, *Optical holography – Principles, Techniques and Applications*, 2 nd ed. (Cambridge University Press, Cambridge, UK). (1996).

[33]. O-P. Kwon, S-L. Kwon, M. Jazbinsek, P. Gunter and S-H. Lee, "High performance reflections gratings in nematiclike photorefractive polymers", Appl. Phys. Lett. 87, 121910-12, (2005).

[34]. F.T. O'Neill, J.R. Lawrence and J.T. Sheridan, "Thickness variation of self-preocessing acrylamide-based photopolymer and reflection holography", Opt. Eng. 40 (4), 533-539, (2001).

Chapter 4
Novel dyes for blue wavelength volume transmission grating recording

4.1. Introduction

One of the major challenges in the area of holographic data storage is the development of suitable storage materials. Holographic media must satisfy stringent criteria, including high dynamic range, high photosensitivity, dimensional stability, optical clarity and flatness, nondestructive readout. Next generation recording media requires an optimal recording material with higher storage capacity and low volume shrinkage. For achieving higher storage capacity, the use of photosensitizer that absorbs in the blue wavelength region is required thus minimizing the fringe spacing and increasing the spatial frequency. Sony and Inphase has developed a new generation of blue laser DVD with a storage capacity up to 50 GB using 400 to 410 nm lasers. The replacement from red to blue laser DVD provides an improvement in storage capacity from 5 GB to 50 GB [1,2].

In this section we introduce series of blue sensitive dyes suitable for high capacity holographic data storage. First we used acridine yellow (AY), then Perylene diimide and finally we synthesize a natural colorant Curcumin and demonstrate their

capability in a photopolymer composition using transmission and reflection volume phase recording.

4.2 Acridine Yellow: a blue photosensitizer.

Acridine yellow is used in microbiology as a mutagen damaging the DNA, as photosensitizer for blue holographic grating recordings at 457,9 nm wavelength in acrylamide based photopolymers. Our approach allows us flexibility in tailoring the media to the particular needs of high density holographic data storage. In order to enhance the RIM up to $4x10^{-3}$, three photopolymers were prepared and the effect of acridine yellow concentration on this parameter is investigated. The influence of exposure intensity on the diffraction efficiency and refractive index modulation is also studied. An angular selectivity study as function of the diffraction efficiency is performed which determines the shrinkage suffered by the recording media.

Photopolymers were prepared by combining AY (λ_{max}=464.2 nm) as radical generator (KODAK) at different proportions. Fig 4.1 shows the molecular structure and UV-Vis spectrum of the acridine yellow that exhibits a maximum absorption peak at 433.6 nm which makes it suitable for blue region recording. Acrylamide was used as monomer, N,N'-methylenebisacrylamide was employed as cross-linking monomer, triethanolamine used as initiator and all dissolved in a poly(vinyl alcohol) solution at 10 and 13% w/v. All the reagents were used without further purification. The average layer thickness measured using a DEK-TAK 6M profilometer was 34 μm.

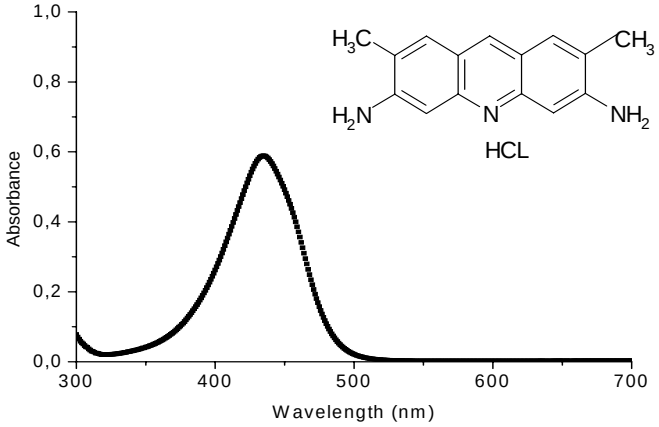

Fig. 4.1 Chemical structure and UV/Vis spectrum of AY solution (water) at 2.629×10^{-4} M of concentration**.**

In fig. 4.2 the cyclic voltammograms of acridine yellow are shown as were recorded in DMF. This measurement allows understanding the limitations of AY as acceptor of electron from TEA (electron donor) during the photoreduction involved in the photopolymerization process. The reduction peak of AY occurs at -1.6 V which enables this dye to be used in the final photopolymer composition.

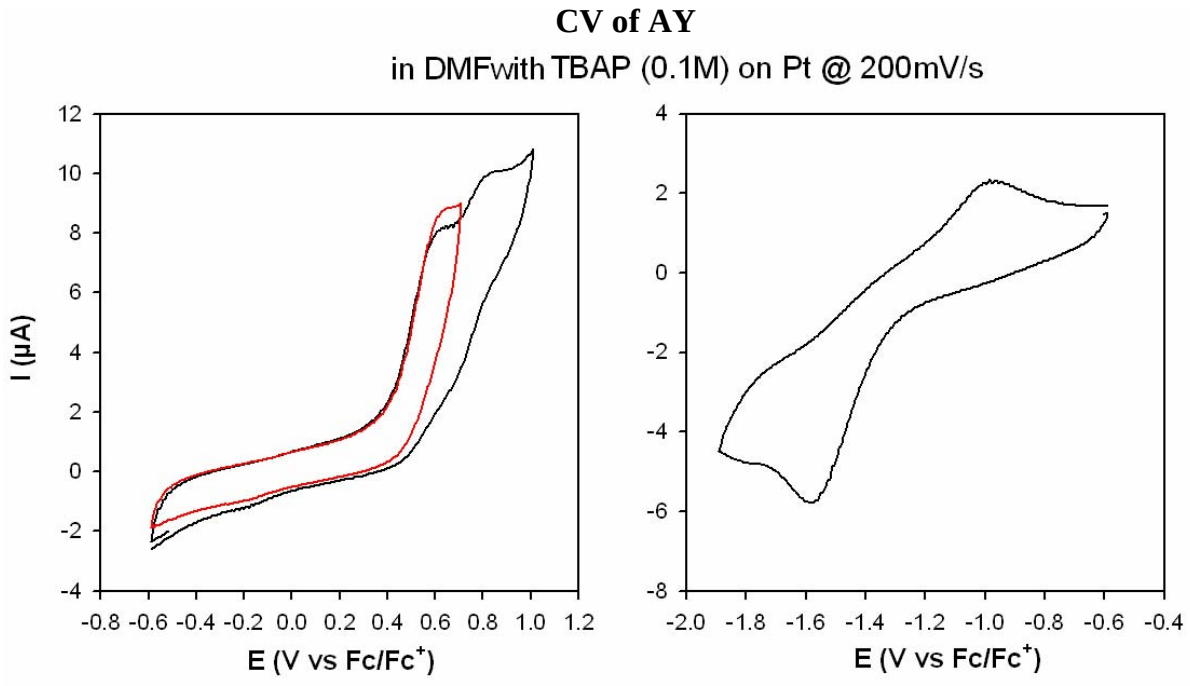

Fig. 4.2 Cyclyc Voltammograms of Acridine Yellow

Two sets of three photopolymers were fabricated varying the acridine yellow concentration mixed with the rest of the components (AA, BSA, TEA) at different PVA solution, 10 % wt/v (Case I) and 13% wt/v (Case II) in order to study the effect of dye concentration and thickness.

4.2.1 Optimization of the acridine yellow concentration.

We demonstrated in last chapter that the quantity of photosensitizer used in the recording material is an important factor, which also controls the diffraction efficiency of the recorded data. As photosensitizer can accelerate the initiation of the polymerization process, light sensitivity, diffraction efficiency as well as RIM can be enhanced by increasing this component in the photopolymer. Also it was observed

that the excess of the photosensitizer has a negative influence on the diffraction efficiency due to additional energy required to bleach this component during the photopolymerization [3,4]. To verify the effect of the acridine yellow on the diffraction efficiency, a series of photopolymers were prepared containing different AY proportions. The photopolymer compositions are summarised in table 4.1.

Table 4.1 Composition of photopolymers using acridine yellow at different AY concentration.

Dye	AA (M)	BSA (M)	TEA (M)	AY (M)
AY1	0.43	0.05	0.57	$5.28x10^{-5}$
AY2	0.43	0.05	0.57	$8.812x10^{-5}$
AY3	0.43	0.05	0.57	$1.376x10^{-4}$

The characterization of holographic gratings storage capacity of this media was carried out using our previously described setup in transmission interference geometry. The parameters used for the recordings are presented in the table 4.2.

Table 4.2 Parameters for gratings recording using AY

Photo-polymer	θ/2 (°)	WB (nm)	RB (nm)	Λ (μm)	SF (lines/mm)	I (mW/cm^2)	θ_B (°)
AY	33.5	457.9	633	0.418	2392	60	49.72

where θ/2 is the half-angle between the interference beams; WB and RB are the writing and reading beam respectively; Λ is the fringe period; θ_B(T,E) are the theoretical and experimental Bragg angle and I is the recording intensity.

Fig.4.2 illustrates the UV-Vis spectra of the photopolymers films prepared using different AY concentration. The square, full circle and triangle curves are attributed to photopolymer AY1-3 varying the AY concentration from $1.376x10^{-4}$ to $5.28x10^{-5}$ M. By blending the AY with the rest of reactants the maximum absorption peak shifts from 433.6 nm to 463.26 nm in all the photopolymers with a thickness of 34 μm. It is observed that by increasing the AY concentration the overall absorption increases.

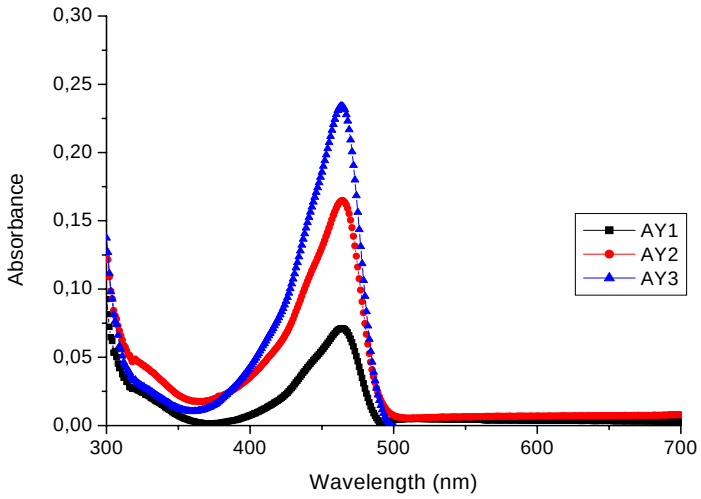

Fig. 4.2 UV-Vis spectra of acridine yellow photopolymer films at different concentrations using PVA at 10%wt/v.

In Fig 4.3 the typical growth of the diffraction efficiency with respect to exposure time and as function of the AY content for the three photopolymers in matrix of PVA solution at 10%wt/v are shown. The exposure intensity was $60mW/cm^2$.

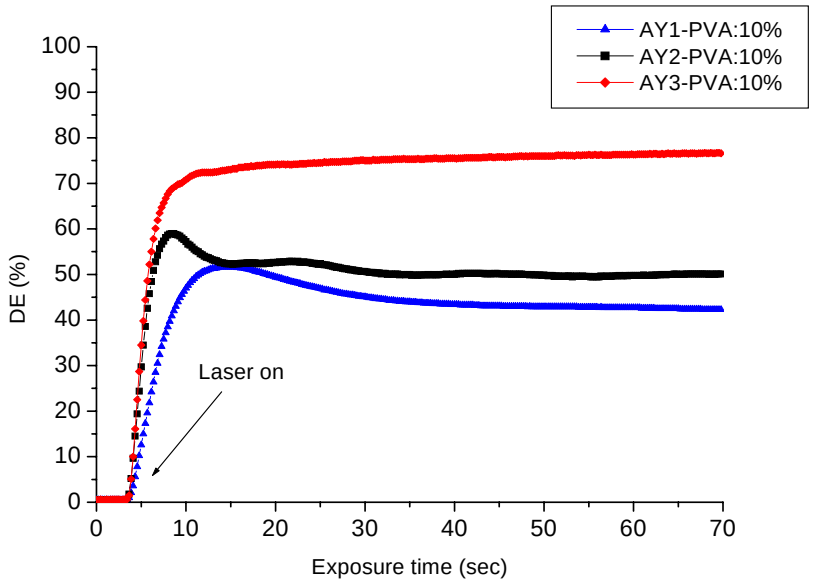

Fig. 4.3 Diffraction efficiency during exposure time of photopolymers AY1-3 using PVA solution at 10%wt/v at different concentration of acridine yellow.

We observed that there was no induction time required for formation of the gratings as the diffraction efficiency started to grow instantly after the exposure. This is in contrast to the acrylate-containing system which requires initial oxygen consummation for the diffraction efficiency to grow, resulting in a delay [5]. We can see that the diffraction efficiency increased by augmenting the dye concentration. This tendency can be explained as the lower diffraction efficiency obtained at the lower concentration of acridine yellow due to existence of lesser molecules capable of starting the polymer chain leading to low level of polymerisation and consequently decay in the diffraction efficiency. After 1.376×10^{-4} M of AY concentration, agglomeration of AY was observed in the samples.

Increasing the concentration of the matrix to 13% wt/v we observed the same performance as the photopolymers with less PVA concentration. The diffraction

efficiency as presented in figure 4.4 increased when higher AY concentration was used.

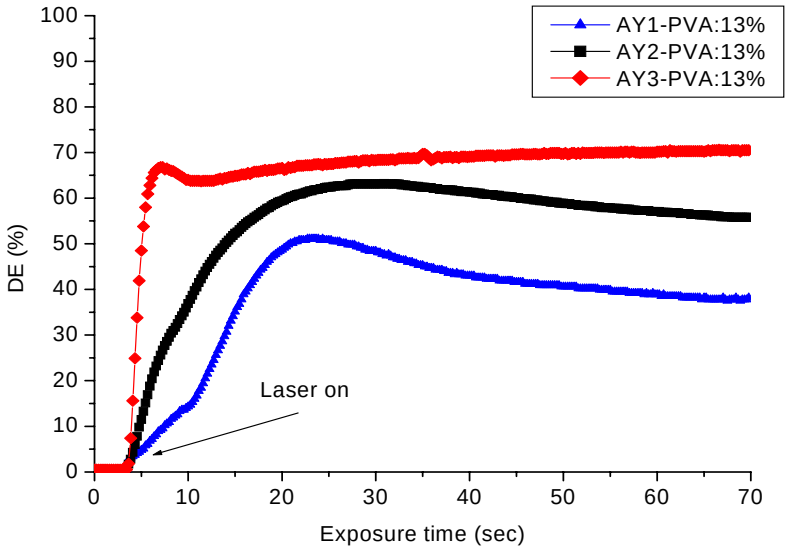

Fig. 4.4 Diffraction efficiency as a function of exposure time for photopolymer AY1-3 using PVA solution at 13%wt/v.

The difference between these two cases (I and II) is the exposure time required to achieve maximum diffraction efficiency was longer for the case of II compared to case I. The efficiency grew up to reach its highest value before stabilizing. The diffraction efficiencies obtained for case II were slightly lesser compare to case I.

For the case I, it was noticeable that the evolution growth of the diffraction efficiency followed different pattern. For photopolymer with higher AY content (AY3), the diffraction efficiency increased and reached a saturation value and then stabilized after approximately 6 sec of exposure. For the other two photopolymers (AY1-2) the behaviour is similar, the diffraction increased until 8 and 15 sec, suffering little decay and then stabilize. Maximum diffraction efficiency of 76.6 % was obtained for the

photopolymer AY3 with the highest amount of AY compare to 45% for the photopolymer with the lowest AY content. Highest sensitivity of 670 cm/J for the photopolymer AY3 was achieved defined earlier. For the cases of AY1-2, lower sensitivities were obtained caused for the retardation of photopolymerization process compare to AY3 [6]. The recording parameters of the photopolymers are shown is table 4.3.

Table 4.3 Properties of acridine yellow photopolymers at 6.136 sec of recording for photopolymers (AY1-3) using PVA solution at 10%wt/v.

Case I	η (%)	d (μm)	Δn	S (cm/J)
AY1	45.6	34	$2.84x10^{-3}$	539
AY2	57.97	34	$3.31x10^{-3}$	608
AY3	70.1	34	$3.80x10^{-3}$	669

The sensitivity relies on the concentration of photosensitizer used because it has an essential effect on photopolymerization rate for a given photopolymer at any particular fringe spacing. As the photosensitizer amount is higher in AY3 the amount of monomer polymerized is expected to increase.

For case II, as well as for the case I, higher diffraction efficiencies were achieved by increasing the dye content reflecting a significant increase of the sensitivity. Higher as 242 sensitivities for the highest AY concentration was found. An increase in the DE represents a positive change in the RIM, reaching as high as $1.34x10^{-3}$ for AY3 (table 4.4). The results obtained for case II concerned for these two optical parameters were

inferior than the one obtained for case I. This effect can be explained as the concentration of AA diminishes when the thickness increases.

Table 4.4 Properties of acridine yellow photopolymers (AY1-3) using PVA solution at 13%wt/v after 6.136 sec.

CaseII	η (%)	d (μm)	Δn	S (cm/J)
AY1	13.6	90	5.46×10^{-4}	111
AY2	35	90	9.16×10^{-4}	178
AY3	64.4	90	1.34×10^{-3}	242

Angular response curves have been used to study the effect of thickness on the performance of above photopolymerizable films [4]. Fig. 4.5, illustrates the diffraction efficiencies as function of reconstruction angle for transmission grating recorded on the three photopolymers measured using a He-Ne beam laser for case I. We observed only the zero and first order diffraction efficiencies as function of the reconstructed angle for all photopolymer layers under a spatial frequency of 2410 lines/mm. Only the first order was noticeable indicating the formation of thick holograms [7]. By fine-tuning the Bragg angle position the diffraction efficiency decreases but doesn't reach to zero. The recording films were rotated with a resolution of 0.1° monitoring the diffracted beam along the Bragg condition. By increasing the AY content in this material the side peaks (first diffracted order) intensity compared to the zero order becomes more uniform and visible. For AY1 these lobes are barely visible compare to AY3 that are more clearly resolved. This can be caused by non-uniformity of the grating formation in good agreement with the

evolution of the diffraction efficiency during time. It was noticed that the FWHM increased slightly by increasing the AY content achieving 0.58° for the case of AY3 corresponding to a high angular selectivity which is an important parameter for quality holographic storage applications.

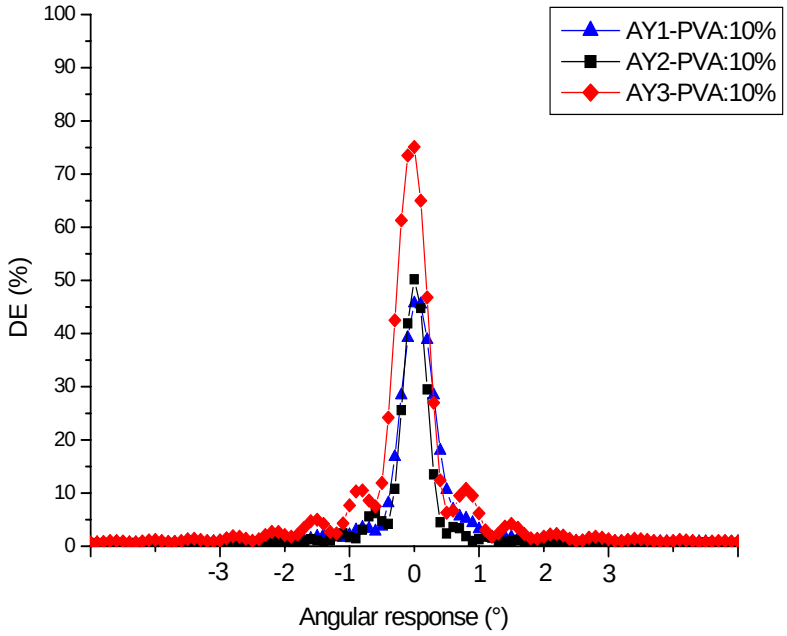

Fig. 4.5 Angular selectivity of diffraction efficiency of photopolymer AY1-3 using PVA solution at 10%wt/v at different dye concentration.

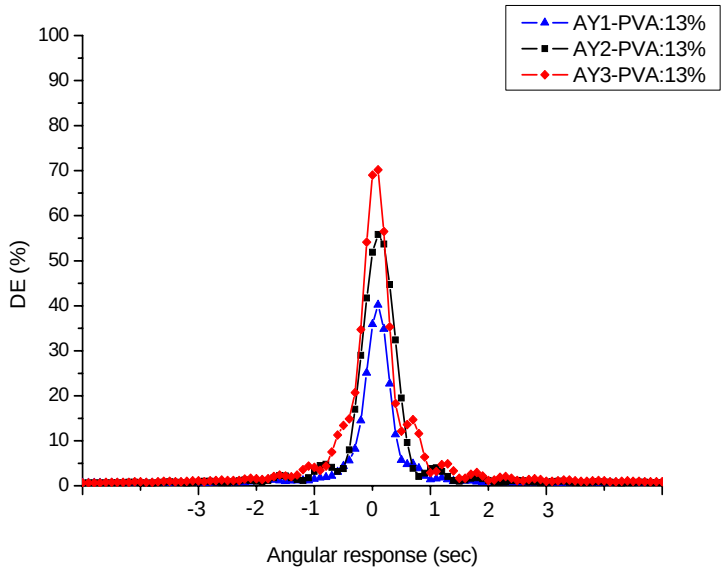

Fig. 4.6 Angular selectivity of diffraction efficiency of photopolymer AY1-3 using PVA solution at 13%wt/v.

For case II, in Fig. 4.6, the corresponding angular scans for the diffraction efficiency are represented for gratings stored in photopolymer with PVA solution at 13% wt/v. In this figure the physical thickness controls the central lobe width.

In figure 4.7 similar compositions in two different recording layer thickness is presented. The narrowing of the principal lobe can be observed when the physical thickness is higher. But this effect can be observed in gratings of 35 μm and 90 μm of thickness because their composition is very similar and the attenuation of index profile limit the optical grating thickness.

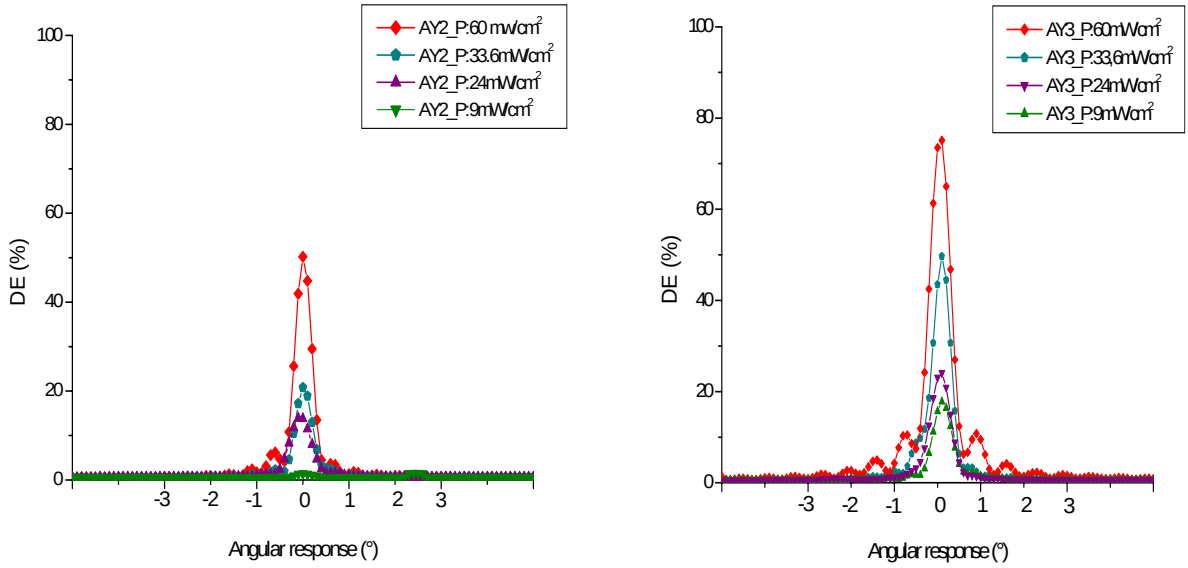

Photopolymer AY2 Photopolymer AY3

Fig. 4.7 Angular selectivity of diffraction efficiency for photopolymer AY2-3 using PVA solution at 10%wt/v at different intensity.

Once the diffraction efficiency is measured, the refractive index modulation was calculated using the Kogelnik's coupled wave theory under Bragg condition. In Fig. 4.8 the refractive index modulation is plotted as function of diffraction efficiency and exposure intensity for the photopolymer with highest AY content (AY3). A remarkable increase of diffraction efficiency was observed by increasing the recording intensity. The diffraction efficiency raised from 17.68% at 9mW/cm^2 to 75% at 60 mW/cm^2 recording intensity. The increase on the diffraction efficiency obtained represents an enhancement of the refractive index modulation from 1.66×10^{-3} to 4×10^{-3} for the lower and the maximum exposure intensity respectively, which is considerably higher than other similar systems [8].

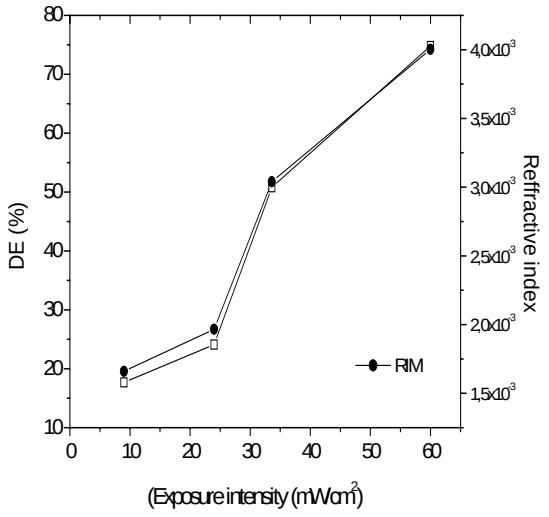

Fig. 4.8 Effect of the exposure intensity on the diffraction efficiency and refractive index for photopolymer AY3 (PVA:10 %wt/v).

Using higher irradiation the free radical concentration becomes high and the termination is favoured leading to the creation of shorter polymer chains. As the polymer pattern being less dense, the observed shrinkage is also less. For the case of low irradiance, the polymerization process is not complete; the reaction sites are numerous so the monomer molecules are forced to diffuse onto longer distances to join a polymer chain in formation. When the polymer density is elevated the diffusion is obstructed and some molecules will not be polymerized [9].

4.2.2 Shrinkage

A study of angular selectivity as function of the diffraction efficiency was investigated in order to determine thus the shrinkage suffered by the films. The existence of shrinkage in the layers results in a change of the thickness of the fringe

spacing, in this case it is required to modify the readout beam angle to achieve maximum diffraction efficiency. This change in the layer thickness [10] is defined as:

$$\Delta d = d_0 \left[\frac{\tan\phi_f}{\tan\phi_i} - 1 \right] \qquad (1)$$

where φ_I and φ_f are the initial and final angle of the recorded grating. Knowing this change the percentage of the shrinkage can be calculated as follows:

$$\% \text{ Shrinkage} = \frac{\Delta d}{d_o} x\, 100 \qquad (2)$$

where Δd and d_o are the fraction of thickness change and the initial thickness of the layer. Considerably small shrinkage of 1% was measured on the photopolymer AY3.

For further understanding of the degree of polymerization of all photopolymers, the photopolymeric layers were irradiated with a collimated light from a Argon ion laser at 457,9 nm for 70 sec in order to polymerize the acrylamide in the samples. 1.2 mg of each sample was milled with 136 mg of KBr pressed in form of disks. Fig. 4.9 shows the FT-IR spectra of polymerized samples containing different AY proportion; measured using FT-IR spectrometer. We observed the stretching vibration of acrylamide at 1675 cm^{-1}. We noticed a decrease in the absorbance by increasing the AY content. For the case of AY1-2 the absorbance are closer compared to AY3 that is much lower. These can explained that more acrylamide molecules are polymerizaed in the AY3 compared to AY1-2, which is concordance with the diffraction efficiency obtained previously where $DE_{AY1\text{-}2}$ are 45 and 50% smaller compare to DE_{AY3} obtained of 75%.

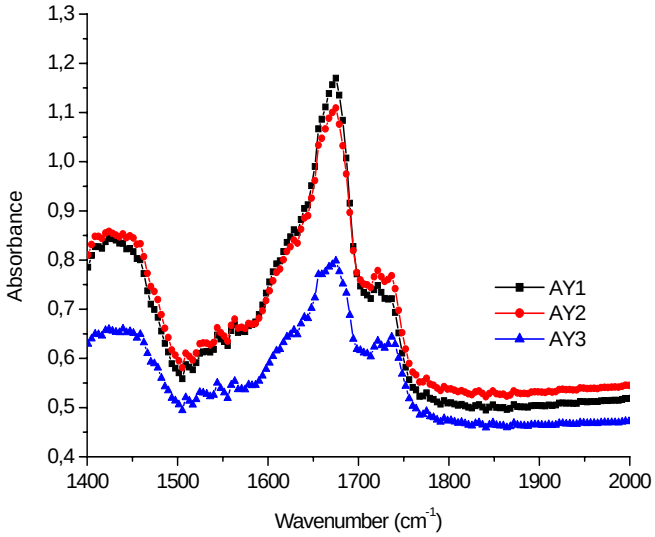

Fig. 4.9 F-TIR spectra of the acridine yellow photopolymers varying its concentration.

Fig 4.10 shows a microscope image of the volume grating created in the acridine yellow photopolymer (AY3) after interferometric exposition at 0.418 μm of grating spacing. This image confirms the formation of well-defined gratings in present photopolymer.

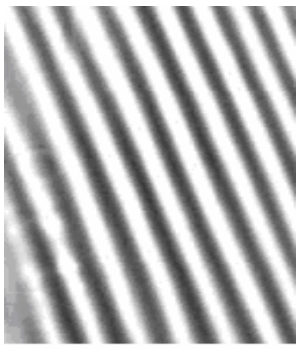

Fig. 4.10 Microscope image of the grating formation of the sample containing 1.367×10^{-4} M of AY concentration.

4.3 Perylene diimide photopolymers

Perylene is a widely studied dye where a diimide functional group attached to the perylene enhances the electron acceptor strength. Also perylene diimide shows the significant overlap in the blue wavelength region. In this section we report our studies on water soluble perylene diimide dye as sensitizer via free radical polymerization in acrylamide base photopolymer.

We fabricated three photopolymer layers (PP1-3) under red light ambiance, by mixing (AA, BSA, TEA) and perylene di-imide (Peryl) as photosensitizer illustrated in fig. 4.11 with an average molecular weight of 502 g/mol.

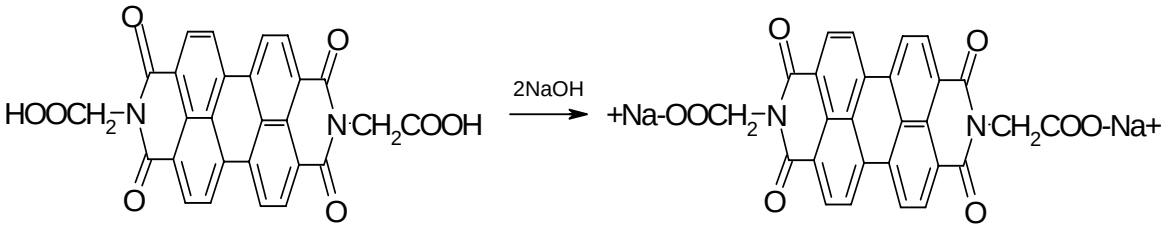

Fig. 4.11 Water soluble molecule of perylene diimide

This photosensitizer presents long wavelength absorption spectra (fig. 4.12) showing two relevant peaks at 494 nm and 529 nm making it suitable to use for recoding under blue wavelength.

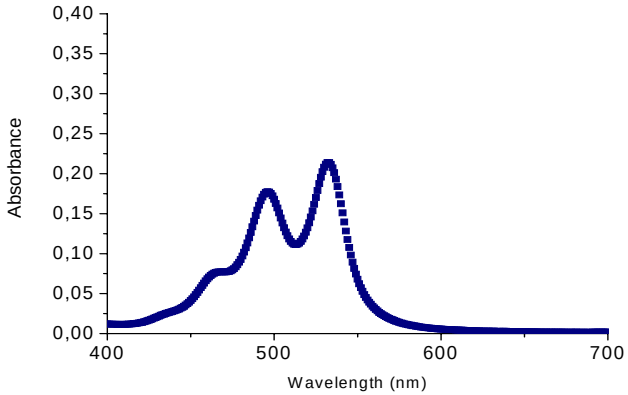

Fig.4.12 Absorption Spectrum of the PP1 photopolymer film with a 90 μm thick layer

This new dye was introduced at our optimised concentration of 6.8 x10^{-4} M in a basic solution (NaOH) using a molar relation of 1:2 respectively. All these components were dissolved in a 13 %wt poly(vinylalcohol) (PVA) solution. The variation for photopolymers PP2-3 was the acrylamide content was increased in 24 and 48% respectively (table 4.5).

Table 4.5 Monomer concentration for the different photopolymers

Monomer conc.	**PP1**	**PP2**	**PP3**
[**AA**] (M)	0.434	0.539	0.643

4.3.1 Photosensitization mechanism

Polycyclic aromatic hydrocarbons such as anthracene and perylene have been used as sensitizer in cationic polymerization (photolysis) using onion salts as coinitiator and THF as monomer [11]. The addition of the sensitizer in polymerization can guide to complex mechanism that involves intermediates. There is evidence that perylene

diimides proceeds the polymerization through singlet and not via triplet excited state initiation due to energy difference between them, 54 and 27 Kcal/mol respectively [12]. This sensitizer is capable to react as electron acceptor as well electron donor.

The photopolymerization process starts when the perylene diimide (D) absorbs a photon from the light then is promoted to an excited singlet state. The singlet state dye reacts with the electron donor, triethanolamine (ED) to produce the radical initiating species that will initiate the polymerization process. Then this species react with the monomer (acrylamide) to form the growing chain. Then this growing chain will react with another and the polymer is produced. A possible mechanism to explain the polymerization process if radicals initiating species are formed though a singlet excited state (exciplex) in this material is shown in the scheme 1.

$D + hv \rightarrow D^*$ (absorption of photon) (a)

$D^* \rightarrow D$ (deactivation (singlet) (b)

$D^* + ED \rightarrow [D\ldots ED]^*$ (formation of radical initiating species) (c)

$\downarrow$

Radical species

$RS^* + M \rightarrow RSM^*$ (formation of growing chain) (d)

$RSM^* + RSM^* \rightarrow$ Polymer (formation of the polymer network) (e)

(scheme 1)

Due to the dye and inhibition effects, some polymers do not react instantaneously to the exposure, negligible polymerization occurs for some period of time at the start of the recording. To study the behaviour of the holographic gratings using a novel perylene- acrylamide based photopolymer the diffraction efficiency was monitored during exposure time. Table 4.6 summarizes the recording parameters.

Table 4.6 Parameters for recording the formation of the gratings using perylene.

Photo-polymer	θ/2 (°)	**WB (nm)**	**RB (nm)**	**Λ (μm)**	**θ_B (°)**	**P (mW)**	**SF (lines/mm)**
PP	33.5	488	633	0.44	45.7	40	2262

where θ/2 is the half-angle between the intereference beams, WB and RB are the writing and reading beam respectively, Λ is the fringe period, θ_B is the theoretical Bragg angle and I is the recording intensity.

In fig.4.13 (a-c) the temporal evolution of the DE for the photopolymer varying the monomer content is presented. The maximum diffraction efficiency achieved was 44% for the photopolymer with smaller acrylamide content compared to 39 and 14% for the photopolymer PP2-3 with higher content (table 4.7).

Table 4.7 Diffraction efficiency and RIM for all the materials.

	PP1	**PP2**	**PP3**
DE (%)	44	39	14
Δn	1.13×10^{-3}	1.054×10^{-4}	5.99×10^{-4}

Once the diffraction efficiency (η) is obtained, we determined the refractive index modulation of all the materials using kogelnik's coupled wave theory (equation 3)

$$\Delta n = \frac{\arcsin\sqrt{\eta}\,\lambda\lambda\cos\theta}{\pi\, d} \qquad (3)$$

where d is the sample thickness (90 μm), λ is the wavelength for the reconstructed beam (633 nm) and θ is the reconstructed angle (45.7°). We observed the same

behaviour as the diffraction efficiency while the acrylamide content increased the RIM decreased.

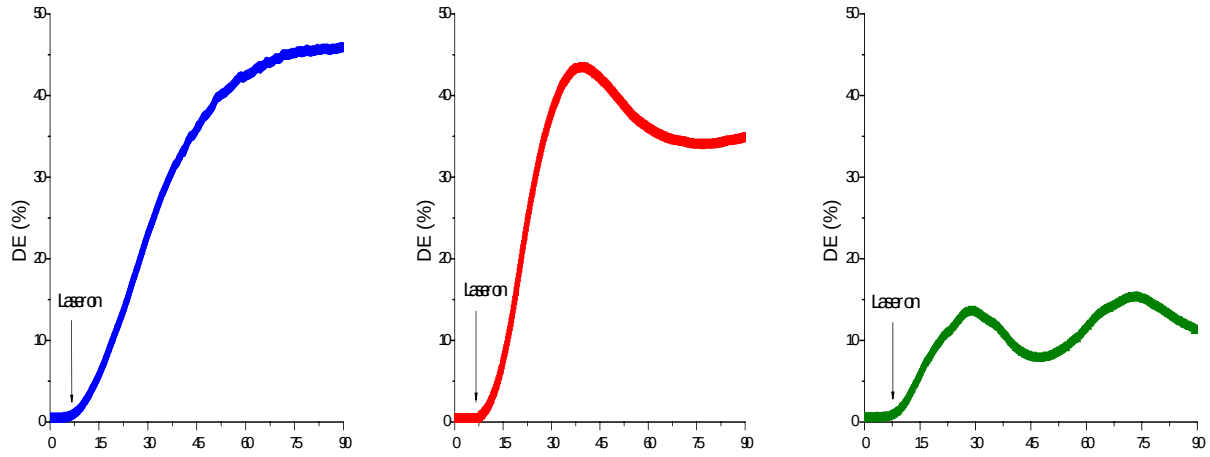

Fig. 4.13. Temporal evolution of diffraction efficiency as function of time for photopolymers PP1-3.

(a) PP1 **(b) PP2** **(c) PP3**

We observed by increasing the concentration up to 24% for photopolymer PP2, a different development in grating was observed, the diffraction efficiency reached to the maximum value and then decreased by 10% and then stabilize at 52.5 sec of exposure time. For the photopolymer PP3 with higher over the content of acrylamide compare to PP2 the grating formation shows dynamic behaviour with exposure time. This variation involves some issues in the grating formation that will be discussed in next sections.

In fig 4.14, grating patterns were visible under optical microscope with a CCD Camera. The bleached areas appear in lighter bands using a thinner layer of 20 μm.

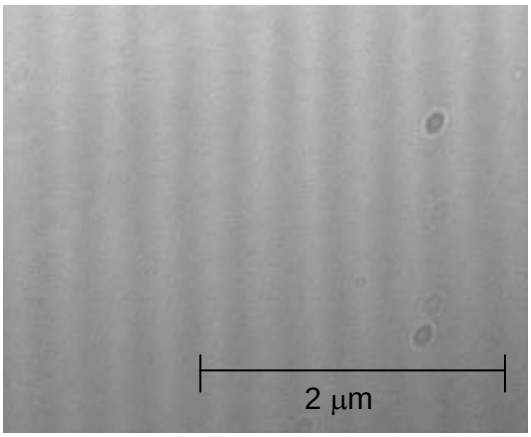

Fig. 4.14 Optical microscope image of grating formation in PP1.

A refractive index modulation (RIM) takes place as a result of the compositional changes between dark and bright regions. The diffusion of the monomer, chain flexibility and mobility of the monomer have a great influence in the amount of photopolymerization as consequence in the refractive index modulation [13] meaning higher is the diffusion of monomer higher RIM will be achieved**.** Another factor that influences the polymeric termination reaction is the formation of new species such as dimmers contributing in a decrease of the polymerization rate [14].

Using perylene as sensitizer, the maximum DE achieved as high as 44% occurred after a long induction period of 52.5 sec of illumination for the photopolymer PP1, this can be attributed to the perylene inhibition effect [15], size of its molecule and its higher transition glass temperature (Tg) in polymer blend superior to 100°C making the polymer chain more rigid restricting the diffusion of monomer to be higher. In an effort to increase the diffraction efficiency we increased the acrylamide content up to 48% more than PP1. We found by increasing the acrylamide content the diffraction

decreased. Observing these results, it's clear that acrylamide concentration has an effect on the declining of the diffraction efficiency as well as the refractive index modulation. This suggests that there is a limit for the acrylamide concentration due to its compatibility and solubility in the photopolymer. This limitation on the content can be a contribution to the presence of hydrogen bonding interactions in the blend.

Certain types of interactions such as hydrogen bonding can modulate the refractive index of a medium through a change in its polarizability [16]. The existence of hydrogen bonds can affect the properties of polymer blends such as mechanical properties. FT-IR spectra were employed to characterize the existence of hydrogen bond on the photopolymers. Mixed samples with oven dried KBr powder then pressed as discs were used to record the spectra using a FT-IR spectrometer (Bio Rad FTS-155) within a range of 4000 and 400 cm^{-1}. As shown in fig. 4.15 two bands appeared close 1738 cm^{-1} attributed to the carbonyl vibration and about 1720 cm^{-1} assigned to the hydrogen-bonded carbonyl groups (shown in region R1). We observed that the spacer length between these two bands decreased as the acrylamide content increased. Longer spacers favour the formation of strong hydrogen bond. Other band at 3402 cm^{-1} (shown in region R2) arise from the hydroxyl vibration region for PP1, as incrementing the monomer content this band shifted to a higher wave number, 3383 and 3384 cm^{-1} for PP2-3 respectively. This indicates that the % of transmission of this group becomes weak by increasing the monomer concentration as well as the glass transition temperature increases.

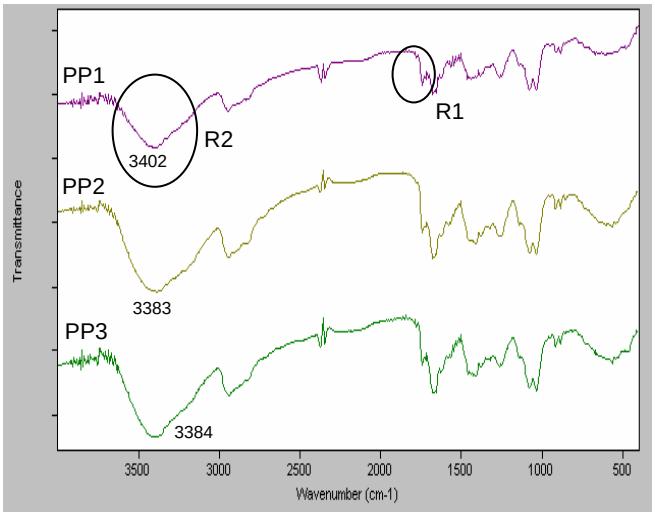

Fig. 4.15 FT-IR spectra for photopolymers PP1-3

The transition glass temperature (Tg) that controls the elasticity of the chain, smaller is its value higher is the stiffness attained by the material [12] is shown in fig. 4.16, was measured by differential scanning calorimetry using a DSC 2010 CE (TA instruments) at a heating rate of 10°C/min from 0 to 200°C. The Tg of the 3 photopolymers was found to be between 110 and 150°C (table 4.8) observing lower temperature was established for PP1 and the highest for PP3 pointing out as the acrylamide content the photopolymer less flexible with lesser thermal stability. The latter can be confirmed by a thermogravimetric analysis; this was performed using TGA 2050 CE (TA instruments) under nitrogen atmosphere. The samples were heated from 0 to 1000°C within a rate of 10°C/min. In fig. 4.17, a 3-step thermal decomposition was observed in all 3 materials, starting the decomposition around 145°C representing a moderate thermal stability in comparison to others perylene based polymer [18]. The first weight loss observed in the polymers was found to be

between 145-165°C about 45-46 %. The maximum weight loss of 54 % (PP1-PP2) and 56 % (PP3) occurred in the second step between 230-240°C arriving almost to 99% of loss in all the samples. In the third degradation step no residue was found, this supports the existence of a decomposition mechanism of the main chain and formation of oligomers, especially dimers and trimers [19]. According to table 4.8 the thermal stability based on the initial temperature occurred between 145 to 165°C pursues the following order: PP1>PP2>PP3 indicating that PP1 has a higher thermal stability than the rest of the materials.

Table 4.8 Tg_i values for the PP1-3

Temp (°C)	PP1	PP2	PP3
Tg	114.5	144.31	149.97

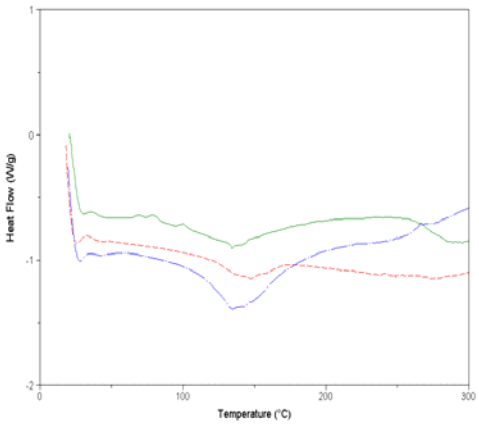

Fig. 4.16 DSC thermograms of PP1-3

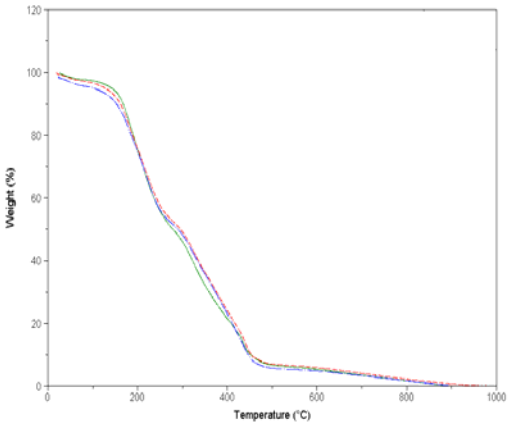

PP1 (green), PP2 (red) and PP3 (blue) lines

Fig. 4.17 Thermogravimetric analysis of PP1-3

From these results, lower crystallization temperature, higher thermal stability, smaller wavenumber of hydroxyl vibration in the spectra, higher spacers length

between carbonyl and hydrogen bonded groups will favour the strong formation of hydrogen bonded between acrylamide molecules and poly (acrylamide) leading to a higher mobility of the monomer molecules to diffuse, thus increasing the refractive index modulation and diffraction efficiency among the photopolymer in study.

Figure 4.18 (a-b) present once the gratings are recorded the angular response for the diffraction efficiency as a function of the reconstructed angle using a He-Ne laser as a probe beam using 2 silicon detectors (Hamamatsu) for photopolymers (PP1-2) with the similar composition (varying the monomer content). The samples were positioned on a computer-controlled rotary stage with a resolution of 0.1°.

We achieved as high as 44 % of diffraction efficiency for PP1 close to the Bragg angle position, while the sample was detuned the diffraction efficiency decreased. The maximum diffraction obtained shows FWHM < 0.46° which represents a high angular selectivity, important quality for holographic storage applications and hardly found in thin films. As we can see only the first diffracted order is visible indicating that the thick holograms were created [5]. We observed by increasing the monomer content in 24 % the angular width of the photopolymer PP2 was found double compare to the first one increasing the FWHM from 0.46 to 0.92° affecting the narrowing of the principal lobe by increasing the monomer content and the secondary lobes have vanished for the case of PP2.

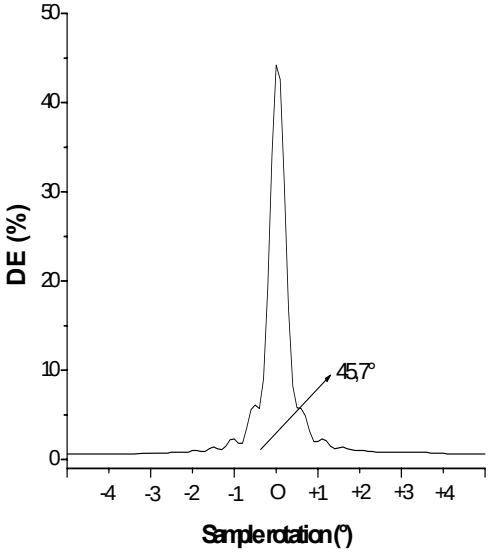

Fig. 4.18a Angular response as function of Diffraction efficiency for PP1.

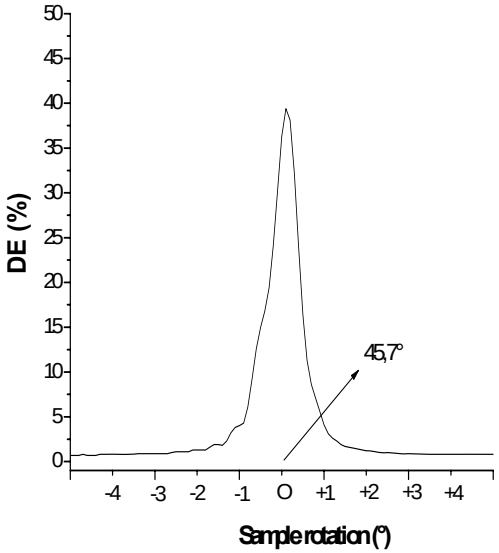

Fig. 4.18b Angular response as function of Diffraction efficiency for PP2

Due to modification in the illuminating angle the grating period is transformed into Λ_f with a value of 0.445 μm, defining it as [20,21]

$$\Lambda_f = \Lambda_o \frac{\cos\theta_f}{\cos\theta_o} \qquad (4)$$

where Λ_o, θ_o and Λ_f, θ_f are the period and angle of the grating before and after shrinkage.

We observed reduced shrinkage of 1.38% which is small (~2 – 3%) according to Gallo et al. [20] and final grating period of which not differs significantly to the original one, making it suitable for HDS applications.

4.4 Curcumin sensitized photopolymer recording

Turmeric is a yellow colour compound found in the Rhizomes of the Curcuma longa plant. Turmeric is a typical spice that provides curry powder, flavour and the yellowish colour in many eastern plates. The important ingredient in turmeric is the curcumin [(E,E)-1,7-bis(4-hydroxy-3-methoxyphenyl)-1,6heptadiene-3,5-one] and is the major yellow-orange pigment extracted from it [22]. This compound is present in the turmeric in a 1 - 2% by weight [23]. Natural curcumin is approved as colouring agent in food, drugs and cosmetics [24]. Curcumin is also known for its antitumor and anticancer properties. It is widely used as household medicine. It has been used to shield sun from the skin burns. Curcumin is found to be an efficient photosensitizer for diaryliodonium salts in cationic polymerization and copolymerization of styrene and methacrylate using photolysis to create photopolymerization [23,25].

In this section we present the results using a novel inexpensive, natural and non toxic photosensitizer: curcumin in acrylamide based photopolymer for transmission holographic recording at 488 nm recording wavelength. The effect of dye concentration and the tuning of the recording wavelength are studied. The angular response as function of diffraction efficiency (DE) is also investigated.

Fig 4.19, illustrates the chemical structure of curcumin.

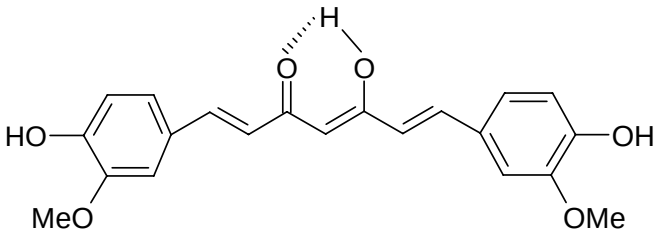

Fig. 4.19 Chemical structure of the curcumin in its enol form.

The cyclic voltammogram (CV) of curcumin is presented in fig 4.20 was recorded in order to try to exaplain the limitations of curcumin as a electron acceptor, role of the dye in the Photopolymerization process. The values were obtained in 0.76mM of curcumin CH_2Cl_2 at a scan rate of 200 mV/s.

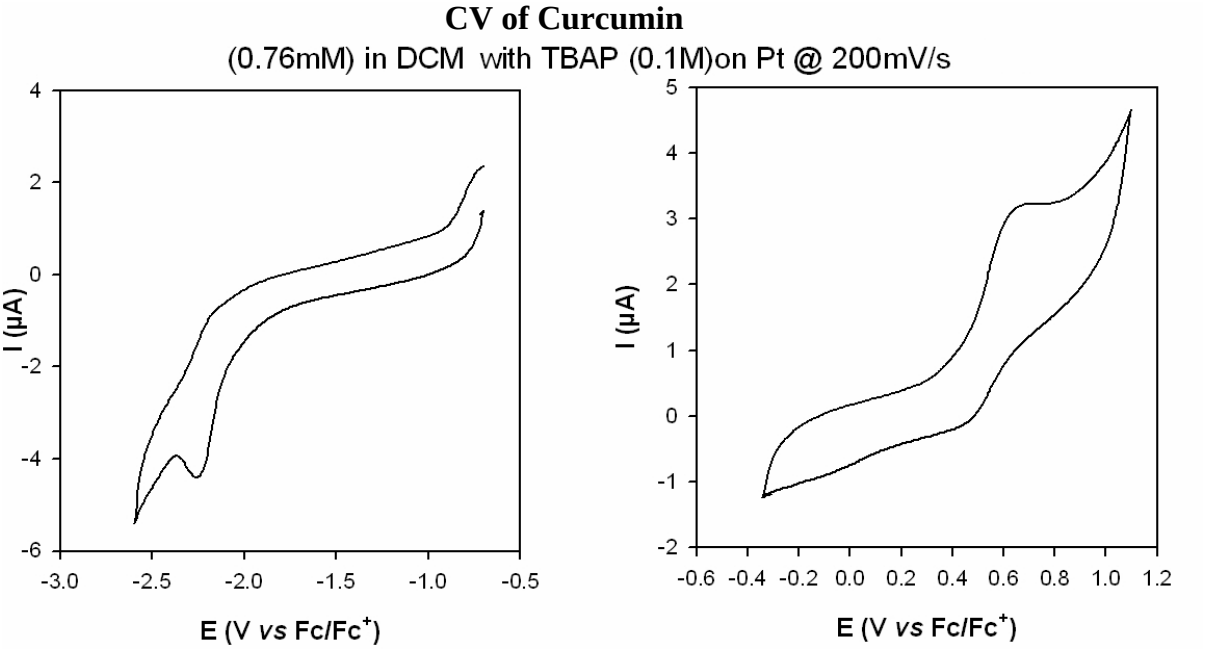

Fig. 4.20 Cyclyc Voltammogram of Curcumin.

4.4.1 Synthesis of curcumin

The isolation of Curcumin from turmeric powder was performed using the method proposed by R. Mohan [22]. Turmeric was acquired from a grocery store. 40 grams of turmeric powder was added into 100 ml of dichloromethane and then stirred magnetically at 40°C for 1 hr. The mixture was suction-filtered and the filtrate was concentrated using a rota-evaporator at 40-50°C. The reddish yellow oily residue was agitated magnetically overnight with 40 ml of hexane. The resulting solid was dissolved in a minimum amount of a solvent mixture (99% dichloromethane and 1% of methanol) loaded onto a column packed with 70 grams of silica gel. The column was eluted with the same mixture. The least polar colored component was concentrated using a rota-evaporator. Curcumin can exist in at least two tautomeric forms, keto and enol. The enol form is more energetically stable in the solid phase and in solution. The final product was verified as curcumin in hydrogen-bond-stabilized enol form by H NMR [26] using DMSO as a solvent due to this compound is not sufficiently soluble in $CDCl_3$ illustrated in fig 4.21. The existence of the extended conjugation, aromatic and enol groups will impart the long-wavelength absorption of this dye [23]. Curcumin displays different solubility in several organic solvents but it is insoluble in water (acidic or neutral water) but becomes soluble in a basic solution of NaOH.

The pre-polymer solutions were prepared by mixing the following materials: the monomer: Acrylamide, N,N′-methylbisacrylamide, Triethanolamine and

Curcuminas (sensitized by previous method) at different concentrations in a 13% (w/v) of poly(vinyl alcohol) matrix solution. The composition of these materials is shown in table 4.9. Curcumin has a broad UV absorption from 300 to almost 500 nm depending on the concentration. This compound is readily soluble and pH dependent due to the phenolic groups in different solvents. Due to the presence of the methoxy and hydroxyl groups, a bathochromic shift is produced at the maximum absorption wavelength of this compound [22]. In Fig. 4.21, It was confirmed by changing the pH from acid to basic using 3 different solvents: Ethanol, DMSO and Basic aqueous solution (NaOH at 0.5 M) where the absorption peak shifts towards red wavelength. The maximum absorption occurs at 427.3 nm, 433,5 nm and 469.32 nm in ethanol, DMSO and aqueous solution respectively.

Table 4.9 Composition of materials inside of the curcumin pre-polymer solutions.

Material	AA (M)	BSA (M)	TEA (M)	Cur (M)
Cur1	0.45	0.05	0.6	$1.54x10^{-4}$
Cur2	0.45	0.05	0.6	$4.86x10^{-4}$
Cur3	0.45	0.05	0.6	$1.01x10^{-3}$

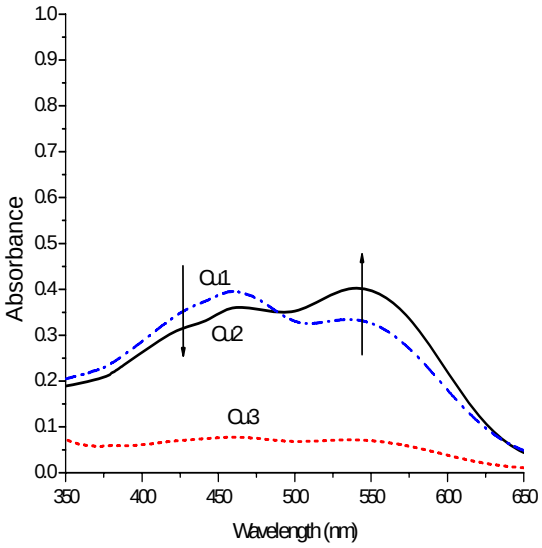

Fig. 4.21a UV spectra for photopolymers Cu1-3 in 50 µm thick films.

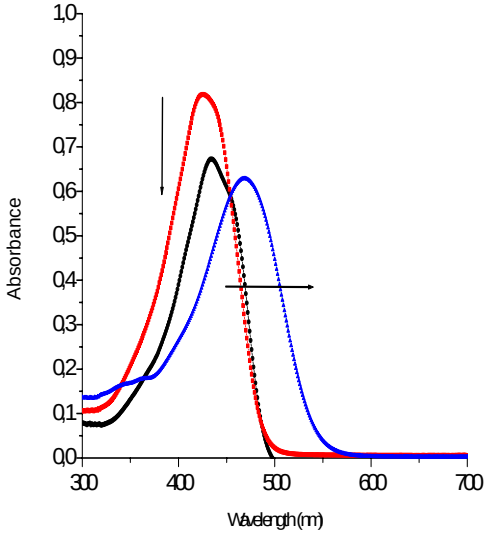

Fig. 4.21b Curcumin UV/Vis spectra in different solvents at 2.7×10^{-4} M of concentration: square, solid circle and triangle curves are assigned in Ethanol anhydrous, DMSO and aqueous basic solution (0.5 M).

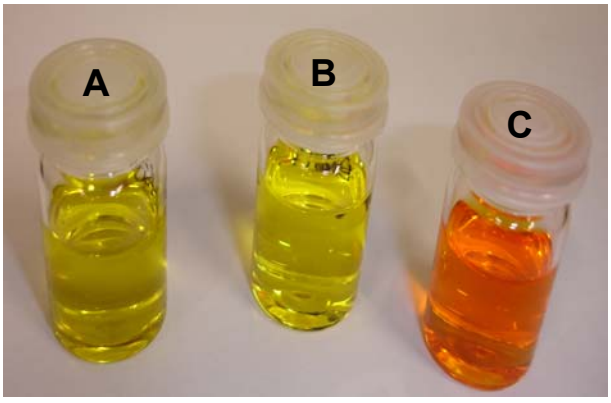

Fig. 4.21c Curcumin solution (M) using different solvent. (a: DMSO, b: Ethanol anhydrous and c: NaOH aqueous solution).

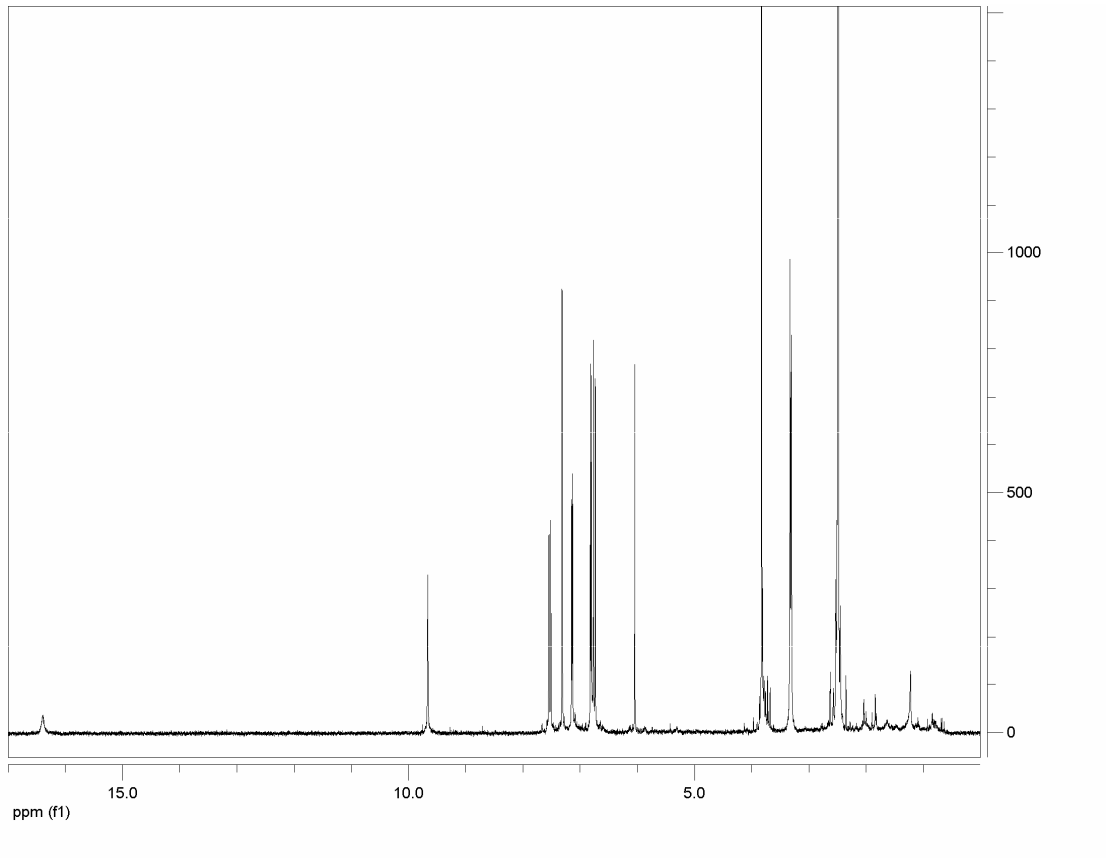

Fig. 4.22 RMN of curcumin using DMSO deuterated as solvent.

The Raman spectrum of the curcumin is shown in figure 4.22. The gratings were formed using the following parameter shown in table 4.10. The diffraction efficiency was defined as the ratio between the diffracted and the sum of transmitted and diffracted intensities.

Table 4.10 Parameter used for grating formation.

Photo-polymer	θ/2 (°)	**WB (nm)**	**RB (nm)**	**Λ (μm)**	**θ_B (°)**	**I (mW/cm²)**	**SF (lines/mm)**
Cu	34.25	488	633	0.433	46.8	133	2306

where θ/2 is the half-angle between the interference beams, WB and RB are the writing and reading beam respectively, Λ is the fringe period, θ_B is the theoretical Bragg angle and I is the recording intensity.

Fig. 4.23a illustrates the evolution of diffraction efficiency during exposure time of curcumin photopolymer (Cur3) monitored using a He-Ne laser beam. As evident from figure 4.23a, no induction period after illumination was observed as the diffraction efficiency increased instantaneously and saturates after exposure of 60 sec yielding diffraction efficiency up to 15.5%.

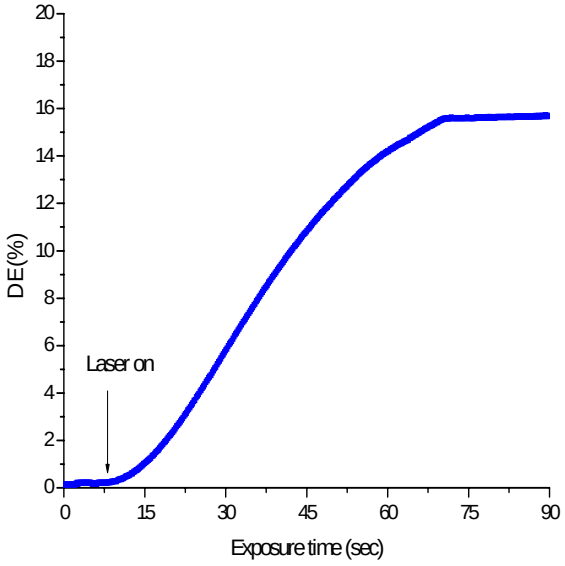

Fig. 4.23a Evolution of diffraction efficiency as function of exposure time for Cu3.

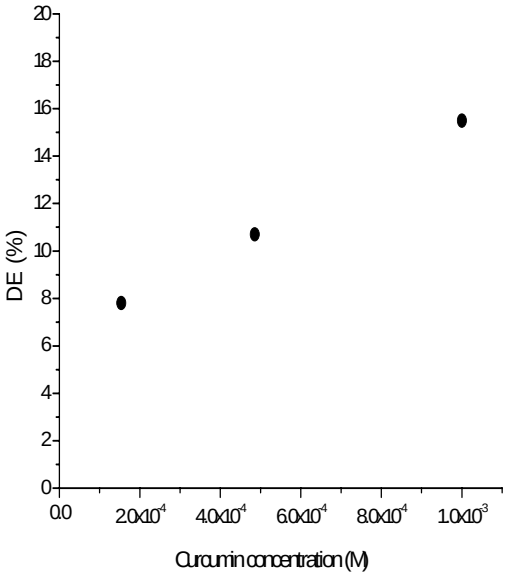

Fig. 4.23b Diffraction efficiency as a function of curcumin concentration.

In Fig. 4.23b, the diffraction efficiency is plotted as function of the curcumin content. A reduction of the diffraction efficiency of the photopolymer is observed by decreasing the proportion of curcumin. The diffraction efficiency decreased from 15.5% to 7.8% for the photopolymer with less curcumin content. This trend can be explained as more acrylamide molecules are expected to polymerize when the concentration is high providing enough dye molecules to initiate the polymerization

process hence an increase in DE [4].Due to limited solubility of curcumin, further increase of curcumin content yielded inferior film quality and hence not presented.

An increase in the curcumin content enhanced the refractive index modulation from $7.8x10^{-4}$ for the photopolymer with the lowest curcumin content to $1.1x10^{-3}$ for the photopolymer with the highest content. We also explored the influence of NaOH content used in the curcumin photopolymers. We prepared different photopolymers keeping the rest of the reactants constant varying the NaOH content. We recorded holographic gratings in all the layers using identical condition for 90 sec of exposure at 133 mW/cm^2. Table 4.11 summarizes the effect of the basic media on the diffraction efficiency using constant curcumin concentration at $2.15x10^{-4}$ M while varying the NaOH content.

Table 4.11 Diffraction efficiencies using different NaOH concentration at $2.18x10^{-4}$ M curcumin concentration.

Basic solution [NaOH] (M)	**DE (%)**
0.29	4.67
0.2	2.89
0.083	1.2

As the NaOH content was decreased the diffraction efficiency was reduced indicating a large impact of the basic media on the curcumin solution. This suggests a better curcumin miscibility when the pH of the aqueous solution was increased.

Fig. 4.24 illustrates the angular response of the curcumin photopolymer as function of diffraction efficiency with a spatial frequency of 2306 lines/mm. By rotating the samples with a resolution of 0.1° the angular selectivity of recorded gratings on the photopolymers was investigated. For this the diffraction efficiency at 633 nm was monitored. The zero diffracted beam was only visible in all the materials. A broader peak of zero diffracted beam is observed by decreasing the curcumin content in the photopolymers. A symmetric shape is observed in all photopolymer around the maximum diffraction efficiency. By increasing the curcumin concentration the FWHM is reduced up to 0.5°, an important feature observed in thick volume holograms [7].

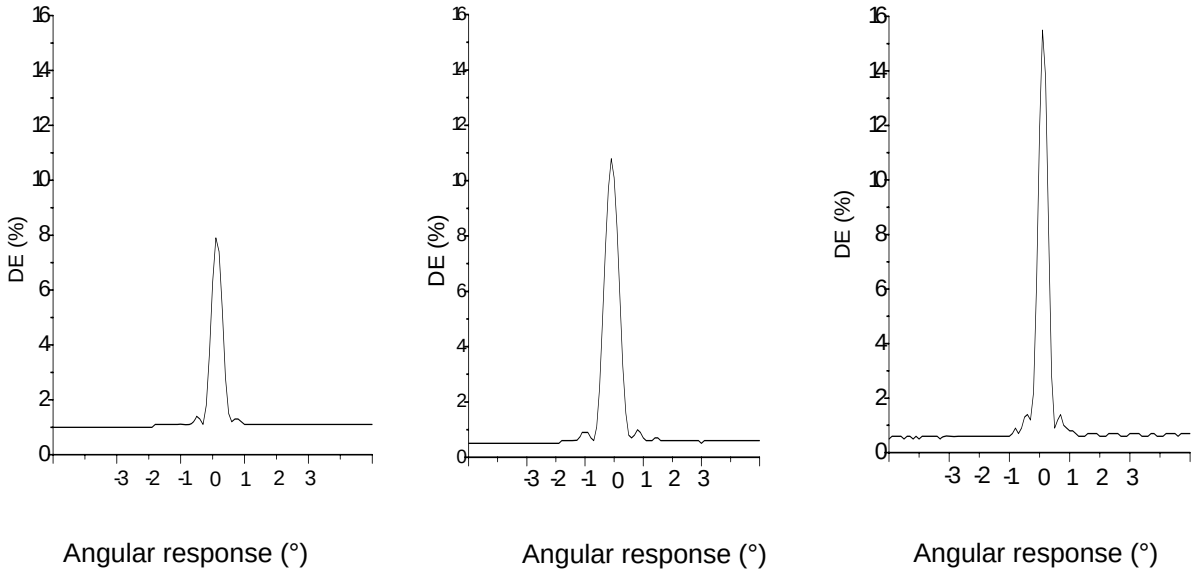

Fig. 4.24 Angular response as function of Diffraction efficiency for all photopolymers;C1, C2,C3.

Due to the long-wavelength absorbance of the photosensitizer, the effect of tuning the recording wavelength on the curcumin photopolymer (Cu3) is investigated. In

Fig. 4.25, the diffraction efficiency is plotted as function of the recording wavelength. Three different lines of Argon-ion laser were used; 488, 476 and 457nm. It was observed that by decreasing the wavelength towards UV region the diffraction efficiency decreases. This can be explained that by decreasing the wavelength the fringe space decreases as well the intensity and the spatial frequency increases. When the intensity decreases the polymerization is not complete and the diffusion is hindered caused by less polymerized acrylamide molecules.

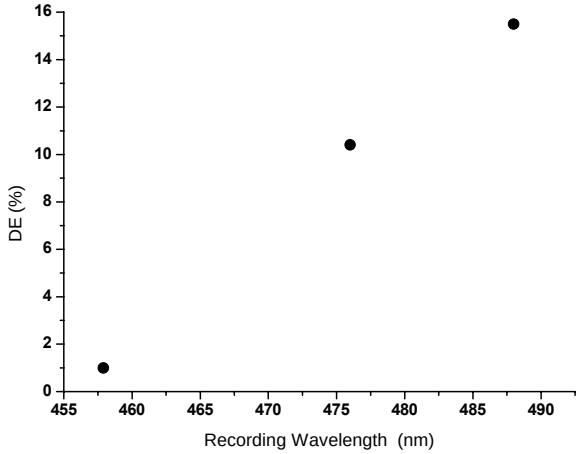

Fig. 4.25 Diffraction efficiencies varying the recording wavelength using a constant curcumin concentration of $1.008x10^{-3}$ M.

We have demonstrated curcumin as a suitable dye for volume data storage applications through formation of transmission gratings in acrylamide based photopolymer. A notice increase in the diffraction efficiency has been achieved by increasing the curcumin concentration leading a increase in the refractive index modulation up to $1.1x10^{-3}$.

4.5. Conclusion

This chapter discloses the novel dyes suitable for blue wavelength recording. We studied two newly synsthesized dyes in water soluble photo polymer systems. Efficient grating formation is achieved in all these blue sensitized photopolymers.

We studied two newly synthesized dyes in water soluble acrylamide photopolymer systems. Efficient grating formation is achieved in all these blue sensitised photopolymers. We found by decreasing the recording wavelength up to blue region we diminished the grating period and we increased the spatial frequency using the same set up from close to 2173 nm to 2410 nm. We have demonstrated Perylene and Curcumin as two novel photosensitizers suitable for blue recording at 488 nm of wavelength with a reduced shrinkage yielding a better efficiency. Shifting the wavelength further to the blue region we found acridine yellow as a appropriate dye for recording at 457 nm of wavelength achieving a high RIM of $4x10^{-3}$ with a shrinkage measured by angular selectivity as lower as 1% making a proper material for holographic data storage.

References

[1] http://www.inphase-technologies.com/downloads/pdf/technology/techTour.pdf

[2] http://www.tapeonline.com/blu-ray.axpx

[3] S. Martin, P.E.L.G. Leclere, Y. L.M. Renotte, V. Toal and Y.F. Lion, "Characterization of an acrylamide-based dry photopolymer holographic recording material", Opt. Engineering 33, 3942-3946 (1994).

[4] M. Ortuño, S. Gallego, C. Garcia, C.Neipp, A. Belendez and I. Pascual, "Optimization of a 1 mm thick PVA/Acrylamide recording material to obtain holographic memories: method of preparation and holographic properties", Appl. Phys. B 76, 851-857 (2003).

[5] C. Sanchez, M.J. Escuti, C Van Heesch, C. W.M. Bastiaansen, D. J. Broer, J. loos and R. Nussbaumer, "TiO_2 nanoparticle-Photopolymer composites for volume holographic Recording", Adv.Funct. Mater 15, 1623-1629 (2005).

[6] W.S. kim, H-S. Chang, Y-C. Jeong,Y-M Lee, J-K. Park, C-W Shin, N. Kim and H-J. Tak, "A new phase-stable photopolymer with high diffraction efficiency based on modified PMMA", Opt. Comm. 249, 65-71 (2005).

[7] H. Kogelnik, Bell Syst. Tech. J. 48, 2909 (1969).

[8] R. Jallapuram, I. Naydenova, S. Martin, R. Howard, V. Toal, S. Frohmann, S. Orlic and H. J. Eichler, "Acrylamide-based photopolymer for microholograpic data storage", Opt. Mater. 28, 1329-1333 (2006).

[9] V. Moreau, Y. Renotte and Y. lion, "Characteriztion of Dupont photopolymer: determination of kinetic parameters in a diffusion model", Appl. Opt. 10, 3427-3435 (2002).

[10] H. Sherif, I. Naydenova, S. Martin, C. McGinn and V. Toal, "Characteriztion of an acrylamide-based photopolymer for data storage utilizing holographic angular multiplexing", J. Opt. A: Pure Appl. Opt. 7, 255-260 (2005).

[11]. M. Magini, M.R. Rodrigues, « A dynamical system to describe the cationic photopolymerization of tetrahydrofuran initiated by systems sensitizer-sulfonium

salt", Polymer, 46, 3489–3495, (2005). J. V. Crivello* and J. L. Lee, "Photosensitized Cationic Polymerizations Using Dialkylphenacylsulfonium and Dialkyl(4-hydroxyphenyl)sulfonium Salt Photoinitiators"
Macromolecules, Vol. 14, No. 5, 1141-1147, (1981).

[12]. S. Icli , S. Demiça, B. Dindar, A. O. Doroshenko and C. Timur, "Photophysical and photochemical properties of a water-soluble perylene diimide derivative", J. P. P. A: Chem, 136, 15–24, (2000)

[13]. W.S. Kim, Y-C Jeong, J-K. Park, C-W Shin and N-Kim, "Diffraction efficiency behaviour of photopolymer based on P5MMA-co-MMA) copolymer matrix", Opt. Mater. Doi:10.1016/j.optmat.2006.09.007, (2006).

[14]. S. Blaya, L. Carretero, R. Mallavia, A. Fimia, R. Madrigal, M. Ulibarrena, D. Levy, "Optimization of an acrylamide-based dry film used for holographic recording", Applied Optics, Vol. 37, No. 32, 7604-7610, 1998.

[15]. D.M. Connor, S.D. Allen, D.M. Collard, C.L.Liotta and D. A. Schiraldi. "Effect of linear comonomers on the rate of crystallization of copolyesters". Journal of applied polymer science. Vol.80, 2896-2704 (2201).

[16]. K. Wu, J. G. Snijders and C. Lin, "Reinvestigation of Hydrogen Bond Effects on the Polarizability and hyperpolarizability of Urea Molecular Clusters" *J. Phys. Chem. B* 2002, *106*, 8954-8958

[17]. A. Sosnik and D. Cohn, "Poly(ethylene glycol)-poly(epsilon-caprolactone) block oligomers as injectable materials", Polymer, 44, 7033–7042, (2003).

[18]. X. He, H. Liu, Y. Li, Y. Liu, F. Lu, Y. Li and D. Zhu, "A New Copolymer Containing Perylene Bisimide and Porphyrin Moieties: Synthesis and Characterization", Macromol. Chem Physic, Vol. 206, Iss. 21, 2199-2205, (2005).

[19]. D. Kucklingl, H-J. P. Adler, L. Ling, W. D. Habicher and K-F Arndt, "Temperature sensitive polymers based on 2-(dimethylmaleinimido)-*N*-ethyl-acrylamide: Copolymers with*N*-isopropylacrylamide", Polymer Bulletin, 44, 269–276 (2000)

[20]. J.T. Gallo and M. Verber, "Model for the effects of material shrinkage on volume holograms", Appl. Opt. 29, 6797- 6804. 1994.

[21]. L. Shou-Jun, L. Guo-Dong, H. Qing-Sheng, W. Min-Xian, Jin Guo-Fan, S. Meng-Quan, W. Tao and W. Fei-Peng, "Holographic grating formation in dry photopolymer film with shrinkage", Chinese Physics, Vol. 13, No. 9, 1428-1431.

[22] A. Anderson, M. Mitchell and R.S. Mohan, "Isolation of Curcumin from Turmeric", J. Chem. Educ. 77, 359-360 (2000).

[23] J.V. Crivello and U.Bulut, "Curcumin: A naturally ocurring lon-wavelength photosensitizer for diaryliodonium salts", J of Polym Sci Part A; Polym Chem 43, 5217-5231, (2005).

[24] E. M. Bruzell, E. Morisbak and H. H. Tonnesen, "Studies on curcumin and curcuminoids. XXIX. Photoinduced cytoxicity of curcumin in selected aqueous preparations", Photochem. Photobiol. Sci. 4, 523-530 (2005).

[25] Mishra and S. Daswal, "Curcumin, A Novel Natural Photoinitiator for the Copolymerization of Styrene and Methylmethacrylate", Journal of Macromolecular Science, Part A: Pure and Applied Chemistry 42, 1667-1678 (2005).

[26] J. Crivello and U. Bulut, "Indian turmeric and its use in cationic Photopolymeriztion", Macrom. Symp. 240, 1-11 (2006).

5

Chapter 5
Nano-composite photopolymer recording media for reduced shrinkage

5.1 Introduction

In previous chapters we explored the potential of photopolymer systems as high capacity data storage media capable of full range recording. With all the excellent properties obtained including high diffraction efficiency at high spatial frequencies, the photopolymer system mainly suffers from the undesired shrinkage after recording. Shrinkage is due to the loss in volume fraction of the recording media as it undergoes polymerization process [1]. The effective film thickness is reduced because of such loss which leads to change in the stored grating period [1]. The basic photopolymer component responsible for such changes during recording process is the non-active component called binder. Almost all polymeric binder materials suffer from loss in volume fraction mainly because of the loss in their mechanical properties caused by polymerization process. To improve the mechanical property of binders like PVA, inorganic based composite materials such as CdS, Carbon nanotubes,

silver, and clays have been employed to prepare polymer nano-composite [2]. Here the crystallization behaviour of polymer material is also crucial since it governs the thermal and stress-strain properties [3]. The crystallisation of PVA is drastically affected by the tactility of main chain, molecular weight and plasticizer amount.

More recently, PVA-based nano-composites have been produced to improve its mechanical properties. Most PVA-based nanocomposites are prepared with the sol–gel method [3]. The main concern for fabricating a polymeric–inorganic nanocomposite is the dispersion of inorganic nanoparticles in a polymer matrix uniformly while avoiding the aggregation. To solve this problem, various processes have been developed. Extensive methods for synthesizing polymeric–inorganic nanocomposites included solgel, *in situ* polymerization, intercalation polymerization, and blending techniques has been used.

Several Attempts have been proposed to improve some features of photopolymers such as enhancement of the refractive index modulation and reduction of the shrinkage by the incorporation of high or low refractive index species such as silica and titania nanoparticles, in addition to the regular photopolymerizable monomers.

Suzuki et al. [4] demonstrated the recording of permanent holographic gratings in the green with high diffraction efficiency in TiO2 nanoparticle-dispersed methacrylate photopolymer films. The photopolymer was prepapred by dispersing the TiO_2 nanoparticles combined with a solution of methyl isobutyl ketone and *n*-butyl alcohol, to methacrylate monomers [~2-methyl-acrylic acid 3-[2-methyl-acryloyloxymethyl)-octahydro-4,7-methano-iden-5-ylmethyl ester] at a wavelength

of 589 nm. The photosensitizer used was titanocene (Irgacure 784, Ciba) at 1 wt% allowing the photosensitivity at wavelengths shorter than 550 nm. The difference between the refractive index of the nanoparticles and the monomers in the solid phase is one, which is greater than that (~0.1) between polymerized monomers and host polymers usually in binder based photopolymers. Diffraction efficiencies near 90% were obtained after 100 seconds of the exposure time with an intensity of 100 mW/cm^2 and a fringe spacing of 1.0 μm. It is shown that the diffraction efficiency as well as the recording sensitivity significantly increased with a raise of nanoparticles content. It is also found that shrinkage during holographic exposure is noticeably suppressed by inclusion of the nanoparticles. The inclusion of nanoparticles represented an enhancement of the refractive index modulation up to $5.1x10^{-3}$.

Kim et al. [5] reported an organic-inorganic photopolymer containing surface-nanoparticles, which exhibits a significant enhancement in optical properties. The photopolymer was prepared using poly(methylmethacrylate-co-methacrylate acid) as a polymer matrix, acrylamide and surface-photoreactive silica nanoparticles as photopolymerizable monomers, triethanolamine and methylene blue as initiator and photosensitizer respectively. The composition of the reactants was: matrix:monomer: TEA:MB was dissolved in the ratio 51:25:24:0.06 wt% in tetrahydrofuran. Two different photopolymers were prepared to verify the effect of the nanoparticles. The photopolymer containing surface-photoreactive nanoparticles showed diffraction efficiency near 90% after 90 sec of exposure and reduced volume shrinkage without affecting the energetic sensitivity using a fringe spacing of about 1 μm.

Sanchez et al. [6] reported another new and efficient inorganic-organic photopolymer for the recording of volume transmission holograms. The mixture comprises a mixture of UV-acrylates and grafted titanium dioxide nanoparticles with an average size of 4 nm. Diffraction efficiencies near 90 % were achieved with a space fringe of 500 nm for the maximum nanoparticles content of 30%. A dramatic increase in efficiency was observed as the nanoparticles concentration was increased. The inclusion of nanoparticles represented an enhancement of refractive index modulation up to 15.5×10^{-3}- an improvement of more than a factor of four over the material without nanoparticles while maintaining high transparency in the visible wavelength range.

Another hybrid photopolymer by incorporating $Zr(O^{i}Pr)_4$ nanoparticles was investigated by F. del Monte et al. [7] Diffraction efficiencies of 97% yielding refractive index modulation up to 1.5×10^{-2} and 69% of diffraction efficiency were achieved for photopolymers with and without Zr nanoparticles respectively in a 35 μm thick film. The components of the holographic material were 2,4-pentadienone and POEA as the first and second photopolymerizable monomers, Irgacure 784 as photoinitiator and the binder of choice was a nanoporous hybrid silica glass.

In present chapter we incorporate inorganic nano-composite materials such as SiO2 nanoparticles in our recording media in order to reduce the overall shrinkage. Furthermore, incorporation of such nano-composite materials often brings the much desired modulation of effective refractive index as the inorganic materials generally exhibit different refractive index. Formation of the transmission volume phase

gratings are demonstrated with excellent control over shrinkage [5,6]. Before going into experimental details it is required to understand the additional photo-physical steps involved in a nano-composite photopolymer media.

5.2 Preparation of PVA/SiO_2 nano-composite based photopolymer recording media

SiO_2 nanoparticles employed have a lower index of refraction (n~1.46) than that of presently used monomers (n=1.55) in our experiments [8]. Firstly the SiO_2 nanoparticles aqueous dispersion is treated with an ultrasonic vibrator [3]. Its pH value is adjusted to a basic one so as to negatively charge the SiO_2 nanoparticles, which act as templates to absorb positively charged polyallilamine hydrochloride (PAH) surfactant chains through electrostatic adsorptive interaction. After incorporation of this pH controlled solution into PVA solution dissolved in water, PVA molecular chains are then assembled on the surface of SiO_2 nanoparticles through hydrogen bonding between hydroxyl groups of the PVA and the amino group of the PAH. Finally the treated SiO_2 nanoparticles are uniformly dispersed in bulk PVA matrix, which then combines with the rest of pre-polymer components [3].

In this experiment we used 17 mg of SiO_2 nanoparticles aqueous dispersion (3.2 ml) which was ultrasonically agitated for 30 min. The pH of the solution was adjusted from acid to a basic with addition of 1.5 ml of 0.2M NaOH water solution. A 0.5 wt% positively charged Poly (allylamine hydrochloride)-(PAH:Aldrich, Mw: 70,000) solution (1.6 ml) was dropped into the SiO_2 dispersion, immediately a precipitation

of the solids appeared. The dispersion was centrifuged and rinsed to eliminate the PAH not absorbed onto the surface of the SiO_2. This step was repeated four times. A 0.5wt% (3.2 ml) PVA solution, Mw: 31,000-50,000 (87-89% hydrolyzed) was dropped into the rinsed SiO_2 dispersion which was ultrasonically stirred for 40 min to produce a stable SiO_2 dispersion. The stable SiO_2 dispersion was dropped into a 10% wt (3.2ml) of a PVA solution with the same molecular weight used previously were ultrasonically stirred for 40 min at room temperature to produce a homogeneous PVA/SiO_2 nanocomposite.

The influence of NaOH quantity plays an important role in the dispersion of the nanoparticles, as it helps the formation of SiO2 solids wrapped in PAH. The formation of solids is indispensable in the functionalization process. The NaOH amount used after nanoparticles aqueous solution in the first step of the nanoparticles functionalization will decide the formation of solids to rinse and then to disperse. If the NaOH amount is less than 1.5 ml in 3.2 ml of nanoparticles-water dispersion no solids are formed, if the quantity is higher than this value the solution becomes transparent, in this way there are no solids formed.

5.2.1 Interaction forces in the nanocomposite

Acute aggregations exist if SiO_2 nanoparticles are dispersed in pure water without any treatment. However, there is a not obvious aggregation after SiO_2 nanoparticles are treated with PAH as the surfaces of negatively charges SiO_2 nanoparticles are

covered by positively charged molecular chain of PAH through electrostatic adsorptive interactions which considerably improve the dispersion of SiO_2 nanoparticles [9].

The amido functional groups of PAH thus covers the surface of SiO_2 nanoparticles, which are then subsequently linked to hydroxyl-functional groups of PVA by hydrogen-bonding interactions. This results in the uniform dispersion of SiO_2 nanoparticles in the PVA matrix [9]. Figure 5.1 schematically demonstrates such process.

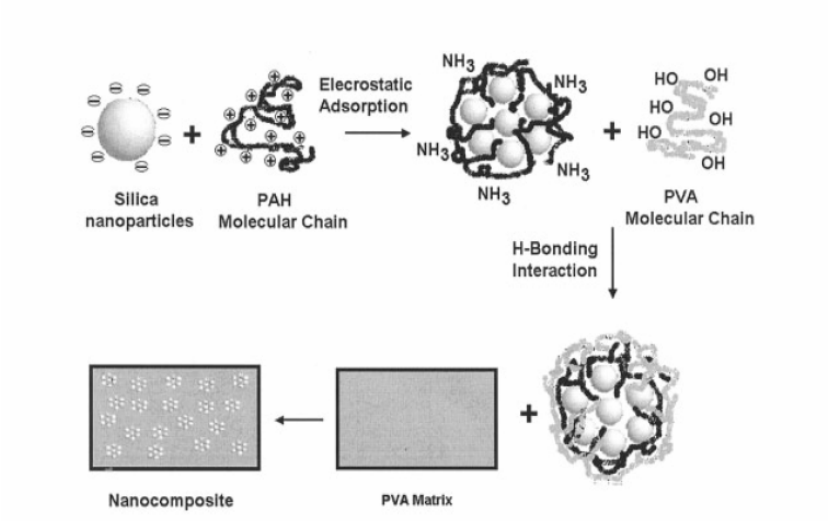

Fig. 5.1 Scheme of the nanocomposite process.

5.2.2 Photopolymerization process incorporating nanoparticles

The polymerization process with nano-particles inside the PVA matrix is slightly different from the general photo polymerization process. When the interfering light pattern reaches the film rapid cross-linking takes place in the high intensity fringes

while there is almost no reaction in the dark areas. As a result of the depletion of highly reactive monomer in the bright regions, the non consumed monomers then start diffusing from dark to bright areas [6].

The consumption of monomers due to photopolymerization breaks the thermodynamical equilibrium balance of monomers and nanoparticles which requires that their volume fraction ratio between two components be constant at any position. Such imbalance leads to migration (diffusion) of monomers from dark to bright regions while photosensitive inorganic nanoparticles experience the counter-diffusion from bright to dark regions since they are not consumed. In this way a permanent RI grating is formed owing to a spatial frequency distribution of the effective RI with periodically distributed nanoparticles and polymerized monomers [8]. Such a dynamic process essentially continues until monomers are consumed completely by the monomolecular and bimolecular termination processes and/or until the increased viscosity of a surrounding medium due to growing polymer networks makes oligomers and nanoparticles immobilize as a result spatially periodic distributions of nanoparticles and if any polymer concentrations are formed in the material [8]. Because unreacted monomers in the dark regions are sooner or later photopolymerized, a fixed RI grating maybe formed owing to a difference in effective refractive indices of periodically distributed nanoparticles and uniformly distributed polymerized monomers.

Such counter-diffusion process is illustrated in Fig. 5.2. The inorganic nanoparticles experience counterdiffusion from the bright to the dark regions, since the particles

are not consumed and their chemical potential increases in the bright regions as a result of depletion of monomers in those areas [10].

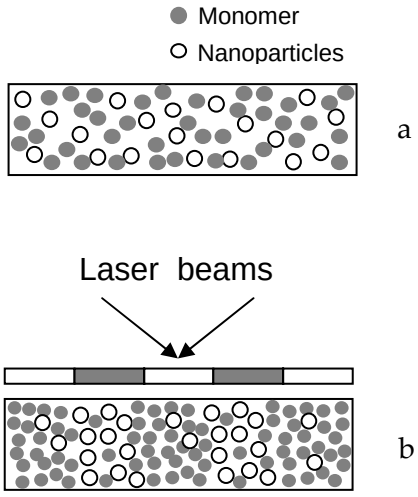

Fig. 5.2 Holographic recording process in a nanoparticle-dispersed photopolymer. (a) before and (b) during holographic exposure.

As a consequence the low reactivity species the monomer and non-reactive nanoparticles counter-diffuse to the dark areas resulting in a compositional modulation [6]. The chemical affinity of the nanoparticles with the low-reactivity monomer could enhance this diffusion of the nanoparticles to the dark areas. This compositional segregation together with the significant difference in refractive index of nanoparticles with respect to the rest of the components of the polymer is expected to enhance the diffraction efficiency of the stored grating structures.

5.2.3 Hydrogen Bond interaction theory

Another dominating effect may come from the formation of hydrogen bonds within the PVA-SiO2 network [11]. Figure 5.3 illustrates the interfacial structure of photopolymer. Before photopolymerization, the acrylamide molecules ought to induce efficient hydrogen bonding with silica nanoparticles (stability of silica/PVA dispersion is lower than that of silica/AA dispersion, thus it could be concluded that acryl amide molecules induce the most strong hydrogen bonding with silica nanoparticles) and then the acrylamide become into poly(acrylamide) by photopolymerization in the illuminates areas [11].

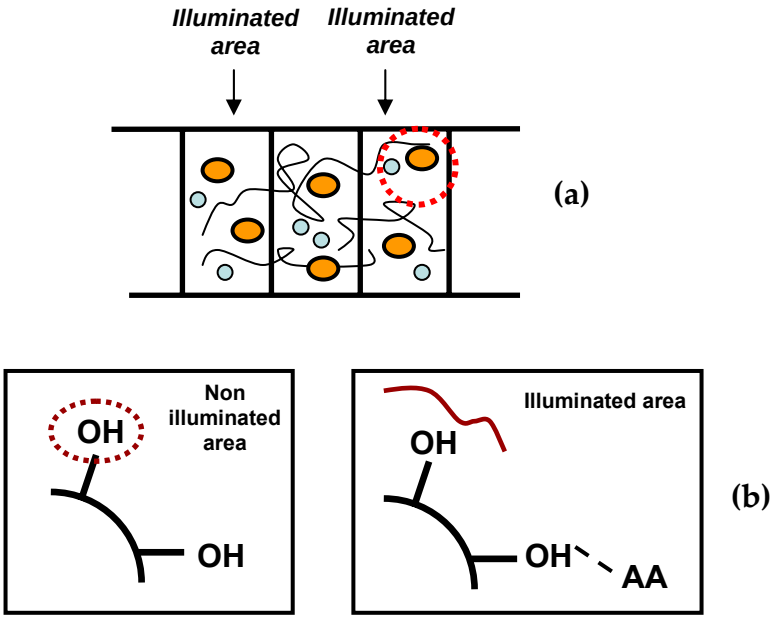

Fig. 5.3 Interfacial structure of nanocomposite_ photopolymer. (a) non_illuminated area (b) illuminated area.

After photopolymerization, acrylamide groups in the PAA chains may form hydrogen bonding with silica nanoparticles in the bright region, while there may be

weak hydrogen bonding in the dark region due to the diffusion of acryl amide molecules into the bright region by the concentration gradient. This difference in the hydrogen bonding strength between the bright region and the dark region may lead to the additional refractive index modulation, in other words, the enhancement in the diffraction efficiency [11].

5.3 Formation of transmission phase gratings in Eosin-nanocomposite photopolymer

We prepared different wt% SiO_2 nano-particle incorporated into PVA matrix with previously described Eosin sensitizer. For successful comparison of the effect of nanoparticles in this recording media It was ensured that the concentration of all the component except SiO_2 remains the same. The final concentration for all three samples is tabulated in table 5.1.

Table 5.1 Composition of pre-polymer solution in 2.5 ml of solution.

Eosin/SiO_2 photopolymer	**[Eosin] (%)**	**[Acrylamide] (M)**	**[BSA] (M)**	**[TEA] (M)**
EOS	0.080	0.452	0.052	0.605
EOS-Si1	0.080	0.452	0.052	0.605
EOS-Si2	0.080	0.452	0.052	0.605

Fig. 5.4 shows the UV-Vis spectra for eosin composite without and for composite containing nanoparticles shows a maximum absorption at the same wavelength of 530 nm. The gradual increase in general absorption features with incorporation of SiO2 nanoparticles indicates towards the amount of scattering taking place as any increase caused by nano-particle is not expected to increase the eosin absorption.

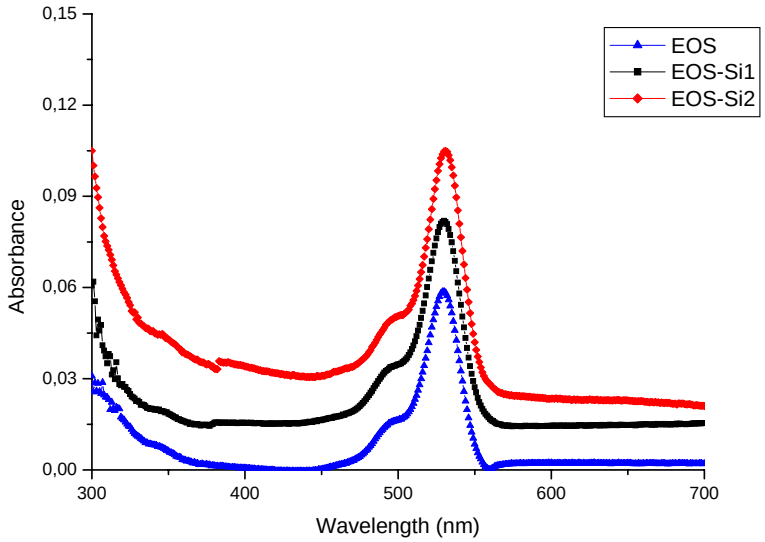

Fig. 5.4 UV/Vis spectra of the Eosin photopolymers and nanocomposites.

Table 5.2 shows the recording and reconstruction parameters used for characterization.

Table 5.2 Experimental parameters for grating formation in Eosin nanocomposite.

Photo-polymer	θ/2 (°)	**WB (nm)**	**RB (nm)**	**Λ (μm)**	**SF (lines/mm)**	**I (mW/cm²)**	**θ_B (°)**
EOS+SiO_2	34	514.5	633	0.46	2173	153.3	43.4 (T)

where θ/2 is the half-angle between the interference beams; WB and RB are the writing and reading beam respectively; Λ is the fringe period; θ_B(T,E) are the theoretical and experimental Bragg angle and I is the recording intensity.

Figure 5.5 illustrates the response of transmission gratings stored in this recording media with respect to increasing exposure time. A dramatic rise in the diffraction efficiency was observed by the addition of SiO_2 nanoparticles compared to the photopolymer without nanoparticles [6]. Also by increasing the nanoparticles loading the time to reach saturation is reduced drastically. The DE increased from 25% to 75% for the composite with higher 0.354 wt% nanoparticles. The less time required for saturation explains the light dispersion created by nano particles which creates a uniform illumination inside the media through out the recording film thickness.

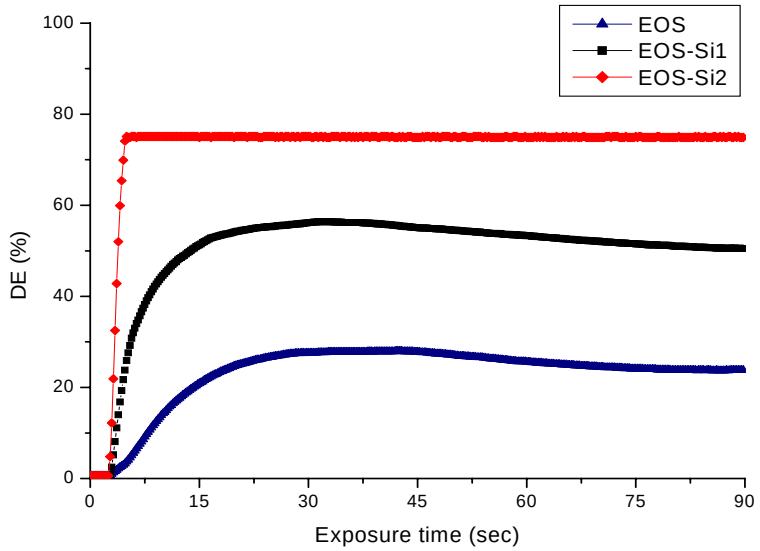

Figure 5.5 Diffraction efficiency with respect to exposure time.

There is a remarkable increase in the DE with exposure time for both cases with nanoparticles. Similar phenomena was reported in previous studies focusing on the nanoparticles-dispersed binder photopolymer and the origin of increase in DE was attributed to a counter-diffusion in DE resulting in the spatially periodic distribution of nanoparticles during holographic exposure. Table 5.3 summarizes the results.

Table 5.3 Optical parameters of photopolymer that contains Eosin + nanocomposites after 2.045 sec using a 25 μm thick layer.

Eosin/SiO_2 photopolymer	**SiO_2 content (%)**	**DE (%)**	**Sensitivity (cm/J)**	**RIM**	**Thickness (μm)**
EOS	0	3.3	232	$1.07x10^{-3}$	25
EOS-Si1	0.208	23.8	623	$3.0x10^{-3}$	25
EOS-Si2	0.354	74.1	1099	$6.1x10^{-3}$	25

We observed that for higher nanoparticles loads the pre-polymer syrup becomes viscous and the dispersion turbidity increases leading to non-uniform grating formation caused by higher surface scattering.

For comparing the amount of film shrinkage, the grating angular response half-width (θ) was obtained from the measurement of the diffraction efficiency as a function of angular deviation from the Bragg condition [5,12]. The angular response of the two photopolymers was measured by rotating the photopolymer from the position satisfying the Bragg condition. Figure 5.6 compares the angular response of the photopolymer with and without nanoparticles: it should be noticed that the

uniformity of grating throughout the depth of the photopolymer is also enhanced by the introduction of small amount of surface-photo reactive nanoparticles.

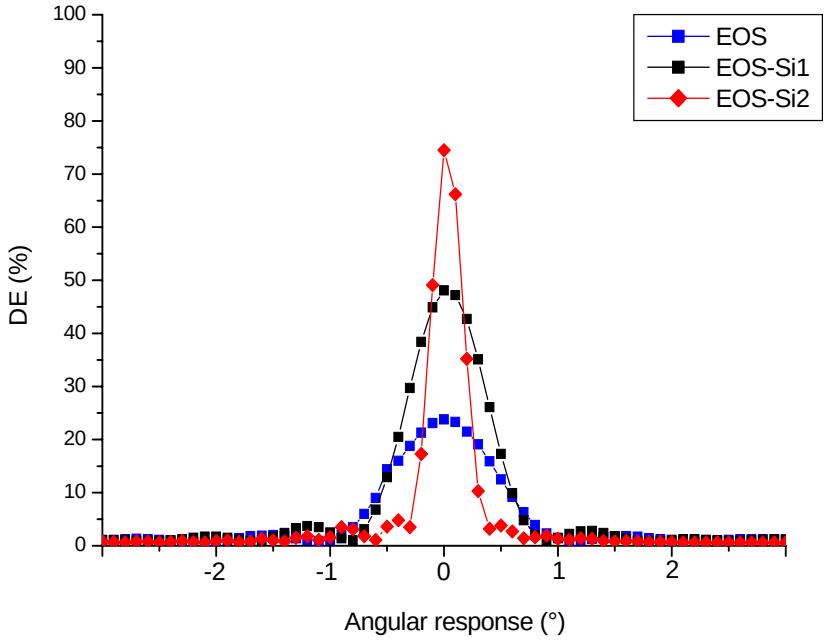

Fig. 5.6 Angular Selectivity of diffraction efficiency for composite without and nanoparticles.

As evident from the above figure, the increase in nano-particle presence inside the recording media narrows the angular selection of the gratings. This is a clear indication of less shrinkage suffered by the films over those without nano-particles as the presence of rigid nano-particles compensates the loss of volume fraction caused by the binder. The Bragg condition in the case of higher amount of nanoparticles was closer to the theoretically calculated Bragg angle while with no to little nanoparticles the Bragg condition varies by angle of 2°. This means the composition with nanoparticles has an ideal response and doesn't suffer from shrinkage as the case of

others. Table 5.4 illustrates the amount of shrinkage taking place in the films with and without nanoparticles.

Table 5.4 Shrinkage calculated using eosin nanocomposite.

Photopolymer	Δd (μm)	Shrinkage (%)
EOS	1.48	5.9
EOS-Si1	1.48	5.9
EOS-Si2	0.47	1.9

5.3.1 Effect of intensity on the EOS-Si2 nanocomposite recording media

In fig. 5.7, the growth of diffraction efficiency is plotted as a function of intensity for the nanocomposite with higher amount of nanoparticles. A clear rise in the diffraction efficiency was observed by increasing the intensity This evolution is different for 40 mW/cm^2 and 100mW/cm^2 where by raising the intensity the diffraction efficiency reached the maximum value and then decays and stabilizes but for the case of maximum intensity at 153 mW/cm^2 the diffraction reaches fast saturation and stabilizes.. Also higher sensitivities were found by increasing the intensity. Table 5.5 summarizes the results obtained by varying the intensity of the recording beams.

Table 5.5 Optical parameters of photopolymer that contains EOS-Si2 nanocomposite varying the recording intensity after 2.045 sec.

Intensity (mW/cm^2)	DE (%)	Sensitivity (cm/J)	RIM	Thickness (μm)
153.3	74.1	1099	$6.1x10^{-3}$	25
100	18	830	$2.5x10^{-3}$	25
40	5.4	1136	$1.3x10^{-3}$	25

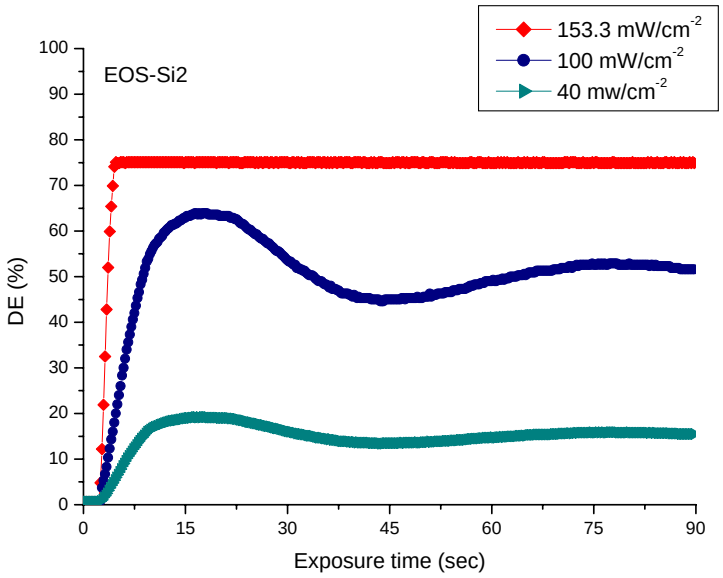

Fig. 5.7 Traces of diffraction vs exposure time for EOS-Si6 photopolymer at different intensities.

The angular response of the recording media with varying intensity is presented in figure 5.8. As we can clearly observe, by decreasing the recording intensity for the photopolymer EOS-Si2 the first diffracted orders start to vanish.

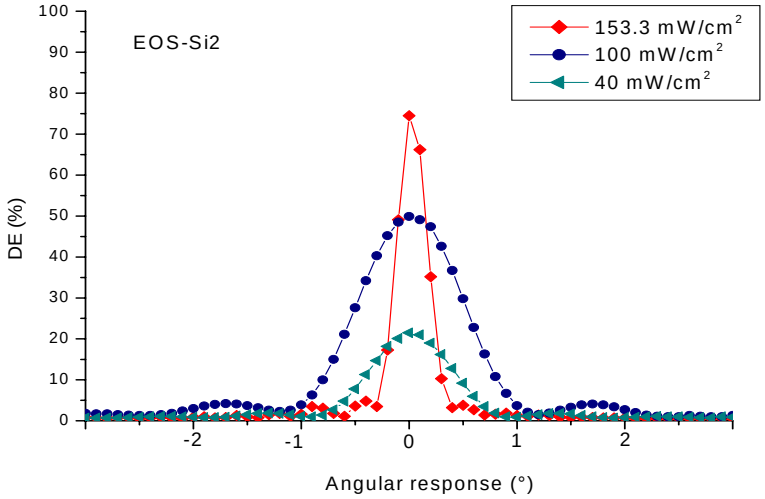

Fig. 5.8 Angular Selectivity of diffraction efficiency of nanocomposite EOS-Si2 at different intensities.

The features for photopolymer with nanoparticles are more clearly resolved. The uplift of the first satellite peaks may result from the non-uniformity in grating strength. Also, by increasing the intensity, the angular width of the zero diffracted order was considerably reduced.

5.3.2 FT-IR and Tg analysis

To clarify the difference in the hydrogen bonding between 'dark' and 'bright' region, we prepared samples firstly illuminated (3mg) then mild with KBR and pressed as disc form for FT-IR measurement photopolymerization of acrylamide molecules, as shown in Fig.5.9. The PVA is a kind of semicrystalline polymer, quite a few crystallites are formed on the surface of the pure PVA fracture, whereas there are no

crystallites on the surface of the PVA/SiO_2 nanocomposite because of the well-dispersed SiO_2 nanoparticles being able to prevent the formation of crystallites [9].

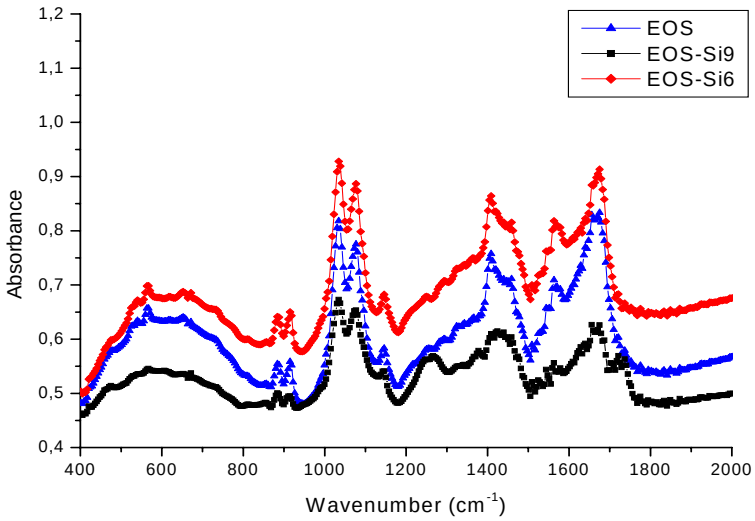

Fig. 5.9 FTIR spectra of the polymerized Eosin photopolymers with and without nanoparticles.

The characteristic absorbing peaks of SiO2 (1100 and 466 cm^{-1}) are not simply overlapped by those of PVA but move to 1089 and 473 cm^{-1}, respectively. This may be due to the interaction between the SiO2 nanoparticles and PVA matrix, which obstructs the formation of intrahydrogen bonding. This further indicates that the PVA matrix and SiO_2 nanoparticles are not simply blended, and complex interactions exist [9].

Figure 5.10 shows the DSC thermogram of photopolymer with and without nanoparticles. The addition of the SiO_2 nanoparticles to the PVA matrix results in a significant increase in Tg, this suggest that the SiO_2 nanoparticles are well dispersed in the PVA matrix due to nanoparticles have huge relative surface areas and strong

absorptive power [9]. The amorphous molecular chains of PVA become stable and interact strongly with the SiO_2 nanoparticles. As a result the SiO_2 nanoparticles restrict the thermal motion of the PVA molecular segment [9]. Because Tg is the limiting temperature for the applications of plastic polymers; an improvement is very important for PVA [7]. The Tg (EOS-without nanoparticles) =90°C and Tg (EOS-Si2, containing nanoparticles)= 94°C resulting Tg(nanocomposite) > Tg (PVA).

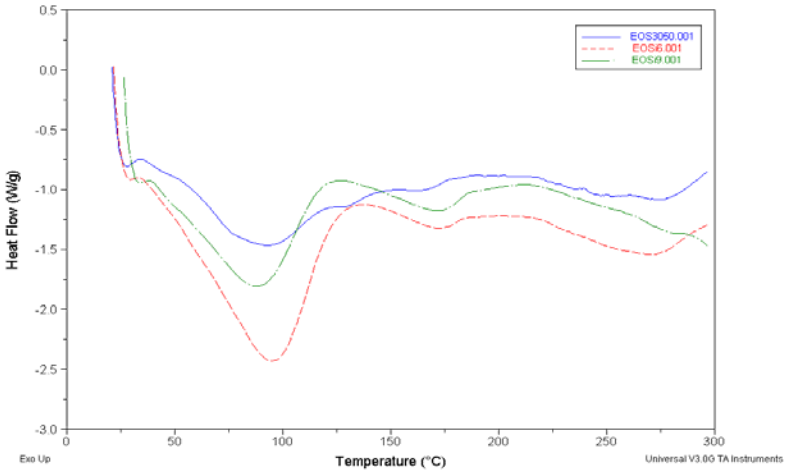

Fig. 5.10 DSC thermogram with Eosin photopolymers containing nanoparticles

Figure 5.11 (a,b) compares the grating surface profile after recording with and without nanoparticels.

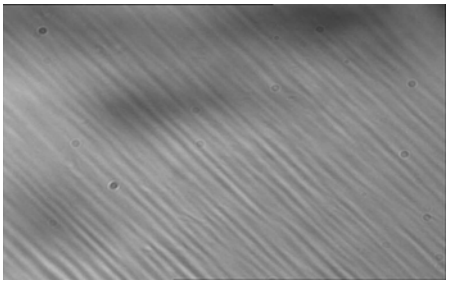

Fig. 5.11a Microscope image with Eosin without nanoparticles.

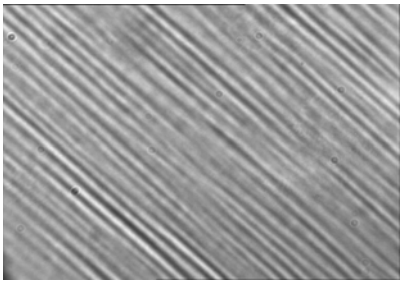

Fig. 5.11b Microscope image with Eosin with nanoparticles.

From the highly resolved features it can be concluded that the incorporation of nano-particles are helpful for high refractive index modulation which essentially gives the higher diffraction efficiency.

Conclusion

We successfully achieved the minimum shrinkage limit of a photopolymer recording system by incorporation of inorganic nanoparticles inside the eosin sensitized recording media. The reason for such decrease in the shrinkage may be attributed to an increase in rigidity of sample material resulting from dispersion of nanoparticles. The structure of photopolymerised polymer and the mechanism of reduction of volume shrinkage due to the rigid silica are conceptually described. Surface-photoreactive nanoparticles introduced in this study are expected to play dual roles with respect to the reduction of volume shrinkage. Due to the rigid silica nanoparticles incorporated in this grating by chemical bonds, the mobility of photopolymerised polymer chains can be reduced and this can lead to a reduction of free volume change and thus to the volume shrinkage of recorded gratings. In addition to the contribution to the reduction in the free volume change during Photopolymerization, the nanoparticles also contribute the rigidity enhancement of the medium which also leads to the reduction of volume shrinkage. It is seen that while shrinkage decreases with an increase of nanocomposite concentration. As the shrinkage decreases, Sensitivity (S), Dynamic sensitivity (S^*) and Δn increases.

References

[1] S. Martin, P. E. L. G. Leclere, Y. L.M. Renotte, V. Toal, Y. F. Lion, "Characterization of an acrylamide-based dry photopolymer holographic recording material", Optical Engineering, Vol. 33, No. 12, 3942-3946, 1994.

[2] Z. Peng, L. X. Kong and S.D. Li, "Dynamic mechanical analysis of poly vinylalcohol/silica nanocomposite", Synthetic Metals 152, 25-28, (2005).

[3] Z. Peng, L. X. Kong and S.D. Li, "Non-isothermal crystallization kinetics of self-assembled polyvinylalcohol/silica nanocomposite", Polymer 46, 1949-1955, (2005).

[4]. N. Suzuki, Y. Tomita and T. Kojima, "Holographic recording in TiO2 nanoparticle-dispersed methacrylate photopolymer films", Appl. Lett. Vol. 81, No. 22, 4121-4123, (2002).

[5] W. S. Kim, Y-Ch. Jeong and J-K Park, "Organic-inorganic hybrid photopolymer with reduced volume shrinkage", Appl. Phys. Lett. 87, 012106-1-3, (2005).

[6] C. Sanchez, M.J. Escuti, C Van Heesch, C. W.M. Bastiaansen, D. J. Broer, J. loos and R. Nussbaumer, "TiO_2 nanoparticle-Photopolymer composites for volume holographic Recording", Adv.Funct. Mater **15**, 1623-1629 (2005).

[7]. F. del Monte, O. Martinez, J. A. Rodrigo, M.L. Calvo and P. Cheben, "A volume holographic sol-gel material with large enhancement of dynamic range by incorporation of high refractive index species. Adv. Mat. 18, 2014-2017, (2006).

[8] N. Suzuki and Y. Tomita, "Diffraction properties of volume holograms recorded in SiO_2 nanoparticle-dispersed methacrylate photopolymer films", Jpn. J. Appl. Phys. 42, L927-L929 Part 2 No. 8A, (2003).

[9] Z. Peng, L. X. Kong and S.D. Li, "Thermal properties and morphology of a polyvinylalcohol/silica nanocomposite prepared with a self-assembled monolayer technique", J. Appl. Pol. Sci. 96, 1436-1442, (2005).

[10] Y. Tomita, N. Suzuki and K. Chikana, " Holographic manipulation of nanoparticles distribution morphology in nanoparticles-dispersed photopolymers", Opt. Lett. 30, No.8, 839-841, (2005).

[11] W. S. Kim, Y-Ch. Jeong, and J-K Park, "Nanoparticle-induced refractive index modulation of organic-inorganic hybrid photopolymer", Opt. Express 14, No. 20 8967-8973, (2006).

[12] N. Suzuki, Y.Tomita and T. Kojima, "Holographic recording in TiO_2 nanoparticle-dispersed methacrylate photopolymer films", Appl. Phys. Lett. 81, No. 22, 4121-4123, (2002).

Conclusions

In chapter 1, we presented the theory of holography and different photosensitive media commonly used for recording purposes focussing in the description of photopolymers. We described the principle of photopolymers, main components exhibiting the materials chosen in our study, the photopolymerization process which undergo once is illuminated by a coherent light (Laser), terminology related to this kind of materials. The diffusion process of the monomer is examined due to its importance in the enhancement of their refractive index modulation. We also discussed the different geometries used for holographic grating recording such as transmission and reflection ones.

In this study we presented the novel water soluble photopolymer systems and their suitability as volume information storage media highlighting on increasing the capacity of the information storage in terms of increased spatial frequency. Different photosensitizing dyes with sensitivity from red to blue spectral region were revised demonstrated spatial frequency as high as 2400 lines/mm arriving close to 6000 lines/mm in transmission and reflection geometry respectively.

In the chapter 2 we presented the optimization of different components of photopolymer system suitable for red wavelength recording in transmission geometry selecting methylene blue as photosensitizer. The diffraction grating

formation was monitored achieving a diffraction efficiency of 40% under a high spatial frequency of 1767 lines/mm with high angular response of 0.5°. By optimizing this component we demonstrated its limitations as a dye in the acrylamide based photopolymers giving an explanation of this phenomenon.

In chapter 3 we studied different photopolymers using Rose Bengal, Erythrosin B, Acridine Orange and Eosin as photosensitizers in transmission as well as reflection geometry recording using green sensitizing dyes, showing a significant advantage of higher capacity grating storage over red sensitized dye studied in chapter 2. An optimization using the different dyes was carried out. An efficient dye is desired to achieve maximum diffraction efficiencies in holographic grating recording in photopolymer. The importance of role as electron acceptor in the photoreaction was studied using CV. We found the maximum diffraction efficiency among all the dyes used of 90% using EryB exhibiting the best acceptor electron nature with a peak reduction of -1.1eV with the highest angular selectivity of 0.48° very important effect, because this effect increases the capacity of the futures holography memories made with photopolymers, compare to the rest of the dyes, 80%, 75% and 70% for RB, AO and Eosin respectively. The effect of the cross-linking agent in photopolymer is also studied by the replacement of the N',N-methylenebisacrylamide for N,N-dimethylacrylamide observing a negative influence (overmodulation process) in the DE evolution due to the drastic decay suffered after achieving its maximum value. The results were analysed with help of optical techniques such as UV/Vis spectra

(layer absorption) DSC (Tg, diffusion of monomer), FTIR measurements (quantity of monomer become polymer) and through diffraction grating formation in the bulk of the recording medium. By changing from transmission to reflection geometry using the same set up we increased more than two times the spatial frequency but lower diffraction efficiencies were achieved. In reflection, we observed by increasing the exposure time the diffraction efficiency was improved. RB was found the more efficient dye in this geometry showing as high as 12.33% of diffraction efficiency.

In chapter 4 we develop novel photopolymer system suitable for blue wavelength recording. Two new water soluble blue sensitizing dyes are synthesized and their information storage capacity is demonstrated. We found between the two novel materials Perylene as more efficient dye at 488 nm of wavelength for creation of holographic grating recording. We demonstrated by increasing the acrylamide content the width of the first lobe (zero diffracted order beam) is increased. By reducing to recording wavelength to 457.9 nm closer UV spectral region we achieved 75% of diffraction efficiency using acridine yellow as dye with reduced shrinkage of 1% making ideal material for data storage. We also discussed by increasing the layer thickness the sensitivity and diffraction efficiency as well as RIM decreased.

Finally; in chapter 5 we studied the response of the refractive index modulation by incorporating low index in-organic nanoparticles in the photopolymer composition. Large modulation of index is thus created in recording system. A better

understanding of the monomer diffusion process involved in the photopolymerization process was achieved. We observed a drastic increase of diffraction efficiency from 25% to 75% as well as the sensitivity and the RIM with the higher load of SiO_2 nanoparticles in the photopolymer. An important diminution of the angular width leading to a reduction of the shrinkage also was found.

For further enhancement of the spatial frequency we propose to find a dye sensible in region close to UV (410 nm). By reducing even more the recording wavelength the spatial frequency will be increased thus increasing the store capacity of the material.